Electronic Supplementary Material (ESI) for ChemComm.

Supporting Information

For

N-Heterocyclic Silylene/Germylene Ligands in Au(I) Catalysis

Nasrina Parvin,[a] Bijoyananda Mishra,[a] Anjana George,[b] Mahesh Neralkar,[a] Jabed Hossain,[a]

Pattiyil Parameswaran,*[b] Srinivas Hotha,*[a] and Shabana Khan*[a]

Contents

S1. Experimental Details

All experiments were carried out under an atmosphere of dry argon or in vaccuo using standard Schlenk technique and in a dinitrogen filled MBRAUN MB 150-G1 glovebox. The solvents used were purified by MBRAUN solvent purification system MB SPS-800. The starting materials **1** and **4** were prepared as reported in the literature. All other chemicals purchased from Aldrich were used without further purification. ^{1}H, ^{13}C, ^{31}P, ^{19}F and ^{29}Si NMR spectra were recorded in Bruker 400 MHz spectrometer, using $CDCl_3$ as solvent with external standards $SiMe_4$ (^{1}H, ^{13}C and ^{29}Si), 85% H_3PO_4 (^{31}P) and CHF_3 (^{19}F). Concentrated solution of the samples in $CDCl_3$ were sealed off in a NMR tube for measurement. Mass spectra were recorded using AB Sciex, 4800 plus MALDI TOF/TOF and HRMS ESI-TOF mass analyzer.

Synthesis of 2:

$AgSbF_6$ (0.171g, 0.5 mmol) was dissolved in DCM and added to the solution of **1** (0.325g, 0.5 mmol) in benzene. Immediately AgCl was precipitated out. After overnight stirring, AgCl was separated out from the reaction mixture by filtration and reduced the volume to 15 mL and kept it at 0^{o}C. Colorless hexagonal shaped crystals suitable for X-ray analysis was observed after one day. Yield: 0.354g (75%). Mp: 145^{o}C (decomposed). ^{1}H NMR (400.31 MHz, $CDCl_3$): δ 0.28 (*s*, 9H, Si*Me*$_3$), 0.43 (*s*, 9H, Si*Me*$_3$), 1.18 (*s*, 18H, C*Me*$_3$), 7.23-7.30 (*m*, 1H, Ph), 7.35-7.44 (*m*, 2H, Ph), 7.48 (*s*, 6H, C_6H_6) 7.52-7.69 (*m*, 2H, Ph) ppm. ^{13}C NMR{^{1}H} (100.67 MHz, $CDCl_3$): δ 3.61 (Si*Me*$_3$), 5.38 (Si*Me*$_3$), 30.65 (C*Me*$_3$), 54.40 (*C*Me$_3$), 126.06, 126.24, 127.20, 127.39, 127.99, 128.68, 130.59 (Ph-*C*), 172.45 (N*C*N) ppm. ^{29}Si\{^{1}H\} NMR (79.495 MHz, $CDCl_3$, 298 K): δ 9.45 (*Si*Me$_3$), 8.39 (*Si*Me$_3$), -6.44 (*Si*N(SiMe$_3$)$_2$) ppm. MALDI: *m/z* $[C_{27}H_{47}N_3Si_3Au]^+$: 616.05 [M-$C_6H_6$]$^+$. Anal Calcd: C, 35.56; H, 5.33; N, 4.44. Found: C, 35.23; H, 5.15; N, 4.57.

Synthesis of 3:

$AgSbF_6$ (0.171g, 0.5 mmol) was dissolved in DCM and added to the solution of **1** (0.350g, 0.5 mmol) in *m*-xylene. Immediately AgCl was precipitated out. After overnight stirring, AgCl was separated out from the reaction mixture by filtration and reduced the volume to 15 mL and kept it at 0^{o}C. Colorless block shaped crystals suitable for X-ray analysis was observed after one day. Yield: 0.329g (68%). Mp: 148^{o}C (decomposed). ^{1}H NMR (400.31 MHz, $CDCl_3$): δ 0.25 (*s*, 9H, Si*Me*$_3$), 0.35 (*s*, 9H, Si*Me*$_3$), 1.14 (*s*, 18H, C*Me*$_3$), 2.40 (*s*, 6H, $C_6H_4(CH_3)_2$, 7.21-7.30 (*m*, 4H,

Ph), 7.35-7.45 (*m*, 3H, Ph), 7.47-7.54 (*s*, 1H, C_6H_6) 7.57-7.64 (*m*, 1H, Ph) ppm. $^{13}C\{^1H\}$ NMR (100.67 MHz, $CDCl_3$): δ 3.39 (Si*Me*$_3$), 4.93 (Si*Me*$_3$), 20.47 ($C_6H_4(CH_3)_2$), 30.40 (C*Me*$_3$), 54.24 (*C*Me$_3$), 122.14, 125.89, 125.99, 127.08, 127.52, 128.12, 130.12, 130.40, (Ph-*C*), 172.38 (N*C*N) ppm. $^{29}Si\{^1H\}$ NMR (79.495 MHz, $CDCl_3$, 298 K): δ 9.34 (*Si*Me$_3$), 8.47 (*Si*Me$_3$), -8.85 (*Si*N(SiMe$_3$)$_2$). MALDI: *m/z* $[C_{27}H_{47}N_3Si_3Au]^+$: 616.05 $[M\text{-}C_6H_4(CH_3)_2]^+$. Anal Calcd: C, 37.00; H, 5.59; N, 4.32. Found: C, 36.73; H, 5.42; N, 4.40.

Synthesis of 4: 30 mL toluene was added into the mixture of 0.232 g (0.5 mmol) of germylene [{PhC(N*t*Bu)$_2$}Ge{N(SiMe$_3$)$_2$}] and 0.147 g (0.5 mmol) of AuCl.SMe$_2$ in a 100 mL schlenk flask. After overnight stirring at room temperature, the reaction mixture was dried completely and filtered in DCM through frit and crystalized in DCM/pentane mixture. Colorless crystals suitable for X-ray analysis was observed at 0^{o}c. Yield: 0.290g (83%). Mp: >240^{o}C. ^1H NMR (400.31 MHz, $CDCl_3$): δ 0.34 (*s*, 9H, Si*Me*$_3$), 0.53 (*s*, 9H, Si*Me*$_3$), 1.20 (*s*, 18H, C*Me*$_3$), 7.35-7.37 (*d*, J= 7.1 Hz, 2H, Ph), 7.44-7.55 (*m*, 3H, Ph) ppm. ^{13}C NMR$\{^1H\}$ (100.67 MHz, $CDCl_3$): δ 3.65 (Si*Me*$_3$), 5.14 (Si*Me*$_3$), 30.82 (C*Me*$_3$), 54.17 (*C*Me$_3$), 126.60, 126.88, 127.17, 127.23, 129.57, 130.79 (Ph-*C*), 168.95 (N*C*N) ppm. MALDI: *m/z* $[C_{21}H_{41}N_3Si_2GeAuClNa]^+$: 720.08 $[M+Na]^+$. Anal Calcd: C, 36.20; H, 5.93; N, 6.03. Found: C, 36.25; H, 5.95; N, 6.07.

Synthesis of 5: $AgSbF_6$ (0.171g, 0.5 mmol) was dissolved in DCM and added to the solution of **4** (0.348g, 0.5 mmol) in benzene. Immediately AgCl was precipitated out. After overnight stirring, AgCl was separated out from the reaction mixture by filtration and reduced the volume to 15 mL and kept it at 0^{o}C. Colorless block shaped crystals suitable for X-ray analysis was observed after one day. Yield: 0.340g (69%). Mp: 210^{o}C (decomposed). ^1H NMR (400.31 MHz, $CDCl_3$): δ 0.39 (*s*, 9H, Si*Me*$_3$), 0.56 (*s*, 9H, Si*Me*$_3$), 1.23 (*s*, 18H, C*Me*$_3$), 7.18-7.24 (*m*, 1H, Ph), 7.36-7.41 (*m*, 5H, Ph), 7.45-7.62 (*m*, 5H, Ph) ppm. ^{13}C NMR$\{^1H\}$ (100.67 MHz, $CDCl_3$): δ 4.69 (Si*Me*$_3$), 6.38 (Si*Me*$_3$), 32.00 (C*Me*$_3$), 55.36 (*C*Me$_3$), 127.02, 128.03, 128.41, 128.70, 128.77, 131.30, (Ph-*C*), 170.74 (N*C*N) ppm. MALDI: *m/z* $[C_{28}H_{50}N_3Si_2GeAu]^+$: 661.97 $[M\text{-}C_6H_6]^+$. Anal Calcd: C, 33.96; H, 5.09; N, 4.24. Found: C, 33.88; H, 5.15; N, 4.21.

Synthesis of 6: $AgSbF_6$ (0.171g, 0.5 mmol) was dissolved in DCM and added to the solution of **4** (0.348g, 0.5 mmol) in toluene. Immediately AgCl was precipitated out. After overnight stirring, AgCl was separated out from the reaction mixture by filtration and reduced the volume to 15 mL and kept it at 0^{o}C. Colorless block shaped crystals suitable for X-ray analysis was

observed after one day. Yield: 0.360g (72%). Mp: 212°C (decomposed). ^{1}H NMR (400.31 MHz, $CDCl_3$): δ 0.29 (*s*, 9H, Si*Me*$_3$), 0.46 (*s*, 9H, Si*Me*$_3$), 1.24 (*s*, 18H, C*Me*$_3$), 2.70 (*s*, 3H, C*H*$_{3,toluene}$), 7.04-7.10 (*m*, 1H, Ph), 7.15-7.18 (*m*, 2H, Ph), 7.28-7.34 (*m*, 1H, Ph), 7.36-7.62 (*m*, 6H, Ph) ppm. ^{13}C NMR{^{1}H} (100.67 MHz, $CDCl_3$): δ 4.77 (Si*Me*$_3$), 6.36 (Si*Me*$_3$), 21.64 (*C*H$_{3,toluene}$), 32.09 (C*Me*$_3$), 55.64 (*C*Me$_3$), 125.49, 127.76, 128.06, 128.30, 128.41, 129.23, 129.39, 129.92, 131.01, 131.42 (Ph-*C*), 138.06 (N*C*N) ppm. MALDI: *m/z* $[C_{29}H_{52}N_3Si_2GeAu]^+$: 662.25 $[M\text{-}C_6H_5CH_3]^+$. Anal Calcd: C, 34.68; H, 5.22; N, 4.18. Found: C, 34.65; H, 5.25; N, 4.11.

Synthesis of 8:

$AgSbF_6$ (0.171g, 0.5 mmol) was dissolved in DCM and added to the solution of **7** (0.310g, 0.5 mmol) in benzene. Immediately AgCl was precipitaed out. After overnight stirring, AgCl was separated out from the reaction mixture by filtration and reduced the volume to 10 mL and kept it at 0°C. Colorless block shaped crystals suitable for X-ray analysis was observed after one day. Yield: 0.330g (71%). Mp: 230°C (decomposed). ^{1}H NMR (400.31 MHz, $CDCl_3$): δ 0.76 (d, 12H, *J*= 6.9 Hz, CH(C*H*$_3$)$_2$), 0.96 (d, 12H, *J*= 6.9 Hz, CH(C*H*$_3$)$_2$), 2.16-2.23 (m, 4H, C*H*(CH$_3$)$_2$), 6.97 (m, 1H, Ph), 7.04 (m, 4H, *J*= 7.8 Hz Ph), 7.22-7.28 (m, 4H, Ph), 7.39 (t, 2H, *J*= 7.8 Hz, C_6H_6) ppm. ^{13}C NMR{^{1}H} (100.67 MHz, $CDCl_3$): δ 24.05, 24.25, 24.56, 28.63, 124.35, 125.08, 130.78, 133.95, 145.08, 184.36 ppm. MALDI: *m/z* $[C_{33}H_{40}N_2Au]^+$: 585.31 $[M\text{-}C_6H_6]^+$. Anal Calcd: C, 44.66; H, 4.96; N, 3.06. Found: C, 44.52; H, 4.51; N, 3.07.

Synthesis of 9: 30 mL toluene was added into 0.420 g of silylene [{PhC(N*t*Bu)$_2$}Si{N(SiMe$_3$)$_2$}] (1 mmol) in a 100 mL schlenk flask and $CoCp(CO)_2$ (0.133 mL, 1mmol) was added into the reaction mixture. After overnight stirring at room temperature, the reaction mixture was dried completely and 15 mL pentane was added into the reaction mixture and kept it at -30°C. Red colored crystals suitable for X-ray analysis was observed after two days. Yield: 0.390g (66%). Mp: 190°C. ^{1}H NMR (400.31 MHz, $CDCl_3$): δ 0.46 (*s*, 9H, Si*Me*$_3$), 0.76 (*s*, 9H, Si*Me*$_3$), 1.25 (*s*, 18H, C*Me*$_3$), 4.87 (*s*, 5H, *Cp*), 6.91-6.97 (*m*, 3H, Ph), 7.06 (*br*, 1H, Ph), 7.30 (*br*, 1H, Ph) ppm. ^{29}Si{^{1}H} NMR (79.495 MHz, $CDCl_3$, 298 K): δ 0.84 (*Si*Me$_3$), 4.90 (*Si*Me$_3$), 50.64 (*Si*N(SiMe$_3$)$_2$) ppm. MALDI: *m/z* $[C_{28}H_{49}N_3Si_3OCo]^+$: 587.20 $[M+H]^+$, 508.21 $[M\text{-}Cp+2H]^+$. IR ν_{CO} (solid): 1873 cm^{-1}. Anal Calcd: C, 57.30; H, 8.42; N, 7.16. Found: C, 57.38; H, 8.45; N, 7.21.

Synthesis of 10: 20 mL hexane was added into 0.646 g (1 mmol) of tris(2,4-di-tert-butylphenyl)phosphite in a 100 mL schlenk flask and $CoCp(CO)_2$ (0.133 mL, 1 mmol) was

added into the reaction mixture and was refluxed for 5 days. After filtration, kept the reaction mixture at -30°C. Red colored crystals suitable for X-ray analysis was observed after two days. Yield: 0.570g (70%). Mp: 174-176°C. ^{1}H NMR (400.31 MHz, $CDCl_3$): δ 1.30 (*s*, 36H, C*Me*$_3$), 1.53 (*s*, 36H, C*Me*$_3$), 4.64 (*s*, 5H, *Cp*), 7.05 (*d*, *J*= 8.6 Hz, 3H, Ph), 7.36 (*s*, 3H, Ph), 7.68 (*d*, *J*= 8.6 Hz, 3H, Ph) ppm. ^{31}P{^{1}H} NMR (161.976 MHz, CDCl3, 298K): δ 155.41 ppm. MALDI: *m/z* $[C_{49}H_{71}PO4Co]^+$: 834.12 $[M\text{-}2H]^+$, 755.18 $[M\text{-}Cp\text{-}H]^+$. IR ν_{CO} (solid): 1956 cm^{-1}. Anal Calcd: C, 72.30; H, 8.79. Found: C, 72.28; H, 8.81.

General procedure for the glycosylation:

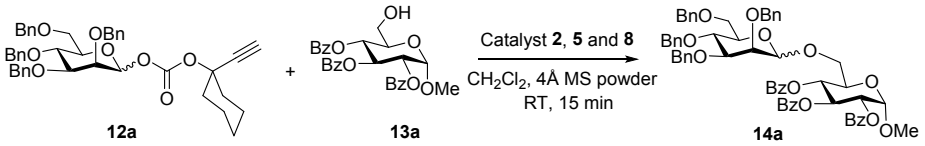

Silylene-Au complex (**2**) (0.014 g, 0.0145 mmol) was added to a solution of donor **12a** (0.100 g, 0.145 mmol) and acceptor **13a** (0.073 g, 0.145 mmol) in anhydrous CH_2Cl_2 (4mL) containing 4Å MS powder (0.200 g) and stirred at 25 ^{0}C for 15 min, concentrated *in vacuo*, and resulting residue was purified by column chromatography (*n*-hexane/EtOAc) to afford disaccharide **14a** (0.113 g, 75%) as a thick syrup.

Similar procedure was adopted for the synthesis of **14b, 14c, 14d, 14e, 14f, 18** and **20** in case of other Au-complexes (**5** and **8**) also.

Preparation of compound 19: To a solution of compound **18** (0.350 g, 0.241 mmol, 1 eq), methanol-CH_2Cl_2 (1:1) (4 mL), a 1 M solution of NaOMe in MeOH (1 mL), was added and stirred for 1 h. The NaOMe was quenched by Amberlite IR-120, filtered, and concentrated in vacuo and the resulting residue was purified by column chromatography (*n*-hexane/EtOAc) to afford trisaccharide di-ol **19** (0.275 g, 92%) as a thick syrup

Compound Characterization Data

Compound (**12a**): Mishra, B.; Neralkar, M.; Hotha, S. *Angew. Chem., Int. Ed.* **2016**, *55*, 7786-7791.

1-*O*-(((1-ethynylcyclohexyl)oxy)carbonyl)-2-*O*-benzoyl-3,4,6-tri-*O*-benzyl α/β-D-mannopyranoside [α:β (1.0:3.0)] (**12b**): Syrup; $[\alpha]^{25}_{D}$ ($CHCl_3$, *c* 1.0): +13.8; IR (cm^{-1}, $CHCl_3$): 3250, 2935, 1730, 1625, 1455, 1260, 1130, 1080, 915, 705; ^{1}H NMR (400.31 MHz, $CDCl_3$): δ

1.19 – 1.27 (m, 2H), 1.40 – 1.45 (m, 4H), 1.50 – 1.60 (m, 6H), 1.67 – 1.73 (m, 2H), 1.78 – 1.86 (m, 2H), 1.88 – 2.01 (m, 2H), 2.03 – 2.15 (m, 2H), 2.38 (s, 1H), 2.41 (s, 1H), 3.67 – 3.73 (m, 2H), 3.76 – 3.91 (m, 7H), 4.03 – 4.25 (m, 1H), 4.50 – 4.67 (m, 8H), 4.73 – 5.35 (m, 5H), 5.38 – 6.34 (m, 3H), 7.12 – 7.19 (m, 14H), 7.27 – 7.34 (m, 16H), 7.38 – 7.43 (m, 4H), 7.52 – 7.57 (m, 2H), 7.99 – 8.01 (m, 4H); $^{13}C\{^{1}H\}$ NMR (100.67 MHz, $CDCl_3$): δ 22.3, 22.4, 22.5, 22.5, 24.9, 25.0, 36.4, 36.7, 36.7, 36.8, 68.1, 68.2, 72.5, 72.7, 73.4, 73.6, 73.6, 75.0, 75.1, 75.2, 75.2, 75.3, 75.6, 76.4, 77.2, 77.4, 78.2, 78.4, 79.8, 79.8, 82.5, 82.5, 93.5, 95.5, 127.7 – 128.0 (12C), 128.1 (6C), 128.4 – 128.5 (16C), 129.5, 129.7, 130.0 (4C), 133.3 (2C), 137.6, 137.9 (2C), 138.0 (2C), 138.1, 151.0, 151.3, 165.1, 165.5; HRMS (ESI-MS): *m/z* $[C_{43}H_{44}O_9Na]^+$: 727.2874 $[M+Na]^+$.

Compound (**12c**): Mishra, B.; Neralkar, M.; Hotha, S. *Angew. Chem., Int. Ed.* **2016**, *55*, 7786-7791.

1-*O*-(((1-ethynylcyclohexyl)oxy)carbonyl)-2,3,5-tri-*O*-benzyl α-D-arabinoside (**12d**): Syrup; $[\alpha]^{25}_D$ ($CHCl_3$, *c* 1.0): +33.2; IR (cm^{-1}, $CHCl_3$): 3020, 1746, 1518, 1215, 1049, 740, 669; ^{1}H NMR (400.31 MHz, $CDCl_3$): δ 1.39 (m, 1H), 1.54 – 1.65 (m, 1H), 1.65 – 1.79 (m, 4H), 1.92 – 2.00 (m, 2H), 2.22 – 2.36 (m, 2H), 2.71 (s, 1H), 3.69 (d, J = 4.9 Hz, 2H), 4.08 (dd, J = 5.8, 2.0 Hz, 1H), 4.23 (d, J = 2.8 Hz, 1H), 4.47 (q, J = 5.0 Hz, 1H), 4.53 – 4.60 (m, 3H), 4.61 (d, J = 2.1 Hz, 2H), 4.70 (d, J = 11.9 Hz, 1H), 6.25 (s, 1H), 7.29 – 7.43 (m, 15H); $^{13}C\{^{1}H\}$ NMR (100.67 MHz, $CDCl_3$): δ 22.6, 22.6, 25.0, 36.7, 37.0, 69.4, 72.1, 72.1, 73.5, 75.2, 78.0, 82.9, 83.4, 83.4, 87.0, 103.2, 127.7, 127.8, 127.8, 127.8, 127.8, 127.8, 128.1, 128.1, 128.1, 128.4, 128.4, 128.4, 128.4, 128.5, 128.5, 137.2, 137.7, 138.0, 151.4; HRMS (ESI-MS): *m/z* $[C_{35}H_{38}O_7Na]^+$: 593.2518 $[M+Na]^+$.

Compound (**12e**): Sureshkumar, G.; Hotha, S. *Glycoconjugate. Journal,* **2012**, *29*, 221-230.
Compound (**12f**): Thadke, S. A.; Mishra, B.; Hotha, S. *Org. Lett.* **2013**, *15*, 2466-2469.
Compound (**13a**): Tiwari, V.; Badavath, V. N.; Singh, A. K.; Kandasamy, J. *Tetrahedron Lett.* **2018**, *59*, 2511–2514.

Methyl 2,3,4-tri-*O*-benzoyl-6-*O*-(2,3,4,6-tetra-*O*-benzyl α/β-D-mannopyranosyl) α-D-glucopyranoside [α:β (3.0:1.0)] (**14a**): Syrup; $[\alpha]^{25}_D$ ($CHCl_3$, *c* 1.0): +44.7; IR (cm^{-1}, $CHCl_3$): 3021, 2931, 1730, 1503, 1455, 1271, 1215, 1101, 919, 748, 699; ^{1}H NMR (400.31 MHz,

$CDCl_3$): δ 3.37 (s, 3H), 3.43 (s, 3H), 3.48 – 3.57 (m, 2H), 3.59 – 3.74 (m, 7H), 3.80 – 4.02 (m, 5H), 4.03 – 4.26 (m, 3H), 4.29 – 4.42 (m, 3H), 4.42 – 4.67 (m, 9H), 4.68 – 5.09 (m, 7H), 5.14 – 5.37 (m, 4H), 5.48 – 5.66 (m, 2H), 6.00 – 6.25 (m, 2H), 7.14 – 7.20 (m, 4H), 7.20 – 7.41 (m, 50H), 7.41 – 7.56 (m, 4H), 7.83 – 8.01 (m, 12H); $^{13}C\{^1H\}$ NMR (100.67 MHz, $CDCl_3$): δ 55.5, 55.6, 66.3, 68.2, 68.7, 69.0, 69.1, 69.5, 69.6, 69.9, 70.7, 70.7, 71.5, 72.1, 72.2, 72.2, 72.3, 72.7, 73.3, 73.5, 74.0, 74.2, 74.8, 74.9, 74.9, 75.1, 75.2, 76.1, 80.0, 82.2, 97.0, 97.1, 98.3, 102.4, 127.5 – 128.2 (24C), 128.3 – 128.5 (28C), 129.0, 129.2, 129.2, 129.2, 129.4, 129.4, 129.8 – 130.0 (12C), 133.2, 133.2, 133.4, 133.5, 133.5, 133.6, 138.3, 138.4, 138.5, 138.5, 138.6, 138.7, 138.8, 139.0, 165.2, 165.2, 165.5, 165.9, 165.9, 166.0; HRMS (ESI-MS): *m/z* $[C_{62}H_{60}O_{14}Na]^+$: 1051.3875 $[M+Na]^+$.

Methyl 2,3,4-tri-*O*-benzoyl-6-*O*-(2-*O*-benzoyl-3,4,6-tri-*O*-benzyl α-D-mannopyranosyl) α-D-glucopyranoside (**14b**): Mp: 64°C; $[\alpha]^{25}_D$ ($CHCl_3$, *c* 1.0): +42.3; IR (cm^{-1}, $CHCl_3$): 3021, 1727, 1453, 1267, 1103, 1099, 1028, 745, 669; ^1H NMR (400.31 MHz, $CDCl_3$): δ 3.45 (s, 3H), 3.67 (dd, J = 11.0, 2.8 Hz, 1H), 3.74 (dd, J = 10.8, 2.9 Hz, 1H), 3.83 (dd, J = 10.8, 3.7 Hz, 1H), 3.87 (d, J = 8.7 Hz, 1H), 4.01 (dd, J = 11.0, 5.3 Hz, 1H), 4.09 – 4.19 (m, 2H), 4.31 (ddd, J = 9.8, 4.9, 3.0 Hz, 1H), 4.48 (d, J = 12.0 Hz, 1H), 4.56 (dd, J = 15.4, 11.2 Hz, 2H), 4.70 (d, J = 12.0 Hz, 1H), 4.75 (d, J = 11.4 Hz, 1H), 4.94 (d, J = 10.9 Hz, 1H), 5.07 (d, J = 1.4 Hz, 1H), 5.28 (d, J = 3.6 Hz, 1H), 5.37 (dd, J = 10.2, 3.6 Hz, 1H), 5.57 – 5.72 (m, 2H), 6.23 (t, J = 9.9 Hz, 1H), 7.22 – 7.43 (m, 23H), 7.43 – 7.59 (m, 4H), 7.94 (m, 2H), 7.99 – 8.07 (m, 4H), 8.12 (m, 2H); $^{13}C\{^1H\}$ NMR (100.67 MHz, $CDCl_3$): δ 55.7, 66.5, 68.3, 69.0, 69.1, 69.8, 70.7, 71.7, 71.9, 72.3, 73.5, 74.3, 75.3, 78.1, 97.1, 98.1, 127.6, 127.6, 127.6, 127.7, 127.7, 128.1, 128.1, 128.3, 128.3, 128.4, 128.4, 128.4, 128.4, 128.4, 128.4, 128.5, 128.5, 128.5, 128.5, 128.6, 128.6, 128.6, 128.6, 129.1, 129.2, 129.4, 129.8, 129.8, 129.8, 130.0, 130.1, 130.1, 130.1, 130.1, 130.1, 133.3, 133.3, 133.5, 133.5, 138.2, 138.6, 138.7, 165.4, 165.7, 166.0, 166.0; HRMS (ESI-MS): *m/z* $[C_{62}H_{58}O_{15}Na]^+$: 1065.3690 $[M+Na]^+$.

Methyl 2,3,4-tri-*O*-benzoyl-6-*O*-(2,3,4,6-tetra-*O*-benzoyl α-D-mannopyranosyl) α-D-glucopyranoside (**14c**): Mp: 72°C; $[\alpha]^{25}_D$ ($CHCl_3$, *c* 1.0): +2.9; IR (cm^{-1}, $CHCl_3$): 3045, 2910, 1720, 1625, 1228, 1035, 970; ^1H NMR (400.31 MHz, $CDCl_3$): δ 3.61 (s, 3H), 3.78 (d, *J* = 10.7 Hz, 1H), 4.09 (dd, *J* = 10.7, 6.1 Hz, 1H), 4.34 – 4.40 (m, 2H), 4.51 – 4.55 (m, 1H), 4.62 (dd, *J* = 11.9,1.7 Hz, 1H), 5.15 (s, 1H), 5.26 (dd, *J* = 10.2, 3.7 Hz, 1H), 5.33 (d, *J* = 3.6 Hz, 1H), 5.58 (td, *J* = 9.9, 1.6 Hz, 1H), 5.76 (dd, *J* = 3.1, 1.7 Hz, 1H), 5.98 (dd, *J* = 10.1, 3.2 Hz, 1H), 6.08 (t, *J* =

10.1 Hz, 1H), 6.21 (t, *J* = 9.9 Hz, 1H), 7.26 – 7.31 (m, 3H), 7.34 (m, 3H), 7.39 – 7.43 (m, 6H), 7.45 – 7.49 (m, 5H), 7.52 – 7.55 (m, 2H), 7.58 – 7.63 (m, 2H), 7.84 – 7.87 (m, 2H), 7.92 – 7.94 (m, 2H), 7.97 – 8.04 (m, 6H), 8.06 – 8.11 (m, 4H); $^{13}C\{^{1}H\}$ NMR (100.67 MHz, $CDCl_3$): δ 55.8, 62.9, 66.6, 67.1, 68.5, 69.1, 69.6, 70.2, 70.5, 70.7, 72.3, 97.1, 97.6, 128.4 (4C), 128.5 (2C), 128.6 (6C), 128.7(2C), 128.9, 129.2, 129.3 (3C), 129.4, 129.5, 129.9 (6C), 130.0 (6C), 130.1 (2C), 133.1, 133.2, 133.2, 133.4, 133.5, 133.6, 133.6, 165.5, 165.5, 165.5, 165.7, 165.9, 165.9, 166.2; HRMS (ESI-MS): *m/z* $[C_{62}H_{52}O_{18}Na]^+$: 1107.3046 $[M+Na]^+$.

Methyl 2,3,4-tri-*O*-benzoyl-6-*O*-(2,3,5-tri-*O*-benzyl α/β-D-arabinofuranosyl) α-D-glucopyranoside [α:β (1.4:1.0)] (**14d**): $[\alpha]^{25}_D$ ($CHCl_3$, *c* 0.5): +74.8; IR (cm^{-1}, $CHCl_3$): 2920, 1724, 1452, 1258, 1102, 1024, 801, 704; ^{1}H NMR (400.31 MHz, $CDCl_3$): δ 3.36 (s, 3H), 3.44 (s, 3H), 3.50 – 3.52 (m, 4H), 3.61 (dd, *J* = 11.6, 5.8 Hz, 1H), 3.66 (dd, *J* = 11.1, 3.1 Hz, 1H), 3.85 – 3.99 (m, 3H), 3.99 – 4.12 (m, 4H), 4.18 – 4.23 (m, 3H), 4.41 – 4.51 (m, 7H), 4.52 – 4.61 (m, 3H), 4.65 (d, *J* = 11.8 Hz, 1H), 4.82 (d, *J* = 11.7 Hz, 1H), 5.05 – 5.07 (m, 2H), 5.18 – 5.27 (m, 4H), 5.54 (dd, *J* = 10.2, 9.4 Hz, 1H), 5.63 (t, *J* = 9.8 Hz, 1H), 6.12 (td, *J* = 9.6, 1.0 Hz, 2H), 7.24 – 7.54 (m, 48H), 7.80 – 8.02 (m, 12H); $^{13}C\{^{1}H\}$ NMR (100.67 MHz, $CDCl_3$): δ 55.5, 55.6, 65.6, 66.0, 68.5, 69.0, 69.2, 69.5, 69.6, 70.6, 70.7, 72.0, 72.0, 72.1, 72.1, 72.2, 72.3, 72.4, 73.3, 73.3, 80.4, 80.5, 83.2, 83.3, 84.2, 88.4, 96.8, 96.9, 101.3, 106.1, 127.5 – 127.9 (15C), 128.2 – 128.3 (15C), 128.4 (12C), 129.0, 129.1 (2C), 129.3 (2C), 129.4, 129.7 (4C), 129.8 (2C), 129.9 (6C), 133.0, 133.0, 133.2, 133.3, 133.3, 133.4, 137.6, 138.0, 138.0, 138.1, 138.1, 138.2, 165.1, 165.3, 165.8, 165.8, 165.8, 165.9; HRMS (ESI-MS): *m/z* $[C_{54}H_{52}O_{13}Na]^+$: 947.3989 $[M+Na]^+$.

Methyl 2,3,4-tri-*O*-benzoyl-6-*O*-(2-*O*-benzoyl-3,4,6-tri-*O*-benzyl α-D-mannopyranosyl) α-D-glucopyranoside (**14e**): See (**14b**).

Methyl 2,3,4-tri-*O*-benzoyl-6-*O*-(2-*O*-benzoyl-3,5-tri-*O*-benzyl β-D-ribofuranosyl) α-D-glucopyranoside (**14f**): Mp: 92°C; $[\alpha]^{25}_D$ ($CHCl_3$, *c* 1.0): +56.4; IR (cm^{-1}, $CHCl_3$): 3020, 1729, 1514, 1272, 1215, 1105, 742, 669; ^{1}H NMR (400.31 MHz, $CDCl_3$): δ 3.33 (s, 3H), 3.44 (dd, J = 10.4, 6.1 Hz, 1H), 3.51 – 3.65 (m, 2H), 3.85 (d, J = 11.3 Hz, 1H), 4.07 – 4.16 (m, 2H), 4.19 – 4.25 (m, 1H), 4.27 (d, J = 11.5 Hz, 1H), 4.40 – 4.41(m, 2H), 4.48 (d, J = 11.4 Hz, 1H), 5.07 – 5.15 (m, 2H), 5.14 – 5.22 (m, 1H), 5.37 – 5.50 (m, 2H), 6.05 (t, J = 9.8 Hz, 1H), 7.05 – 7.46 (m, 22H), 7.76 – 7.80 (m, 2H), 7.81 – 7.85 (m, 2H), 7.87 – 7.91 (m, 2H), 7.95 – 7.99 (m, 2H); $^{13}C\{^{1}H\}$ NMR (100.67 MHz, $CDCl_3$): δ 55.6, 66.6, 68.9, 69.8, 70.6, 71.2, 72.2, 73.0, 73.3, 74.3, 78.0, 80.8, 96.9, 105.9, 127.6, 127.7, 127.7, 127.8, 128.0, 128.0, 128.3, 128.3, 128.3, 128.3,

128.4, 128.4, 128.4, 128.4, 128.5, 128.5, 128.5, 128.5, 129.1, 129.1, 129.3, 129.7, 129.7, 129.7, 129.9, 129.9, 129.9, 129.9, 130.0, 130.0, 133.1, 133.3, 133.4, 133.4, 137.6, 138.2, 165.3, 165.5, 165.9, 165.9; HRMS (ESI-MS): *m/z* $[C_{54}H_{50}O_{14}Na]^+$: 945.3099 $[M+Na]^+$.

Methyl 2,4-di-*O*-benzyl-α-D-mannopyranoside (**17**): Syrup; $[\alpha]^{25}_D$ ($CHCl_3$, *c* 0.5): +14.0; IR (cm^{-1}, $CHCl_3$): 3568, 3017, 2925, 910, 738, 564; ^1H NMR (400.31 MHz, $CDCl_3$): δ 2.48 (s, 2H), 3.30 (s, 3H), 3.58 (ddd, *J* = 9.8, 4.4, 2.8 Hz, 1H), 3.68 (t, *J* = 9.5 Hz, 1H), 3.71 (dd, *J* = 3.7, 1.6 Hz, 1H), 3.77 (dd, *J* = 11.9, 4.4 Hz, 1H), 3.84 (dd, *J* = 11.8, 2.9 Hz, 1H), 3.98 (dd, *J* = 9.2, 3.7 Hz, 1H), 4.59 (d, *J* = 11.8 Hz, 1H), 4.65 (d, *J* = 11.1 Hz, 1H), 4.70 (d, *J* = 11.8 Hz, 1H), 4.73 (d, *J* = 1.6 Hz, 1H), 4.88 (d, *J* = 11.2 Hz, 1H), 7.29 – 7.36 (m, 10H); $^{13}C\{^1H\}$ NMR (100.67 MHz, $CDCl_3$): δ 54.9, 62.3, 71.3, 71.8, 73.2, 74.9, 76.4, 78.4, 98.3, 127.9, 128.0, 128.0, 128.1, 128.1, 128.2, 128.5, 128.5, 128.7, 128.7, 137.7, 138.4; HRMS (ESI-MS): *m/z* $[C_{21}H_{26}O_6Na]^+$: 397.1635 $[M+Na]^+$.

Methyl 2,4-di-*O*-benzyl-3,6-di-*O*-(2-*O*-benzoyl-3,4,6-tri-*O*-benzyl-α-D-mannopyranosyl)-α-D-mannopyranoside (**18**): syrup; $[\alpha]^{25}_D$ ($CHCl_3$, *c* 0.5): +12.4; IR (cm^{-1}, $CHCl_3$): 3265, 3025, 2955, 1725, 917, 730, 571; ^1H NMR (400.31 MHz, $CDCl_3$): δ 3.22 (s, 3H), 3.65 – 3.71 (m, 3H), 3.73 – 3.85 (m, 5H), 3.87 – 3.96 (m, 2H), 4.02 – 4.10 (m, 4H), 4.13 – 4.19 (m, 2H), 4.47 (s, 1H), 4.49 – 4.50 (m, 3H), 4.51 – 4.56 (m, 3H), 4.65 – 4.68 (m, 4H), 4.71 – 4.76 (m, 3H), 4.80 (d, *J* = 11.0 Hz, 1H), 4.87 – 4.92 (m, 2H), 5.10 (d, *J* = 1.8 Hz, 1H), 5.33 (d, *J* = 1.7 Hz, 1H), 5.73 (t, *J* = 2.9 Hz, 1H), 5.77 (t, *J* = 2.6 Hz, 1H), 7.16 – 7.40 (m, 44H), 7.52 – 7.56 (m, 2H), 8.02 – 8.04 (m, 2H), 8.07 – 8.09 (m, 2H); $^{13}C\{^1H\}$ NMR (101.67 MHz, $CDCl_3$): δ 54.9, 66.6, 68.8, 68.8, 69.1, 69.2, 69.5, 71.1, 71.2, 71.7, 71.9, 72.5, 72.5, 73.5, 73.6, 74.3, 74.5, 75.1, 75.1, 75.3, 77.6, 77.6, 78.3, 78.7, 98.3, 98.3, 99.8, 127.5, 127.6 (5C), 127.7 (2C), 127.8 (4C), 127.9 (4C), 128.0 (4C), 128.1 (4C), 128.3 (2C), 128.4 (10C), 128.5 (6C), 128.6 (2C), 130.0, 130.1 (5C), 133.2, 133.2, 138.0, 138.0, 138.0, 138.3, 138.6, 138.6, 138.7, 138.8, 165.6, 165.6; HRMS (ESI-MS): *m/z* $[C_{89}H_{90}O_{18}Na]^+$: 1469.6021 $[M+Na]^+$.

Methyl 2,4-di-*O*-benzyl-3,6-di-*O*-(3,4,6-tri-*O*-benzyl-α-D-mannopyranosyl)-α-D-mannopyranoside (**19**): syrup; $[\alpha]^{25}_D$ ($CHCl_3$, *c* 1.0): +46.1; IR (cm^{-1}, $CHCl_3$): 3554, 3275, 3037, 2963, 925, 716, 552; ^1H NMR (400.31 MHz, $CDCl_3$): δ 2.37 (s, 2H), 3.23 (s, 3H), 3.58 – 3.73 (m, 6H), 3.75 – 3.93 (m, 8H), 3.93 – 4.03 (m, 2H), 4.08 – 4.14 (m, 2H), 4.44 – 4.57 (m, 7H),

4.57 – 4.62 (m, 5H), 4.62 – 4.70 (m, 3H), 4.83 (t, J = 10.7 Hz, 2H), 5.07 (d, J = 1.8 Hz, 1H), 5.21 (d, J = 1.7 Hz, 1H), 7.12 – 7.34 (m, 40H); $^{13}C\{^{1}H\}$ NMR (101.67 MHz, $CDCl_3$): δ 54.9, 66.2, 68.2, 68.8, 68.9, 69.5, 71.3, 71.6, 71.6, 72.1, 72.2, 72.4, 73.5, 73.7, 74.4, 74.6, 75.0, 75.1, 75.1, 75.2, 77.9, 79.1, 79.7, 80.2, 98.3, 99.8, 101.6, 127.6, 127.7 (8C), 127.8 (2C), 127.9 (5C), 128.0 (6C), 128.1 (2C), 128.4 (8C), 128.5 (2C), 128.6 (6C), 138.0, 138.0, 138.2, 138.4, 138.4, 138.4, 138.6, 138.7; HRMS (ESI-MS): *m/z* $[C_{75}H_{82}O_{16}Na]^+$: 1261.5495 $[M+Na]^+$.

Methyl 2,4-di-*O*-benzyl-3,6-di-*O*-(2-*O*-(2,3,4,6-tetra-*O*-benzoyl α-Dmannopyranosyl) -3,4,6-tri-O-benzyl α-D-mannopyranosyl)-α-D-mannopyranoside (**20**): syrup; $[\alpha]^{25}_D$ ($CHCl_3$, *c* 0.5): +8.4; IR (cm^{-1}, $CHCl_3$): 3272, 3045, 2964, 1720, 1130, 945, 730, 583; ^{1}H NMR (400.31 MHz, $CDCl_3$): δ 3.25 (s, 3H), 3.55 – 3.75 (m, 6H), 3.78 – 3.86 (m, 2H), 3.86 – 3.95 (m, 3H), 3.99 – 4.04 (m, 5H), 4.11 – 4.18 (m, 2H), 4.29 (dt, J = 12.4, 2.5 Hz, 1H), 4.36 – 4.46 (m, 3H), 4.47 – 4.60 (m, 9H), 4.61 – 4.63 (m, 3H), 4.65 – 4.68 (m, 3H), 4.70 – 4.75 (m, 1H), 4.80 (s, 1H), 4.92 (t, J = 10.5 Hz, 2H), 5.04 (d, J = 2.5 Hz, 1H), 5.13 (d, J = 2.5 Hz, 1H), 5.21 (d, J = 2.5 Hz, 1H), 5.34 (d, J = 2.5 Hz, 1H), 5.86 (d, J = 2.8 Hz, 1H), 5.89 – 5.98 (m, 3H), 6.13 (td, J = 10.1, 2.0 Hz, 1H), 6.19 (td, J = 10.1, 2.0 Hz, 1H), 6.88 – 7.06 (m, 5H), 7.06 – 7.23 (m, 15H), 7.28 – 7.33 (m, 26H), 7.35 – 7.46 (m, 14H), 7.51 – 7.64 (m, 4H), 7.83 – 7.91 (m, 8H), 8.04 – 8.06 (m, 4H), 8.12 – 8.14 (m, 4H); $^{13}C\{^{1}H\}$ NMR (101.67 MHz, $CDCl_3$): δ 54.9, 62.7, 62.7, 66.4, 66.7, 66.9, 69.2, 69.2, 69.4, 69.6, 70.3, 70.3, 70.5, 70.6, 71.7, 71.9, 71.9, 72.2, 72.6, 72.7, 73.2, 73.4, 74.7, 74.8, 74.9, 74.9, 75.1, 75.4, 77.1, 77.4, 77.9, 78.7, 79.4, 79.7, 98.3, 99.5, 99.5, 99.8, 101.1, 127.1 (2C), 127.4 (2C), 127.5 – 127.7 (14C), 127.9 (2C), 128.0 (4C), 128.3 (4C), 128.4 (12C), 128.5 (12C), 128.7 (4C), 129.1, 129.2, 129.4, 129.5, 129.7, 129.7, 129.9 – 130.0 (16C), 130.1, 130.2, 133.0, 133.1, 133.1, 133.1, 133.4, 133.4, 133.4, 133.4, 138.2, 138.3, 138.3, 138.3, 138.5, 138.5, 138.7, 138.8, 165.2, 165.2, 165.4, 165.5, 165.5, 165.6, 166.2, 166.3; HRMS (ESI-MS): *m/z* $[C_{143}H_{134}O_{34}Na]^+$: 2418.8691 $[M+Na]^+$.

Table S1.1 Attempts of disaccharide synthesis using carbonate donors with different catalysts.[a]

Entry	Catalyst	Mol %	Yield (%)
1	**1**	10	-
2	TfOH	10	10
3	$AgSbF_6$	10	-
4	$[Et_3O]+ [SbCl_6]-$	10	20
5	$PPh_3AuCl/AgSbF_6$	10	75
6	**1**/$AgSbF_6$ (*in situ*) (DCM)	10	42
7	**1**/$AgSbF_6$ (*in situ*) (DCM+benzene)	10	55
8	$[IPr_2Au]^+[SbF_6]^-$	10	-

[a]Reagents and conditions: **12c** (1 equiv.), **13a** (1 equiv.), Catalyst, DCM, room temperature,12 h

Table S1.2 Attempts of disaccharide synthesis using orthoester donors with different catalysts.[b]

Entry	Catalyst	Mol %	Yield (%)
1	$AgSbF_6$	10	30% (**14f**), 10% (**16**)
2	$PPh_3AuCl/AgSbF_6$	10	65% (**14f**), 30% (**16**)
3	$AuBr_3$	10	55% (**14f**), 15% (**16**)
4	**1**/$AgSbF_6$ *(in situ)* (DCM)	10	76% (**14f**), 20% (**16**)
5	**1**/$AgSbF_6$ *(in situ)* (DCM+benzene)	10	90% (**14f**), 2% (**16**)
6	$[IPr_2Au]^+[SbF_6]^-$	10	-

[b]Reagents and conditions: **12f** (1 equiv.), **13a** (1 equiv.),Catalyst, DCM, room temperature,12 h.

S2. Molecular Structure:

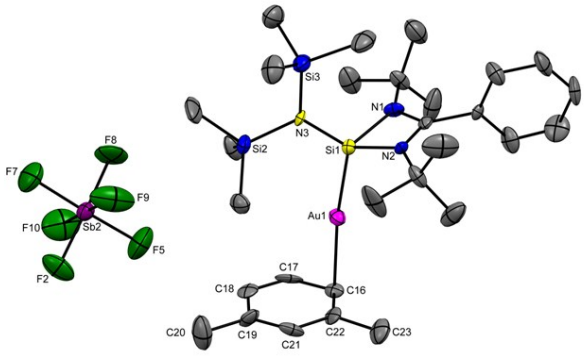

Figure S1. The molecular structure of **3** (ellipsoid are shown at the probability level of 50%). Hydrogen atoms are omitted for clarity.

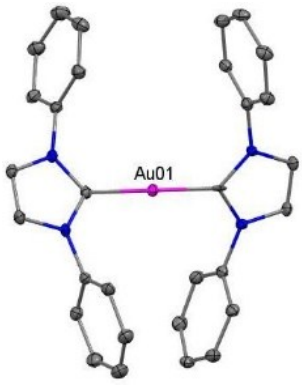

Figure S2. The molecular structure of the deactivated catalyst of **8** (ellipsoids are shown at the probability level of 30%). Hydrogen atoms, *i*Pr groups and SbF_6 anion are omitted for clarity.

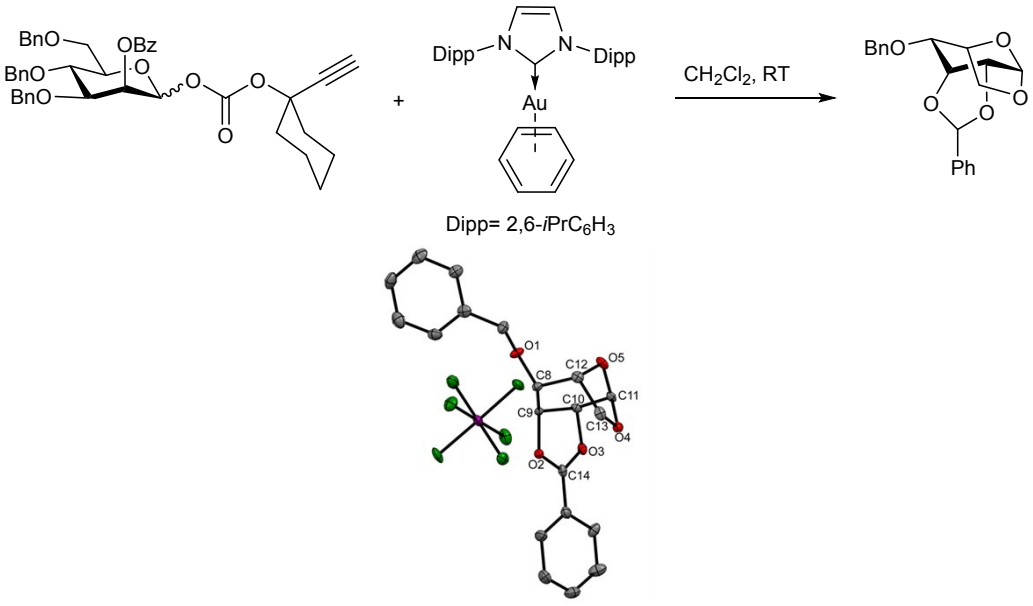

Figure S3. The molecular structure of the product obtained from the stoichiometric reaction of alkyne and catalyst **8** (ellipsoid are shown at the probability level of 50%). Hydrogen atoms are omitted for clarity.

S3. Crystal Data and Structure Refinements for 2, 3, 4, 8, 9 and 10.

X-ray Crystallography Details: Single crystals of suitable size, coated with paraffin oil was mounted for all the complexes. Crystal data for all the complexes were collected on a Bruker Smart Apex Duo diffractometer at 100 K using Mo Kα radiation (λ = 0.71073 Å). Collected data were integrated by using SAINT and then absorption correction was done by multi-scan method using SADABS program. All the structures were solved by direct methods and refined by full-matrix least-squares methods against F^2 (SHELXL-2014/6). Crystallographic Information File (CIF) for the structures has been deposited to the Cambridge Crystallographic Data Centre as supplementary publication nos. 1819357 (**2**), 1819358 (**3**), 1990445 (**4**), 1954430 (**8**), 1990448 (**9**), 1990449 (**10**). These CIF can be obtained free of charge from The Cambridge Crystallographic Data Centre via www.ccdc.cam.ac.uk/data_request/cif.

Table S2. Crystal Data and Structure Refinement for 2, 3, 4, 8, 9 and 10.

	2	**3**	**4**
Chemical formula	$C_{27}H_{47}AuF_6N_3SbSi_3$	$C_{29}H_{51}AuF_6N_3SbSi_3$	$C_{21}H_{39}AuClGeN_3Si_2$
Formula weight	930.66	958.71	694.74
Temperature	100(2)	100(2)	100(2)
Wavelength	0.71073	0.71073	0.71073
Crystal system	monoclinic	monoclinic	monoclinic
Space group	$P2_1/n$	$P2_1/c$	$P2_1/c$
Unit cell dimentions	a=11.831(7) Å	a=22.214(7) Å	a=8.9235(5)Å
	b=21.434(14) Å	b=18.276(6) Å	b=18.5223(13)Å
	c=14.563(10) Å	c=18.686(6) Å	c=17.8450(12) Å
	α= 90°	α=90°	α= 90°
	β= 98.575(18)°	β=93.012(7)°	β= 101.332(2)°
	γ=90°	γ=90°	γ=90°
Volume	3652(4) Å^3	7576(4) Å^3	2892.0(3)Å^3
Z	4	8	4
Density (calculated)	1.693 g/cm^3	1.681 g/cm^3	1.596 g/cm^3

Absorption coefficient	4.903 mm^{-1}	4.729 mm^{-1}	6.294 mm^{-1}
F(000)	1824	3776	1368
Theta range for data collection	2.28 to 25.25°	2.23 to 25.16°	2.20 to 25.25°
Index ranges	-14<=*h*<=14 -25<=*k*<=25 -17<=*l*<=17	-26<=*h*<=26 -21<=*k*<=21 -22<=*l*<=22	-10<=*h*<=10 -22<=*k*<=22 -21<=*l*<=21
Reflections collected	87805	104634	81573
Independent reflections	6620 [R(int)= 0.1276]	13512 [R(int)= 0.2456]	5233 [R(int)= 0.0618]
Coverage of independent reflections	99.9%	99.4%	100%
Function minimized	$\Sigma\, w(Fo^2 - Fc^2)^2$	$\Sigma\, w(Fo^2 - Fc^2)^2$	$\Sigma\, w(Fo^2 - Fc^2)^2$
Data/ restraints/ parameters	6620/ 0/ 382	13512/ 108/ 849	5233/ 0/ 274
Goodness-of-fit on F2	1.015	1.078	1.119
Δ/ σ max	0.001	0.001	0.002
Final R indices	4974 data; [$I>2\sigma(I)$] *R1*= 0.0363, *wR2*= 0.0622	7556 data; [$I>2\sigma(I)$] *R1*= 0.0800, *wR2*= 0.1492	4144 data; [$I>2\sigma(I)$] *R1*= 0.0280, *wR2*= 0.0597
	all data, *R1*= 0.0649, *wR2*= 0.0708	all data, *R1*= 0.1724, *wR2*= 0.1766	all data, *R1*= 0.0457, *wR2*= 0.0668
Largest diff. peak and hole	0.946 and -0.912 $eÅ^{-3}$	2.265 and -1.323 $eÅ^{-3}$	0.501 and -0.787 $eÅ^{-3}$
R. M. S deviation from mean	0.132 $eÅ^{-3}$	0.252 $eÅ^{-3}$	0.145 $eÅ^{-3}$

	8	**9**	**10**
Chemical formula	$C_{33}H_{42}AuF_6N_2Sb$	$C_{27}H_{46}CoN_3OSi_3$	$C_{55}H_{75}CoO_4P$
Formula weight	899.40	571.87	890.05

Temperature	100(2)	100(2)	100(2)
Wavelength	0.71073	0.71073	0.71073
Crystal system	monoclinic	triclinic	triclinic
Space group	$P2_1/c$	*P-1*	*P-1*
Unit cell dimentions	a=13.4432(9) Å	a= 9.741(9) Å	a=12.132(3) Å
	b=14.6762(9) Å	b=17.157(15) Å	b=13.703(5) Å
	c=17.3789(8) Å	c=18.969(15)Å	c=17.467(6) Å
	α= 90°	α=102.473(13)°	α=112.033(7)°
	β= 100.2060(10)°	β=91.56(2)°	β=104.987(7)°
	γ=90°	γ=91.73(2)°	γ=92.737(8)°
Volume	3374.5(3) Å^3	3092(5) Å^3	2565.8(14) Å^3
Z	4	4	2
Density (calculated)	1.770 g/cm^3	1.228 g/cm^3	1.152 g/cm^3
Absorption coefficient	5.201 mm^{-1}	0.695 mm^{-1}	0.408 mm^{-1}
F(000)	1752	1224	958
Theta range for data collection	2.25 to 25.25°	2.20 to 25.25	2.19 to 25.25
Index ranges	-16<=h<=16 -17<=k<=17 -20<=l<=20	-11<=h<=11 -20<=k<=20 -22<=l<=22	-12<=h<=13 -16<=k<=16 -20<=l<=20
Reflections collected	108354	85325	19606
Independent reflections	6111 [R(int)= 0.0432]	11186 [R(int)= 0.1194]	8546 [R(int)= 0.1786]
Coverage of independent reflections	99.9%	99.8%	91.9%
Function minimized	$\Sigma\, w(Fo^2 - Fc^2)^2$	$\Sigma\, w(Fo^2 - Fc^2)^2$	$\Sigma\, w(Fo^2 - Fc^2)^2$
Data/ restraints/ parameters	6111/ 0/ 396	11186/0/655	8546/0/552
Goodness-of-fit on F2	1.037	1.696	1.050
Δ/ σ max	0.002	0.042	0.000

Final R indices	5485 data; [*I>2σ(I)*] *R1*= 0.0201, *wR2*= 0.0401	8239 data; [*I>2σ(I)*] *R1*= 0.1474, *wR2*= 0.3961	3619 data; [*I>2σ(I)*] *R1*= 0.1149, *wR2*= 0.2600
	all data, *R1*= 0.0251, *wR2*= 0.0420	all data, *R1*= 0.1738, *wR2*= 0.4128	all data, *R1*= 0.2596, *wR2*= 0.3260
Largest diff. peak and hole	2.132 and -1.629 eÅ^{-3}	7.657 and -1.648 eÅ^{-3}	0.618 and -0.793 eÅ^{-3}
R. M. S deviation from mean	0.082 eÅ^{-3}	0.257 eÅ^{-3}	0.112 eÅ^{-3}

S4. Deduction of hapticities in 2, 3 and 8

The assignment of hapticity number for the complexes having low hapticities (η^1-η^3), has always been a complicated task as the difference between M-C bond distances is very less. Therefore, we used a method proposed by Alvarez and co-workers to deduce the hapticity of the metal-arene complexes given in *Organometallics,* 2014, **33**, 6660-6668.

Table S3. Deduction of hapticities in 2, 3 and 8

Complex	**M-C[a] (d_1, d_2, d_3)**	**Distance ratio ρ_1**	**Distance ratio ρ_2**	**η**
2	2.37, 2.60, 2.77	1.09	1.16	1
3	2.31, 2.73, 2.78	1.18	1.20	1
8	2.29, 2.34, 2.88	1.02	1.25	2

[a] M (=Au), $d_1<d_2<d_3$, [b]$\rho 1 = d_2/d_1$, [c]$\rho 2 = d_3/d_1$, if $\rho_1 \approx \rho_2 \gg 1$ then η^1 , if $\rho_2 > \rho_1 \approx 1$ then η^2, and if $\rho_1 \approx \rho_2 \approx 1$ then η^3

S5. Computational Details.

Computational Methodology

Geometry optimizations were performed using GGA DFT functional BP86[1] with def2-SVP2[2] basis set using Gaussian 09[3] software. Single point calculations were carried out using meta-GGA functional M06[4] with def2-TZVPP[2] level of theory on the optimized geometries.

Solvent effects were incorporated in single point calculations using PCM model[5] by incorporating dichloromethane solvent (DCM). ΔE and $\Delta E^{\#}$ represent reaction enthalpy and enthalpy of activation respectively calculated by adding electronic energy at the M06/PCM/def2-TZVPP level of theory and zero point energy at the BP86/def2-SVP level of theory. ΔG and $\Delta G^{\#}$ represent the Gibbs free energy of reaction and Gibbs free energy of activation respectively, calculated by adding electronic energy at the M06/PCM/def2-TZVPP level of theory and the thermal correction to Gibbs free energy at 298.15 K and 1 atm at the BP86/def2-SVP level of theory. The population analysis was performed by natural bond orbital (NBO)[6] method at M06/PCM/def2-TZVPP//BP86/def2-SVP level of theory.

The model compound **A** for alkynyl glycosyl carbonate (glycosyl donor) was constructed by avoiding all –OR substitution on the carbohydrate ring with hydrogen, except at the nearest C atom of the anomeric carbon. At the nearest C of the anomeric carbon –O-CO-CH_3 group is retained to understand the anchimeric assistance of the protecting group on the oxocarbenium ion. Also cyclohexyl group in the leaving group is replaced by two methyl groups.

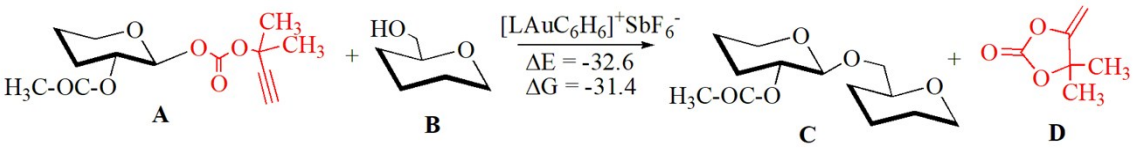

Scheme S1. Overall glycosidation reaction at the M06/PCM/def2-TZVPP//BP86/def2-SVP level of theory. ΔE and ΔG (in kcal/mol) represent reaction enthalpy and Gibbs free energy of reaction respectively at the M06/PCM/def2-TZVPP//BP86/def2-SVP level of theory.

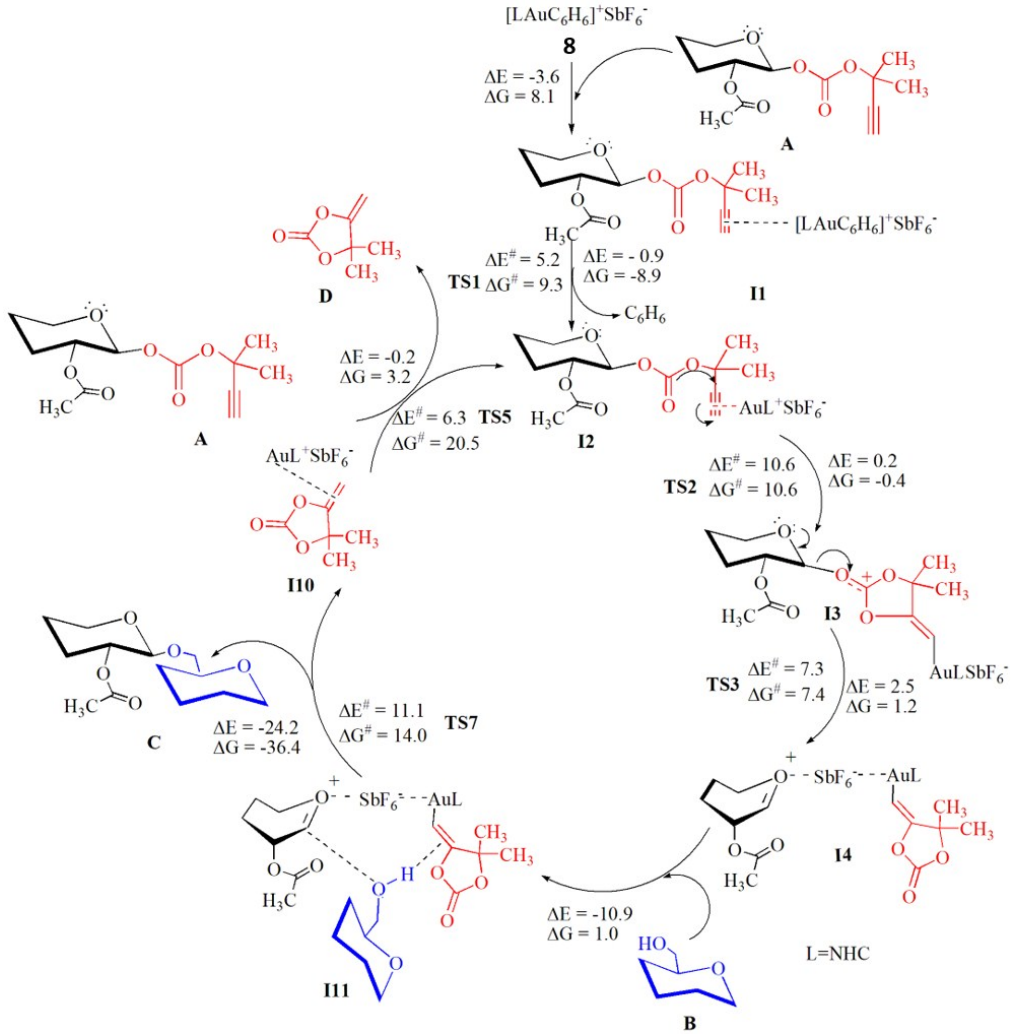

Scheme S2. Mechanism for glycosidation reaction by remote activation using **8** through intermediate **I11**. Energies are given in kcal/mol. ΔE and $\Delta E^{\#}$ (in kcal/mol) represent reaction enthalpy and enthalpy of activation respectively at the M06/PCM/def2-TZVPP//BP86/def2-SVP level of theory. ΔG and $\Delta G^{\#}$ (in kcal/mol) represent the Gibbs free energy of reaction and Gibbs free energy of activation respectively, at same level of theory at 298.15 K and 1 atm.

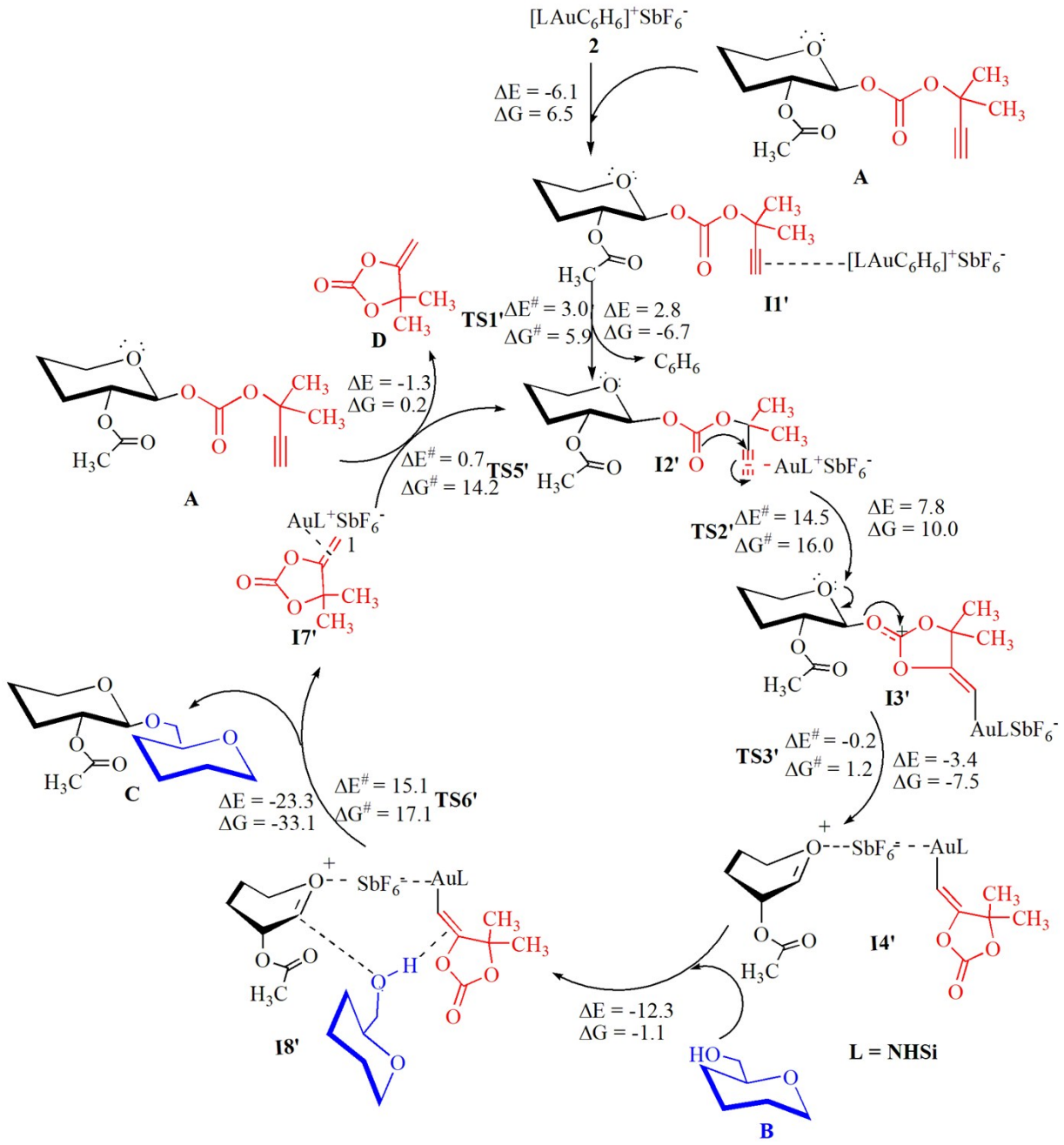

Scheme S3. Mechanism for glycosidation reaction by remote activation using **2** through intermediate **I8′**. Energies are given in kcal/mol. ΔE and $\Delta E^{\#}$ (in kcal/mol) represent reaction enthalpy and enthalpy of activation respectively at the M06/PCM/def2-TZVPP//BP86/def2-SVP level of theory. ΔG and $\Delta G^{\#}$ (in kcal/mol) represent the Gibbs free energy of reaction and Gibbs free energy of activation respectively, at same level of theory at 298.15 K and 1 atm.

*The transition state TS6′ is obtained using additional keywords IOP(1/8=1) int = finegrid guess = mix

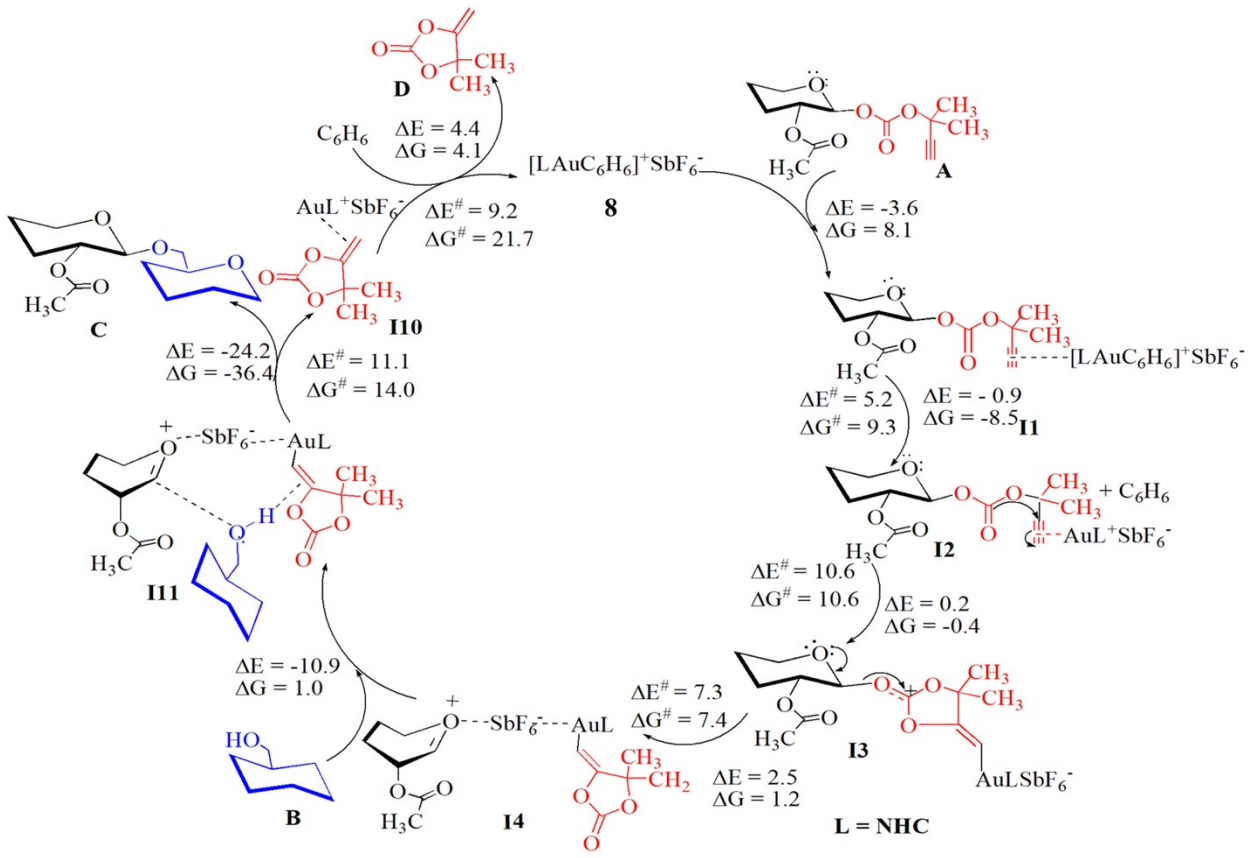

Scheme S4. Mechanism for glycosidation reaction by remote activation in presence of **8** with regeneration of catalyst. ΔE and $\Delta E^{\#}$ (in kcal/mol) represent reaction enthalpy and enthalpy of activation respectively at the M06/PCM/def2-TZVPP//BP86/def2-SVP level of theory. ΔG and $\Delta G^{\#}$ (in kcal/mol) represent the Gibbs free energy of reaction and Gibbs free energy of activation respectively, at same level of theory at 298.15 K and 1 atm.

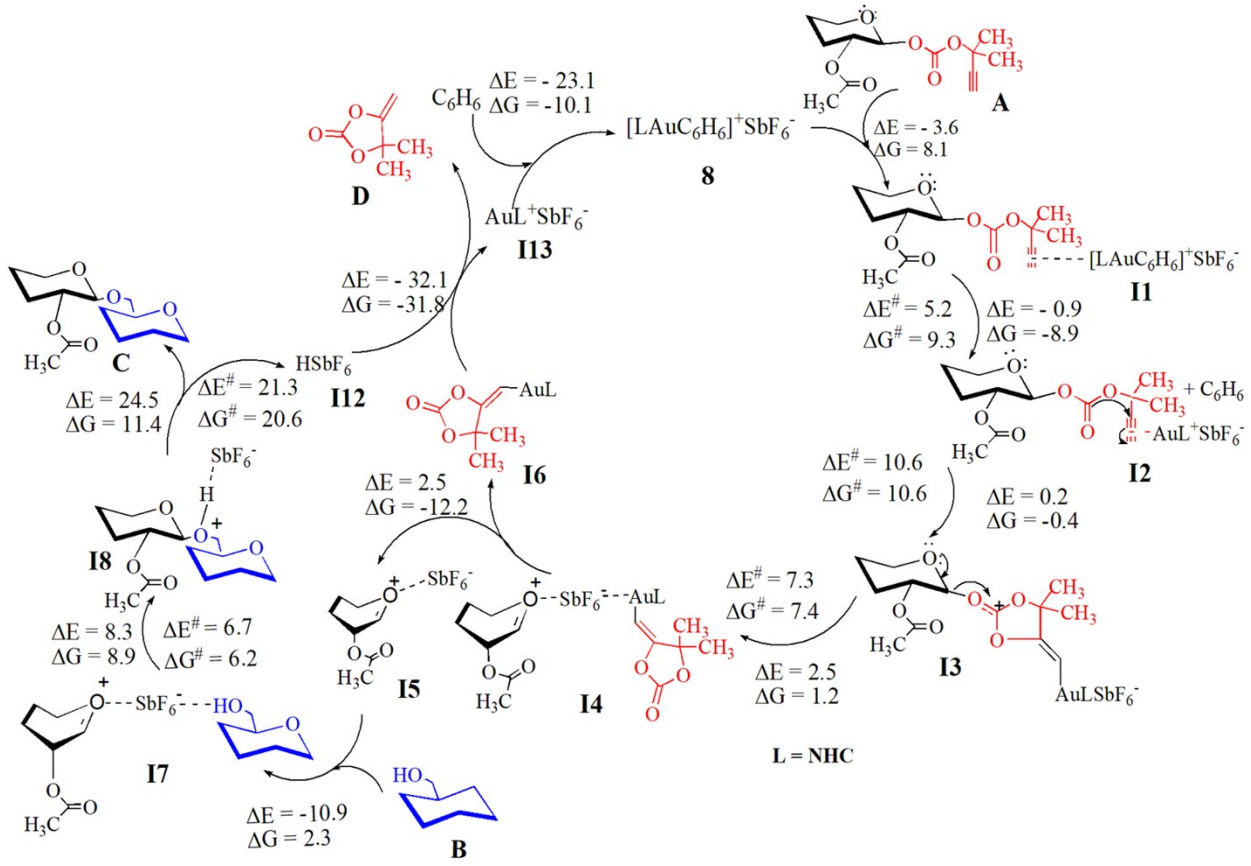

Scheme S5. Mechanism for glycosidation reaction by remote activation in presence of **8** through the intermediate **I13**. ΔE and $\Delta E^{\#}$ (in kcal/mol) represent reaction enthalpy and enthalpy of activation respectively at the M06/PCM/def2-TZVPP//BP86/def2-SVP level of theory. ΔG and $\Delta G^{\#}$ (in kcal/mol) represent the Gibbs free energy of reaction and Gibbs free energy of activation respectively, at same level of theory at 298.15 K and 1 atm.

Discussion: We have carried out quantum mechanical calculations to explore the mechanism of model glycosidation reaction[36,37] between alkynyl glycosyl carbonate A (glycosyl donor), and an acceptor B (ROH) catalyzed by N-heterocyclic carbene/silylene supported Au(I)-benzene complexes **8** and **2** at the M06/PCM/def2-TZVPP//BP86/def2-SVP level of theory by considering DCM as solvent. The overall reaction is highly exothermic (Scheme S2, ΔE = -32.6 kcal/mol) and exergonic (ΔG = -31.4 kcal/mol). We have calculated different reaction pathways for glycosidation reaction (see SI for the details). Herein, we explain the most feasible mechanism of the glycosidation reaction catalyzed by N-heterocyclic carbene supported Au(I)-benzene complex **8** (Scheme 6).

Other plausible mechanisms are given in the Supporting Information. The optimized geometries (BP86/def2-SVP) and important geometrical parameters of reactants, products, intermediates, and transition states are given in supporting information (Figures S10 to S12).

The first step of the reaction involves the interaction of gold catalyst **8** with alkynyl glycosyl carbonate **A** to form a weakly bound complex **I1**, where the carbonyl oxygen of the carbonate group has a slight bonding interaction with hydrogen atoms of the benzene ring coordinated to Au (O···H distance = 2.487 Å). The reaction energy and Gibbs free energy for this step are found to be -3.6 kcal/mol and 8.1 kcal/mol, respectively. In the next step, the alkynyl group replaces the arene ring in **I1** to form Au-alkyne complex **I2**. The formation of **I2** is exothermic by 0.9 kcal/mol, and exergonic by 8.9 kcal/mol and corresponding energy barrier is low ($\Delta E^{\#}$ = 5.2 kcal/mol and $\Delta G^{\#}$ = 9.3 kcal/mol). The metal coordination stabilizes the π*-MO (LUMO+1, E = -2.09 eV, Figure 4) centered on C≡C bond in **I2** as compared to the corresponding MO on **A** (LUMO+1, E = -0.54 eV, Figure 4). This facilitates the intramolecular nucleophilic addition of the lone pair on carbonyl oxygen to π*-MO of **I2** resulting the vinylgold complex **I3**. The reaction energy for the generation of **I3** is only slightly endothermic (0.2 kcal/mol) and exergonic (-0.4 kcal/mol) and the corresponding energy barrier is not very high ($\Delta E^{\#}$ = 10.6 kcal/mol and $\Delta G^{\#}$ = 10.6 kcal/mol).

In the next step, the glycosidic bond undergoes cleavage to form the intermediate **I4**, which is also facilitated by the donation of lone pair of electrons on pyranose oxygen to σ*- orbital glycosidic bond. The formation of **I4** is slightly endergonic process (1.2 kcal/mol) and endothermic (2.5 kcal/mol), and the corresponding change in free energy barrier is 7.4 kcal/mol. The bound complex **I4** is then separated into two intermediates viz. oxocarbenium ion **I5** and the cyclic carbonate vinyl gold complex **I6**. The oxocarbenium ion **I5** is now susceptible to interact with nucleophiles such as the aglycone (ROH) molecule (**B**) leading to new complex **I7**. The nucleophilic attack of alcohol oxygen atom O_{OH}, which is a part of aglycone moiety in **I7** on to the anomeric carbon of the oxocarbenium ion, produces a new intermediate **I8**. The corresponding energy values are given in Scheme 6. Subsequently, **I8** interacts with the vinyl gold complex **I6** to from a weakly bound complex **I9**. The HOMO of **I9** (Figure S9a) is □-MO of C=C bond with

comparatively higher coefficient on C_{AuL}. Note that the natural charge on C_{AuL} is -0.64 e, whereas that in the other carbon atom of C=C is slightly positive (0.20 e). Hence, this promotes the electrophilic addition of positively charged H_{SbF6-} (0.55 e) to electron rich C_{AuL}. This results in the cleavage of Au–C_{AuL} σ bond, leading to the formation of Au-alkene π complex **I10** and the disaccharide molecule **C**. The product formation step is highly exothermic as well as exergonic (ΔE = -30.4 kcal/mol and ΔG = -41.3 kcal/mol). The alkynyl group in alkynyl glycosyl carbonate **A** now competes with the alkene in **I10** to coordinate with Au(I) and leads to the formation of **I2**, and thus the catalytic cycle continues. This step is exothermic by -0.2 kcal/mol, and endergonic by 3.2 kcal/mol and the corresponding kinetic energy barrier is $\Delta E^{\#}$ = 6.3 kcal/mol, and $\Delta G^{\#}$ = 20.5 kcal/mol.

The reaction mechanism for the glycosidation reaction catalyzed by silylene-supported gold-benzene complex **2** is given in Scheme S6. The extent of elongation of C≡C bond length in **I2** (1.257 Å) is larger than that in **I2′** (1.244 Å). Hence, the C≡C in NHC supported Au(I)-alkyne complex (**I1**) is more activated by the donation of π electrons from an alkyne to Au as well as a greater back donation from Au→alkyne in comparison with Au(I)-alkyne complex supported by silylene (**I2′**). The activation of alkyne, and thereby formation of intermediate **I3** is more favorable in the case of reaction catalyzed by **8**. The barrier for the formation of similar intermediate **I3′**, catalyzed by **2** is highly energy demanding. Both step-wise, as well as the concerted mechanism, indicate that the energy barrier for the product formation step is high in the case of reaction catalyzed by **2**. The DFT studies on the glycosidation reaction between glycosyl carbonate **A** and an aglycone molecule **B** (ROH) catalyzed by N-heterocyclic carbene/silylene supported Au(1)-benzene complexes **8** and **2**, indicate that the NHC supported complex **8** is better catalyst than **2**.

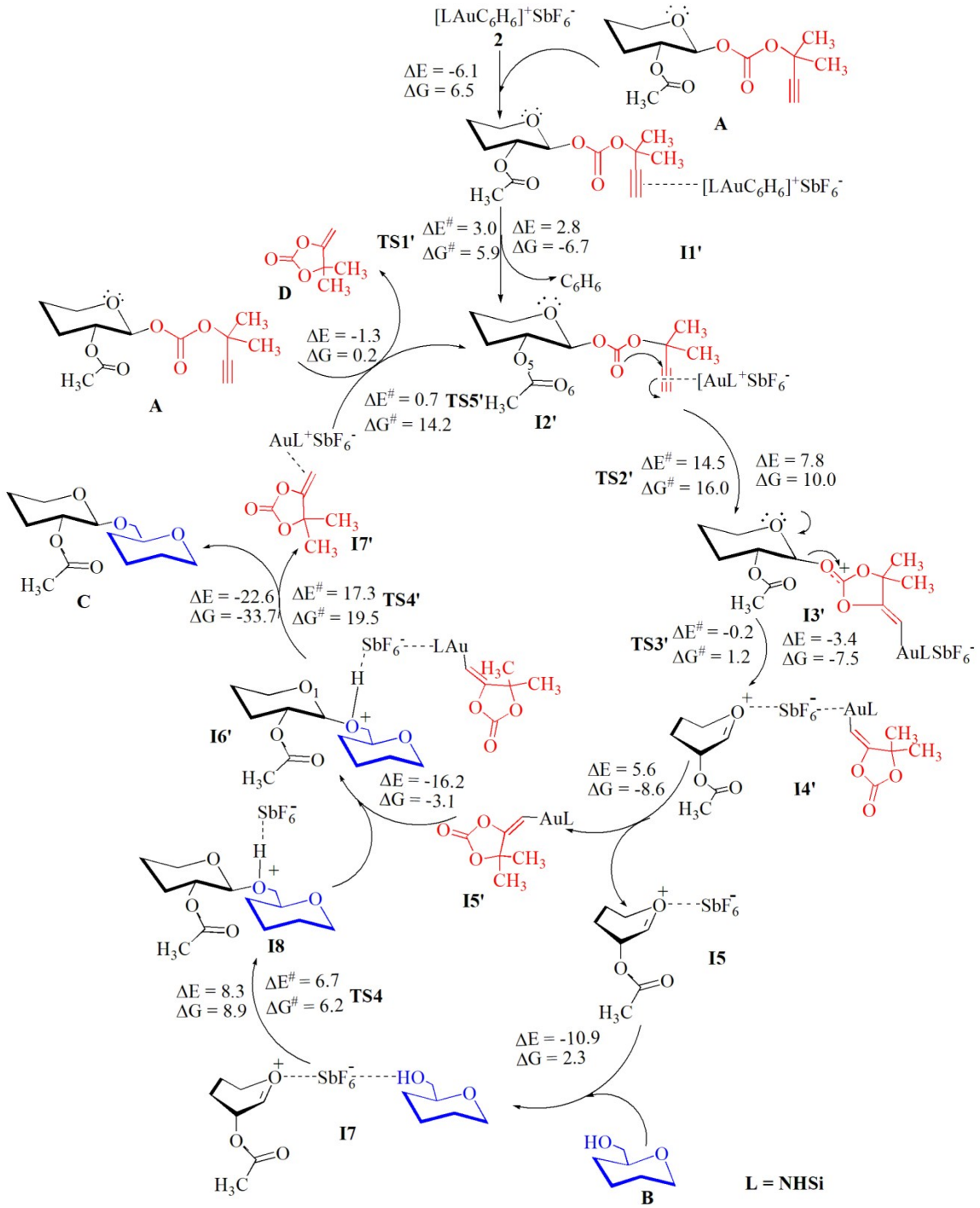

Scheme S6: Feasible mechanism for glycosidation reaction by remote activation in the presence of **2**. ΔE and $\Delta E^{\#}$ (in kcal/mol) represent reaction enthalpy and enthalpy of activation respectively at the M06/PCM/def2-TZVPP//BP86/def2-SVP level of theory. ΔG and $\Delta G^{\#}$ (in kcal/mol) represent the Gibbs free energy of reaction and Gibbs free energy of activation respectively, at same level of theory at 298.15 K and 1 atm.

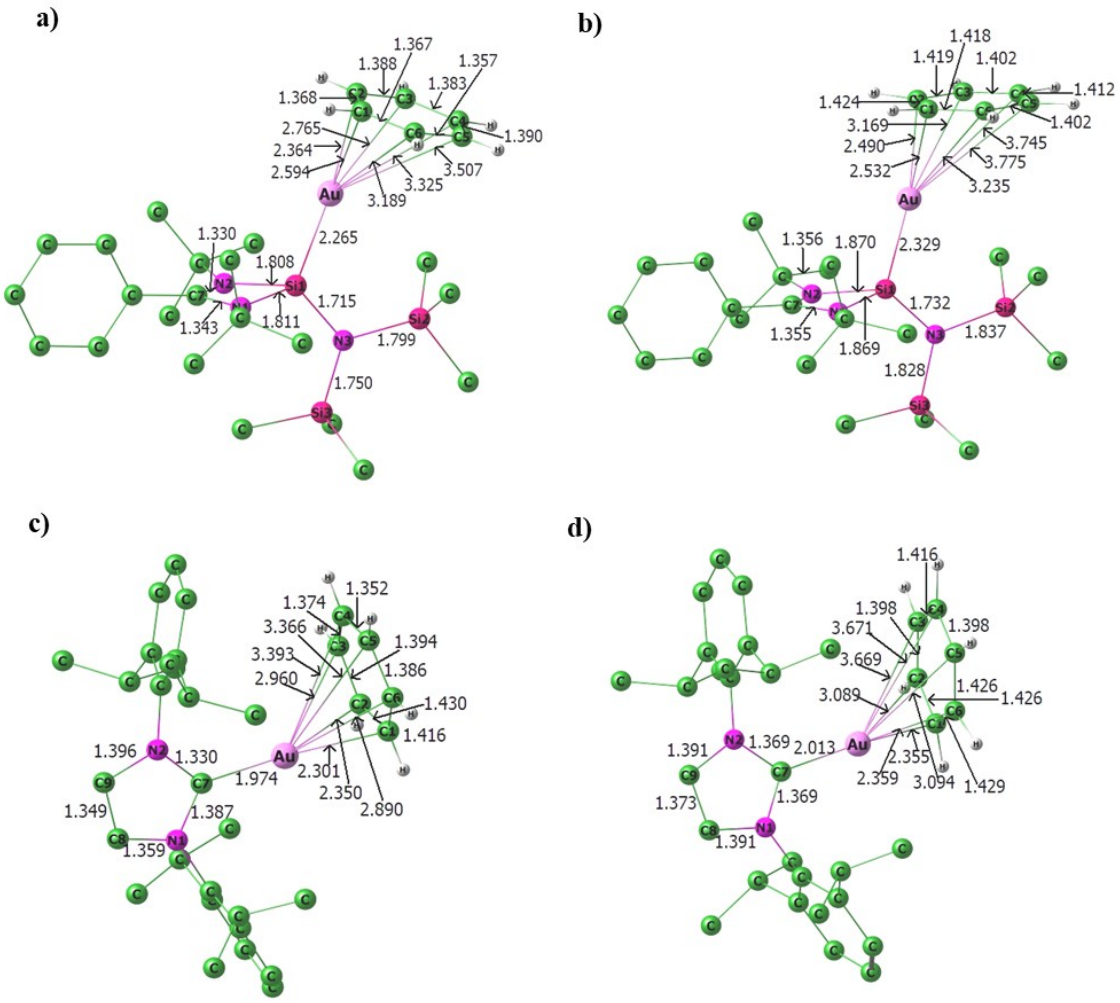

Figure S4. a) Experimental and b) optimized (BP86/def2-SVP) geometry of complexes **2** (**L^1L^2SiAuBz**$^+$, where L^1 = $N(SiMe_3)_2$, L^2 = (Ph)C(N*t*-Bu)$_2$ and Bz = C_6H_6), (c) Experimental and d) optimized (BP86/def2-SVP) geometry of **8** (**NHCAu(Bz)**$^+$, NHC=N-heterocyclic carbene with (i-Pr)$_2$Ph substituent on each N.

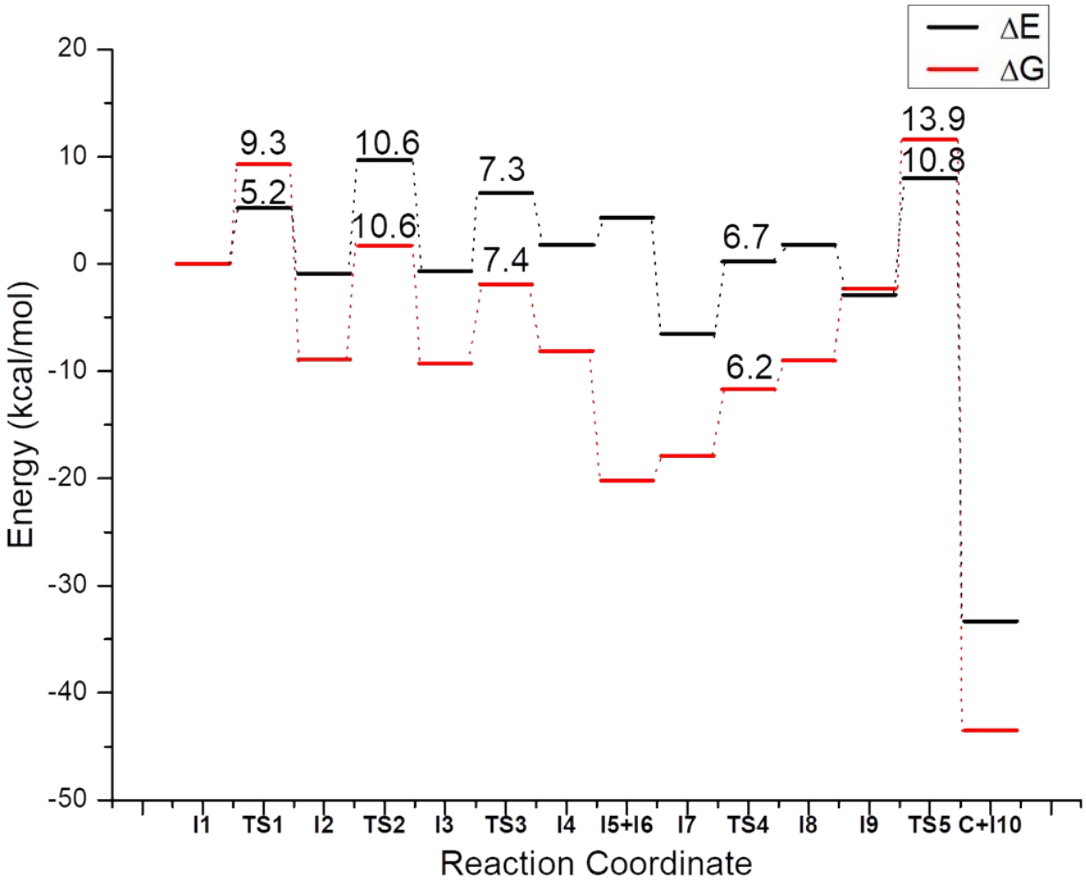

Figure S5. Energy profile diagram for glycosidation reaction by remote activation in presence of **8** as per the mechanism given in Scheme 7. Energies are given in kcal/mol at M06/PCM/Def2-TZVPP//BP86/Def2-SVP level of theory. Activation energy for each step is also given above in kcal/mol.

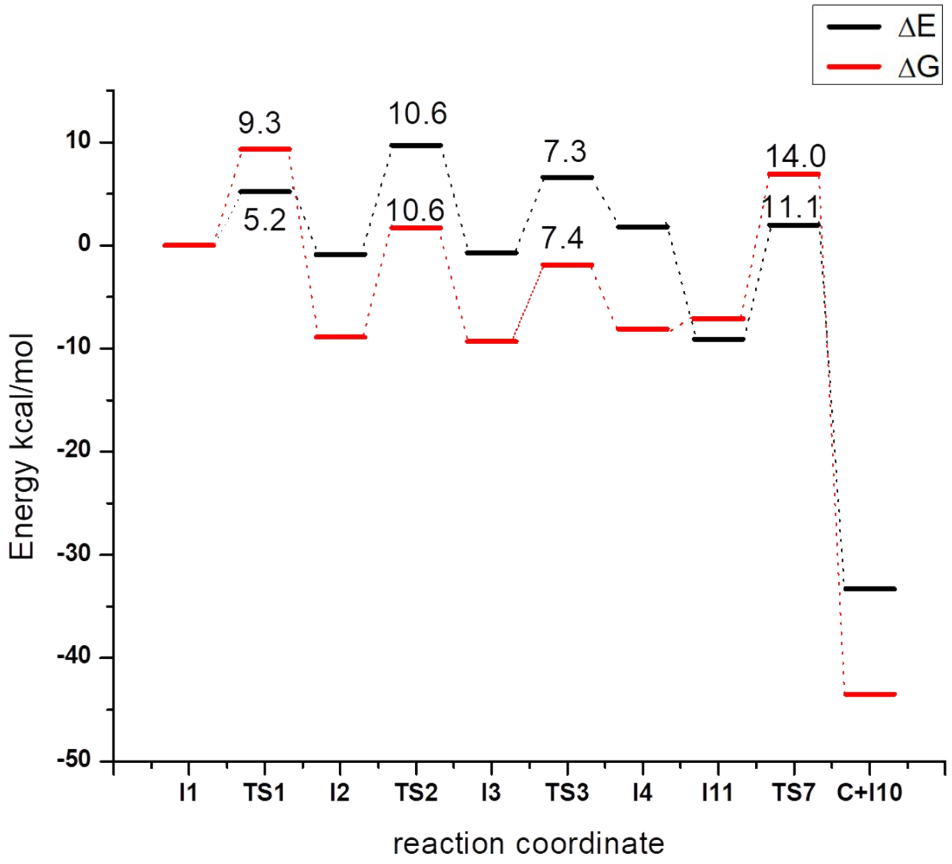

Figure S6. Energy profile diagram for (Scheme S2) of glycosidation reaction by remote activation in presence of **8**. Energies are given in kcal/mol at M06/PCM/def2-TZVPP//BP86/def2-SVP level of theory (DCM solvent). Activation energy for each step is given above in kcal/mol.

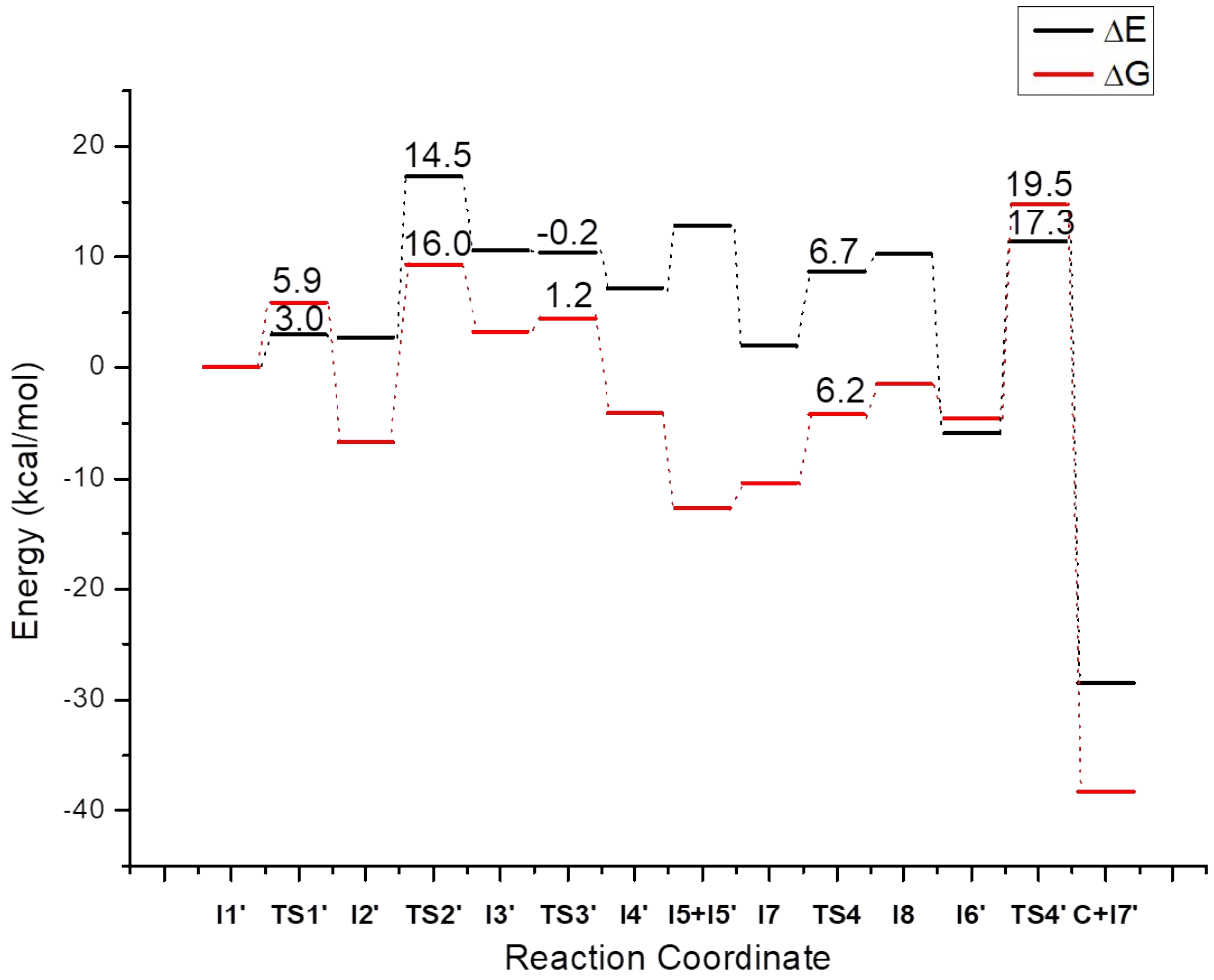

Figure S7. Energy profile diagram for glycosidation reaction by remote activation in presence of **2** as per the mechanism given in Scheme S6. Energies are given in kcal/mol at M06/PCM/def2-TZVPP//BP86/def2-SVP level of theory. Activation energy for each step is given above in kcal/mol.

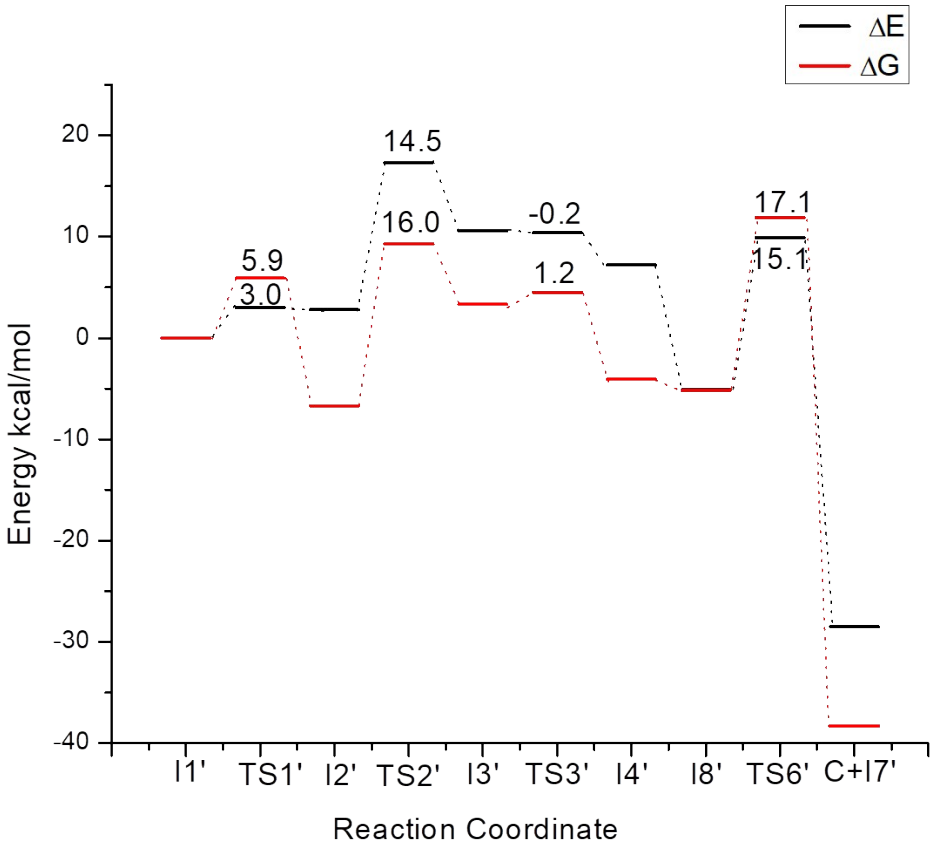

Figure S8. Energy profile diagram for of glycosidation reaction by remote activation in presence of **2** as per the mechanism given in Scheme S3. Energies are given in kcal/mol at M06/PCM/def2-TZVPP//BP86/def2-SVP level of theory. Activation energy for each step is given above in kcal/mol.

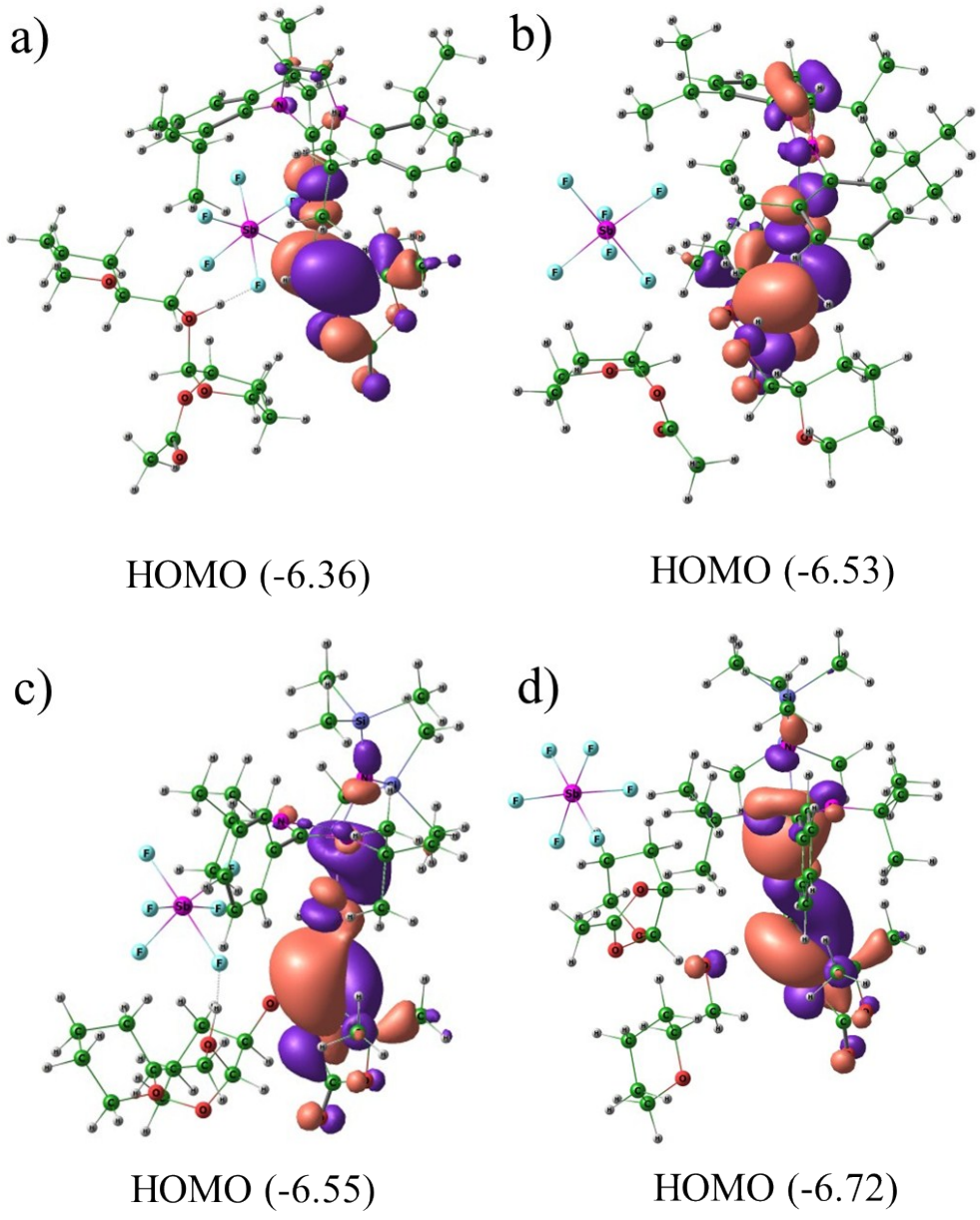

Figure S9. Important molecular orbitals of at M06/PCM/def2-TZVPP//BP86/def2-SVP level of theory of a) **I9** and b) **I11** c) **I6′** and d) **I8′**. Eigen values (eV) are given in parenthesis.

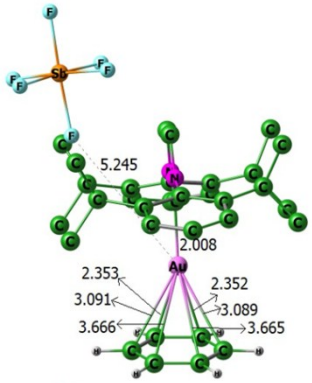

5

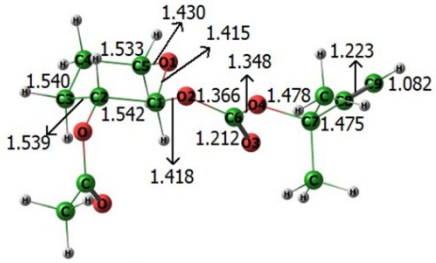

A

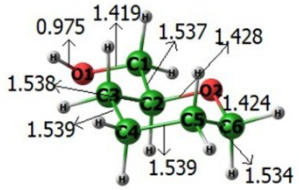

B

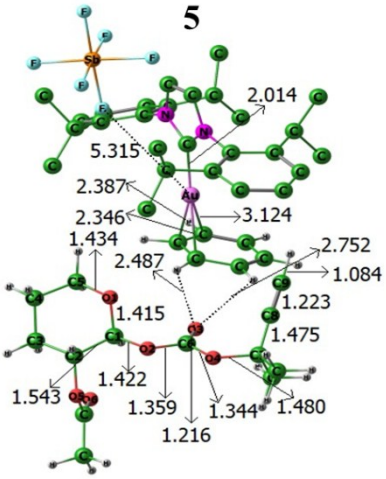

I1

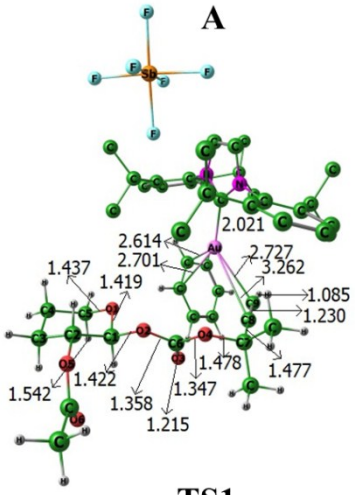

TS1

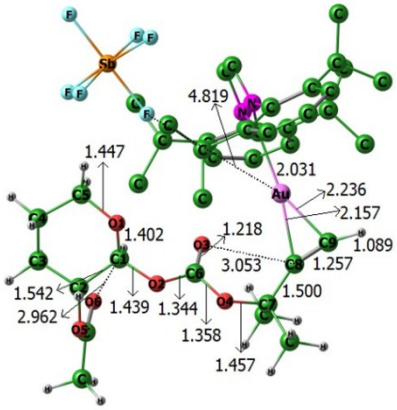

I2

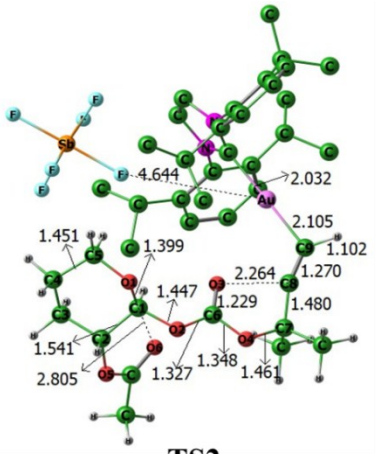

TS2

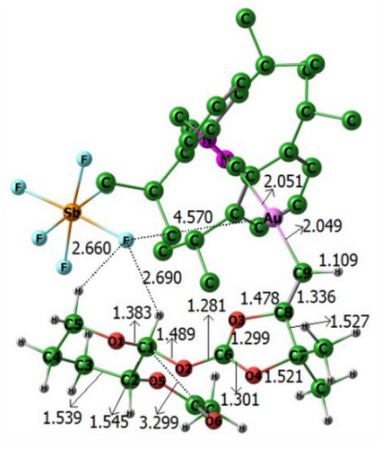

I3

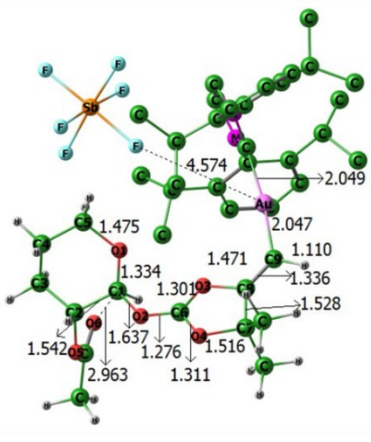

TS3

Figure S10. Optimized geometries and important geometrical parameters of reactants, intermediates and transition states at the BP86/def2-SVP level of theory. Distances are given in angstroms and angles in degrees.

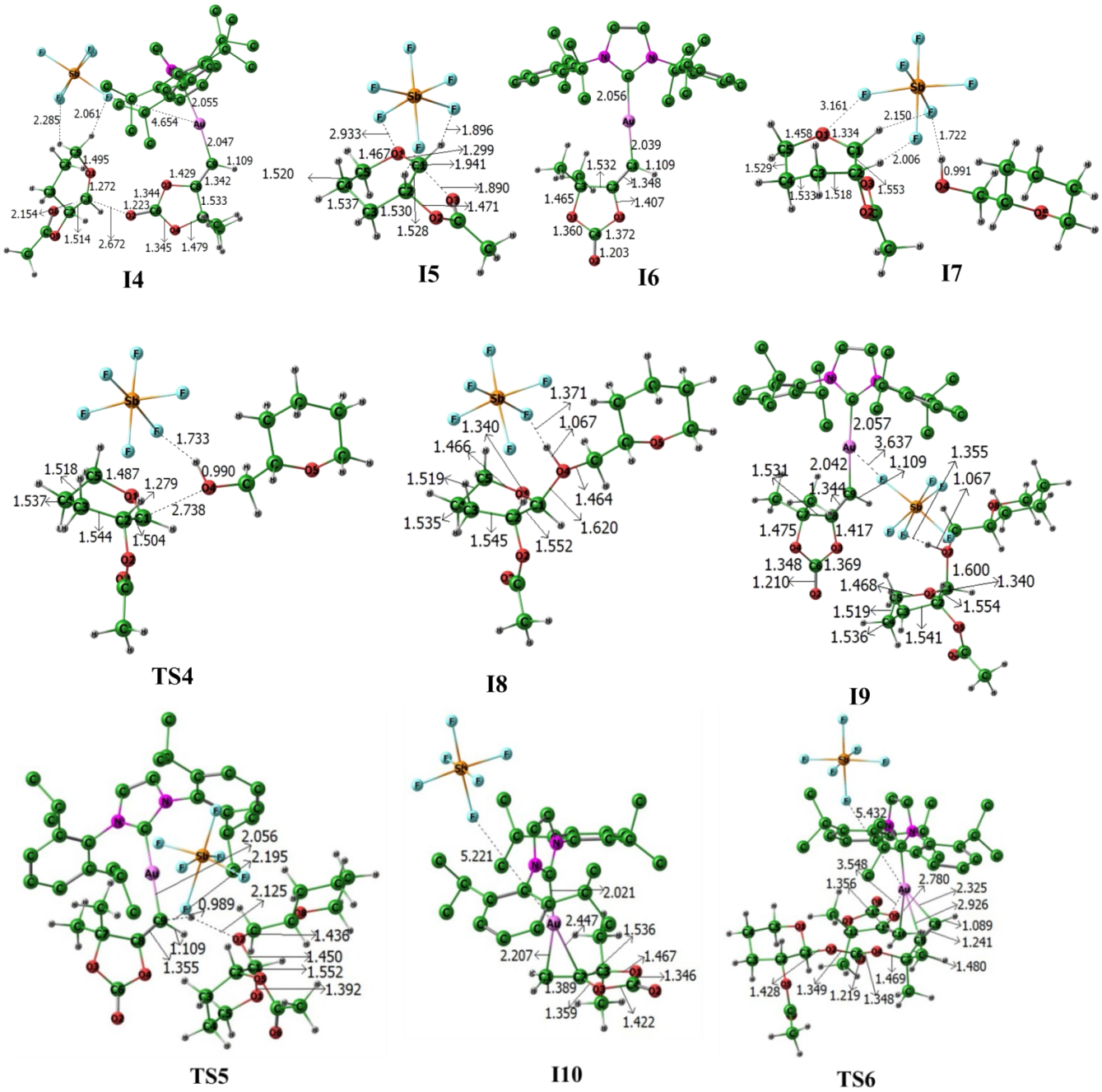

Figure S11. Optimized geometries and important geometrical parameters of intermediates, transition states and products at the BP86/def2-SVP level of theory. Distances are given in angstroms and angles in degrees.

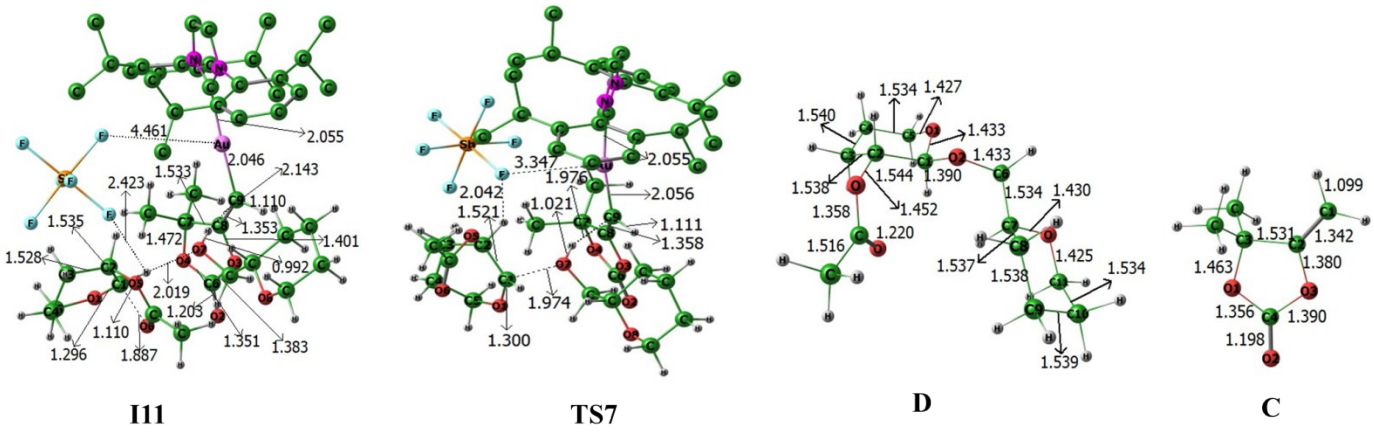

Figure S12. Optimized geometries and important geometrical parameters of intermediates, transition states and products at the BP86/def2-SVP level of theory. Distances are given in angstroms and angles in degrees.

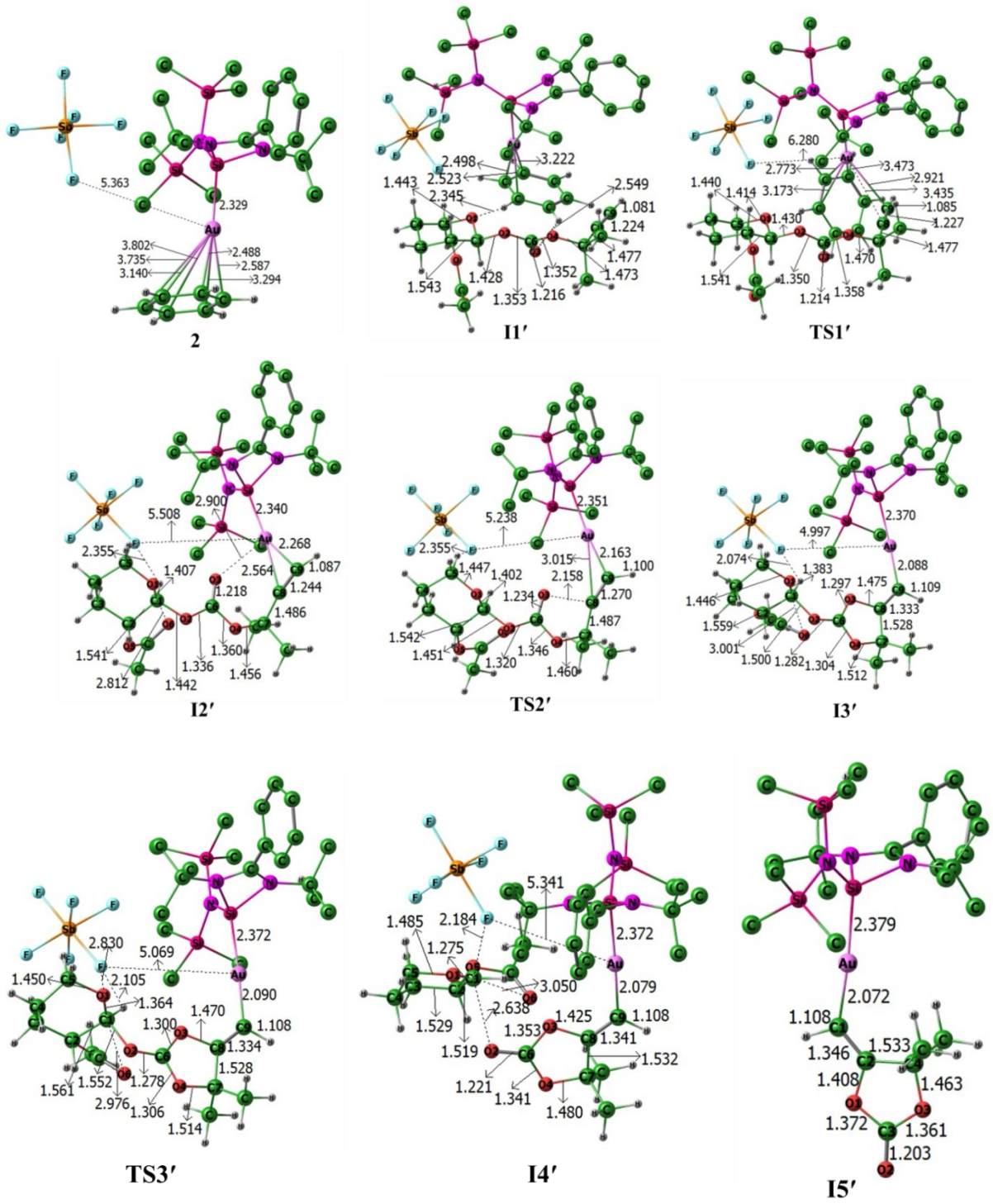

Figure S13. Optimized geometries and important geometrical parameters of intermediates and transition states at the BP86/def2-SVP level of theory. Distances are given in angstroms and angles in degrees.

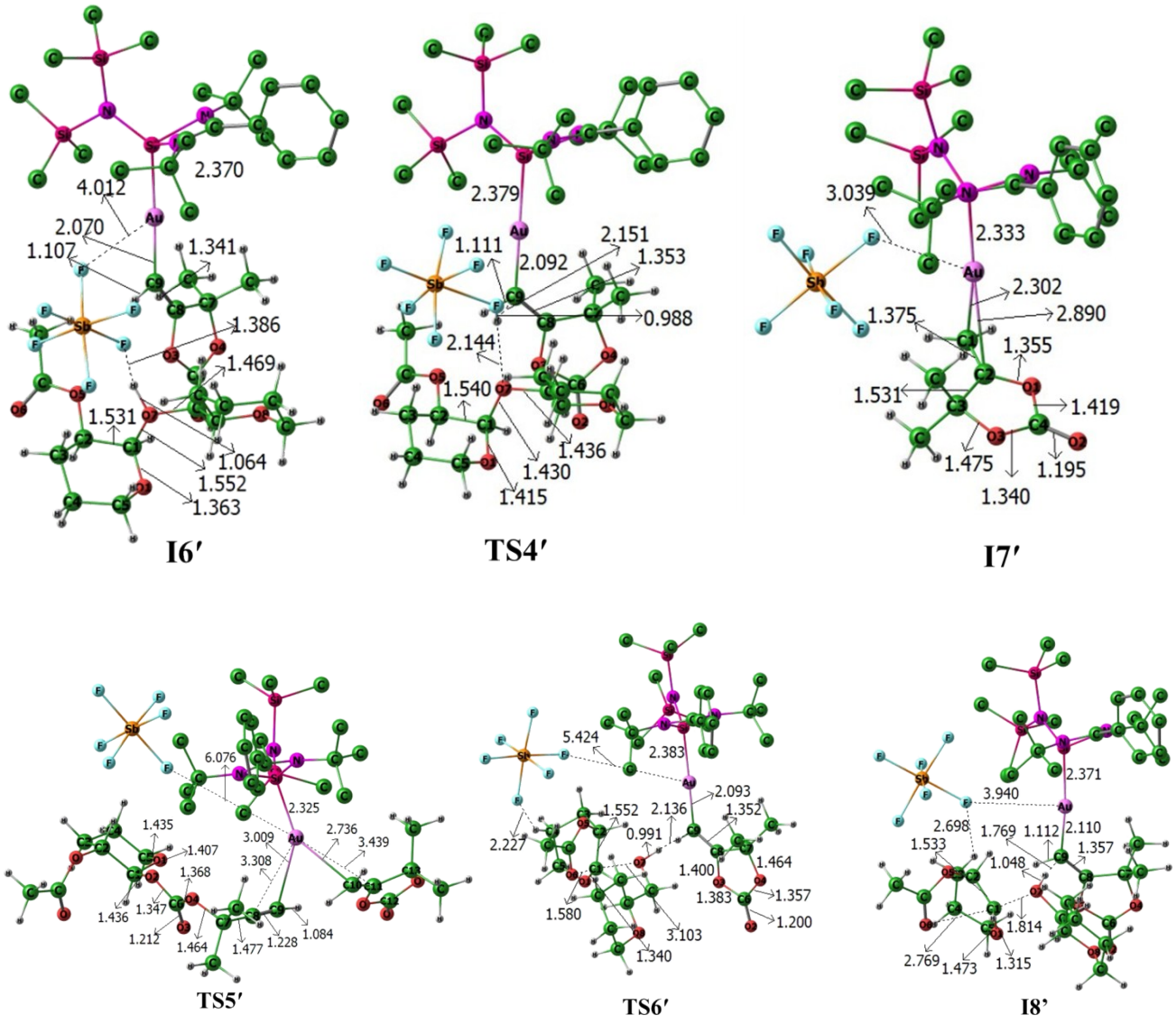

Figure S14. Optimized geometries and important geometrical parameters of intermediates and transition states mentioned at the BP86/def2-SVP level of theory. Distances are given in angstroms and angles in degrees.

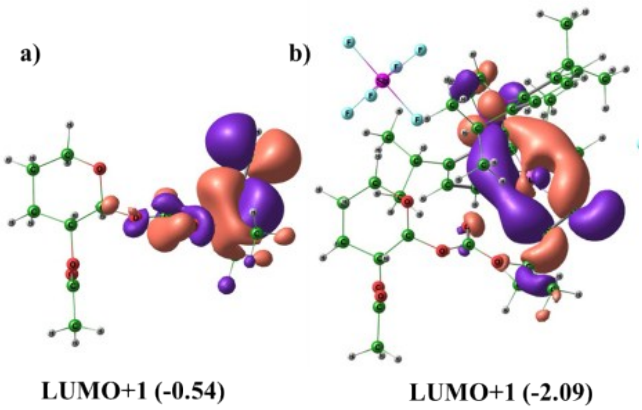

Figure 15: The low lying π* -molecular orbitals centered on C≡C in a) A and b) I2 at the M06/PCM/def2-TZVPP//BP86/def2-SVP level of theory. Eigen values (eV) are given in parenthesis.

References

1. (a) Becke, A. D. *Phys. Rev. A* **1988***, 38,* 3098–3100. (b) Perdew, J. P. *Phys. Rev. B* **1986**, *33*, 8822–8824.
2. Weigend, F. and Ahlrichs, R. *Phys. Chem. Chem. Phys.* **2005**, *7*, 3297–3305.
3. Frisch, M. J.; Trucks, G. W.; Schlegel,H.B.; Scuseria, G. E.; Robb, M. A.; Cheeseman, J. R.; Scalmani, G.; Barone, V.; Mennucci, B.; Petersson, G. A.; Nakatsuji, H.; Caricato, M.; Li, X.; Hratchian, H. P.; Izmaylov, A. F.; Bloino, J.; Zheng, G.; Sonnenberg, J. L.; Hada, M.; Ehara, M.; Toyota, K.; Fukuda, R.; Hasegawa, J.; Ishida, M.; Nakajima, T.; Honda, Y.; Kitao, O.; Nakai, H.; Vreven, T. ; Montgomery, J. A.; Jr.; Peralta, J. E.; Ogliaro, F.; Bearpark, M.; Heyd, J. J.; Brothers, E.; Kudin, K. N.; Staroverov, V. N.; Keith, T.; Kobayashi, R.; Normand, J.; Raghavachari, K.; Rendell, A.; Burant, J. C.; Iyengar, S. S.; Tomasi, J. ; Cossi, M.; Rega, N.; Millam, J. M.; Klene, M.; Knox, J. E.; Cross, J. B.; Bakken, V.; Adamo, C.; Jaramillo, J.; Gomperts, R.; Stratmann, R. E.; Yazyev, O.; Austin, A. J.; Cammi, R.; Pomelli, C.; Ochterski, J. W.; Martin, R. L.; Morokuma, K.; Zakrzewski, V. G.; Voth, G. A.; Salvador, P.; Dannenberg, J. J.; Dapprich, S.; Daniels, A. D.; Farkas, O.; Foresman, J. B.; Ortiz, J. V.; Cioslowski, J.; Fox, D. J. *Gaussian 09 (Revision B.01), Gaussian, Inc., Wallingford CT*.
4. Zhao, Y. and Truhlar, D. G. *Theor. Chem. Acc.* **2008**, *120*, 215–241.
5. (a) Miertus, S., Scrocco, E. and Tomasi, J. *J. Chem. Phys.* **1981***, 55*, 117–129. (b) Tomasi, J. and Cammi, R. *J. Comput. Chem.*. **1995**, *16,* 1449–1458.
6. (a) Reed, A. E., Curtiss, L. A. and Weinhold, F. *Chem. Rev.* **1988***, 88,* 899–926. (b) Glendening, E. D., Reed, A. E., Carpenter, J. E. and Weinhold, F. *NBO Version 5.9.*

S6. IR Spectrum of 9 and 10.

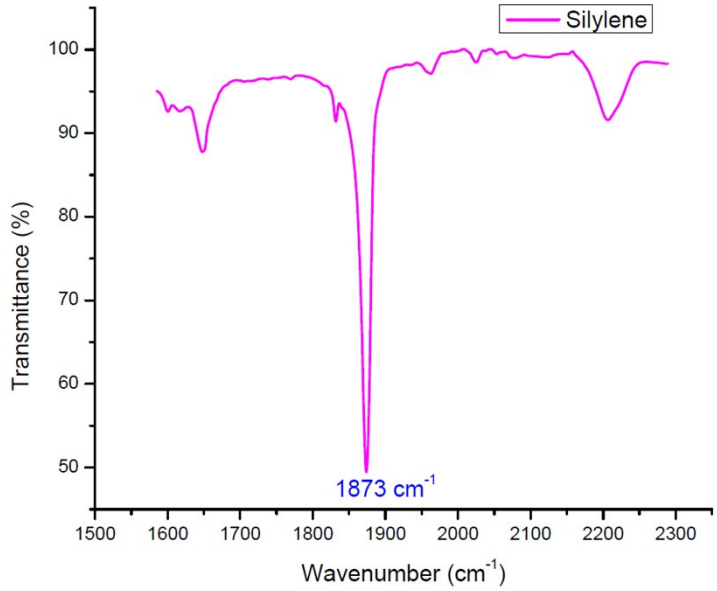

Fig S15. IR Spectrum of **9** in solid state

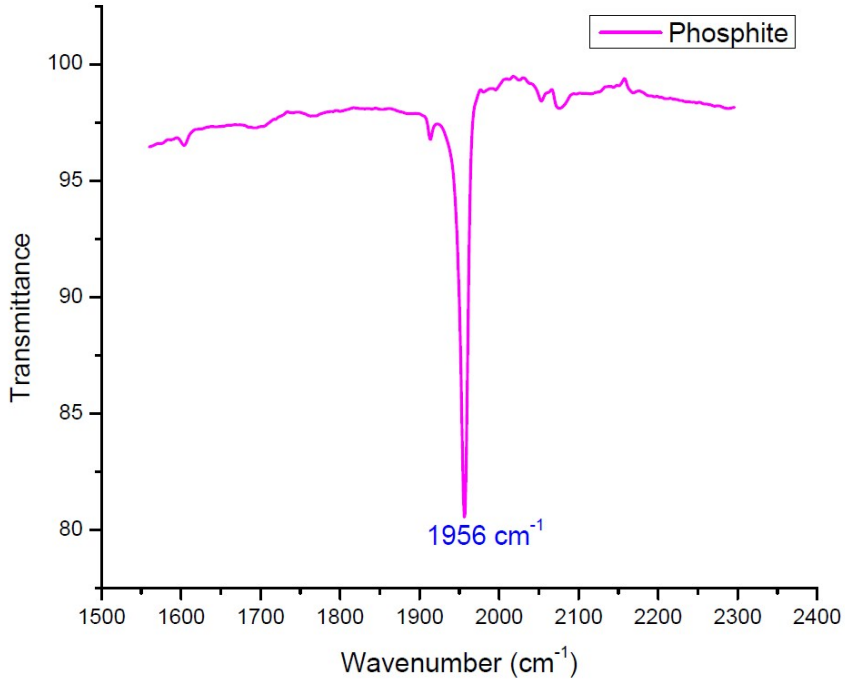

Fig S16. IR Spectrum of **10** in solid state

S7. NMR Spectra of 2, 3, 4, 5, 6, 8, 9, 10, 12b, 12d, 14a, 14b, 14c, 14d, 14f, 17, 18, 19 and 20.

^{1}H NMR spectrum (400.31 MHz, $CDCl_3$) of compound **2**

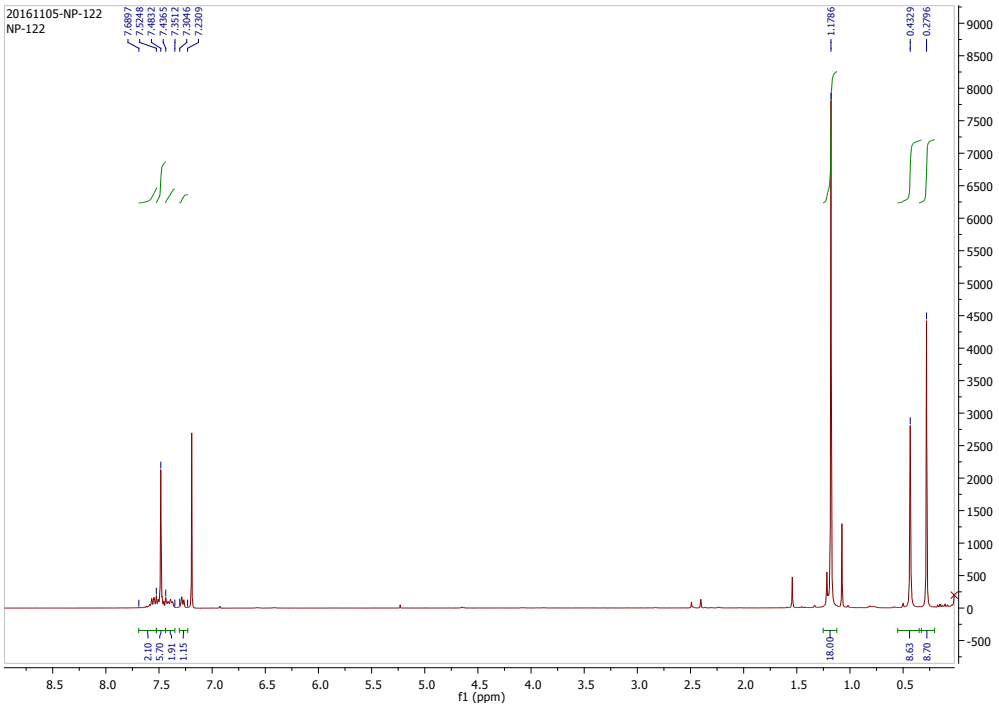

^{13}C NMR Spectrum (100.67 MHz, $CDCl_3$) of compound **2**

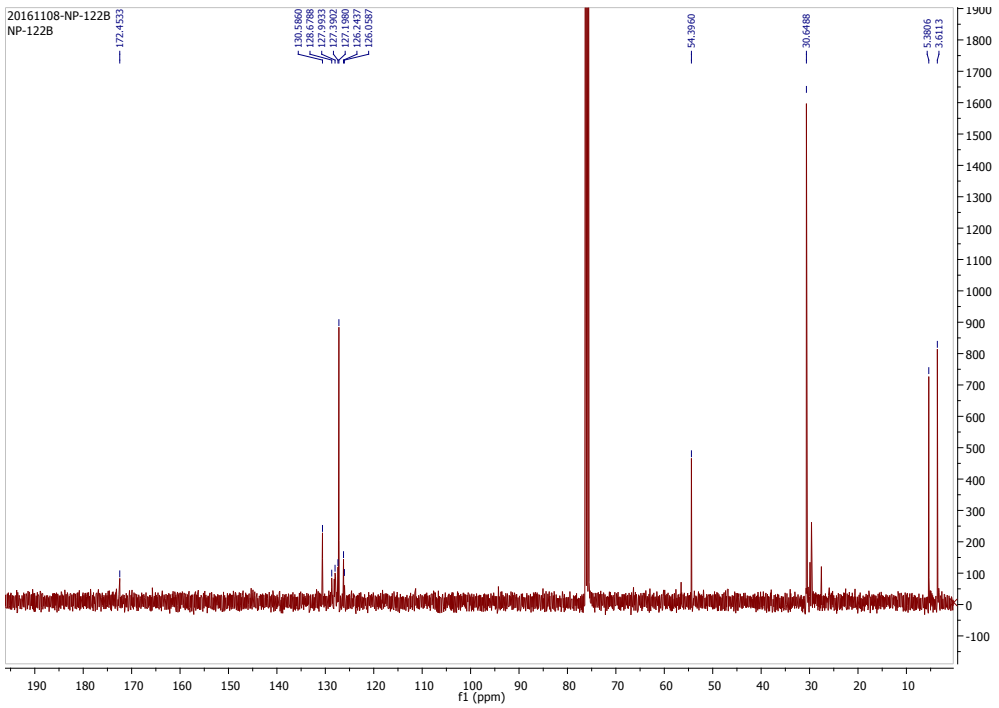

^{29}Si NMR Spectrum (79.495 MHz, $CDCl_3$) of **2**

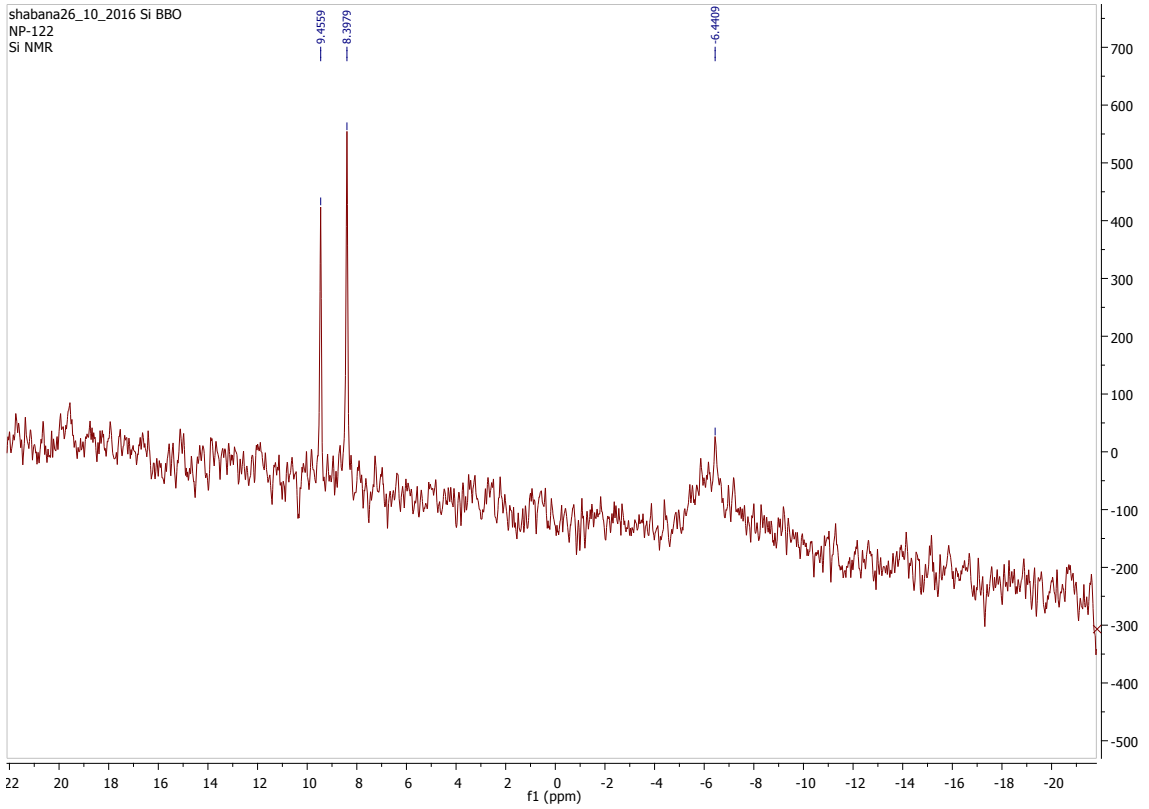

^{1}H NMR spectrum (400.31 MHz, $CDCl_3$) of compound **3**

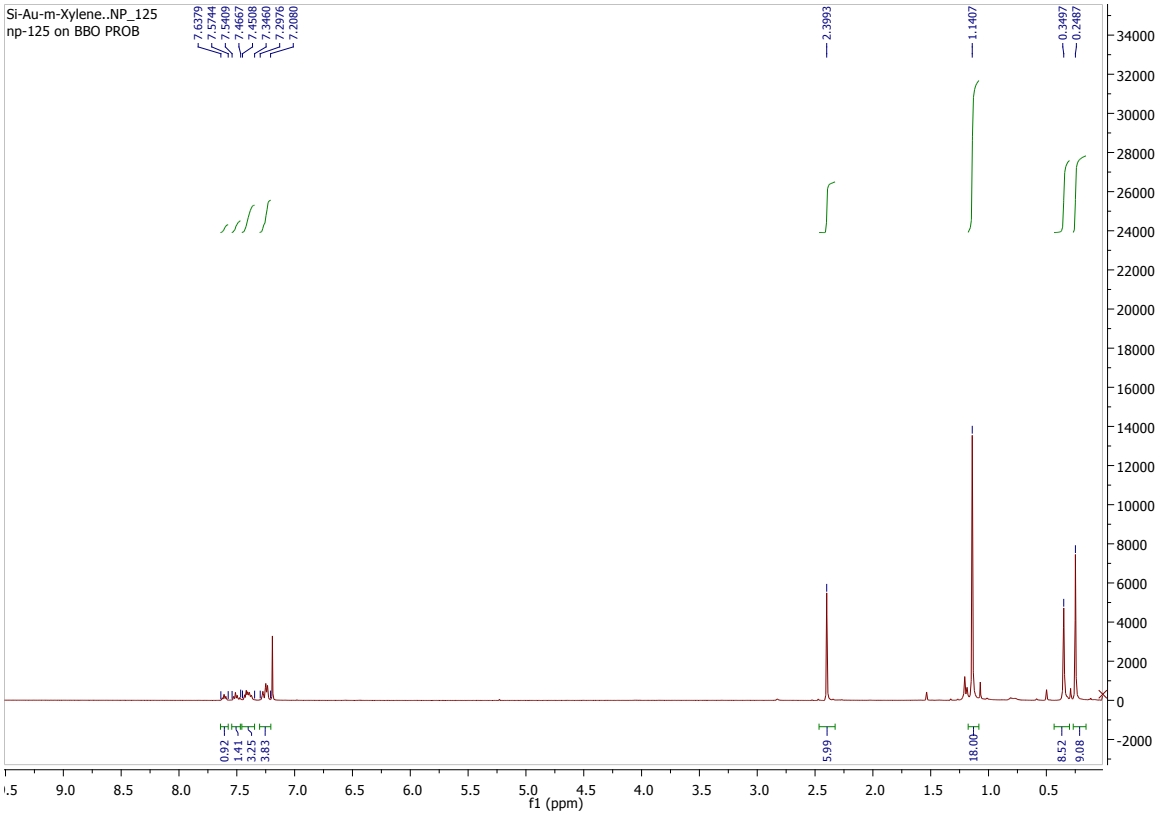

^{13}C NMR Spectrum (100.67 MHz, $CDCl_3$) of compound **3**

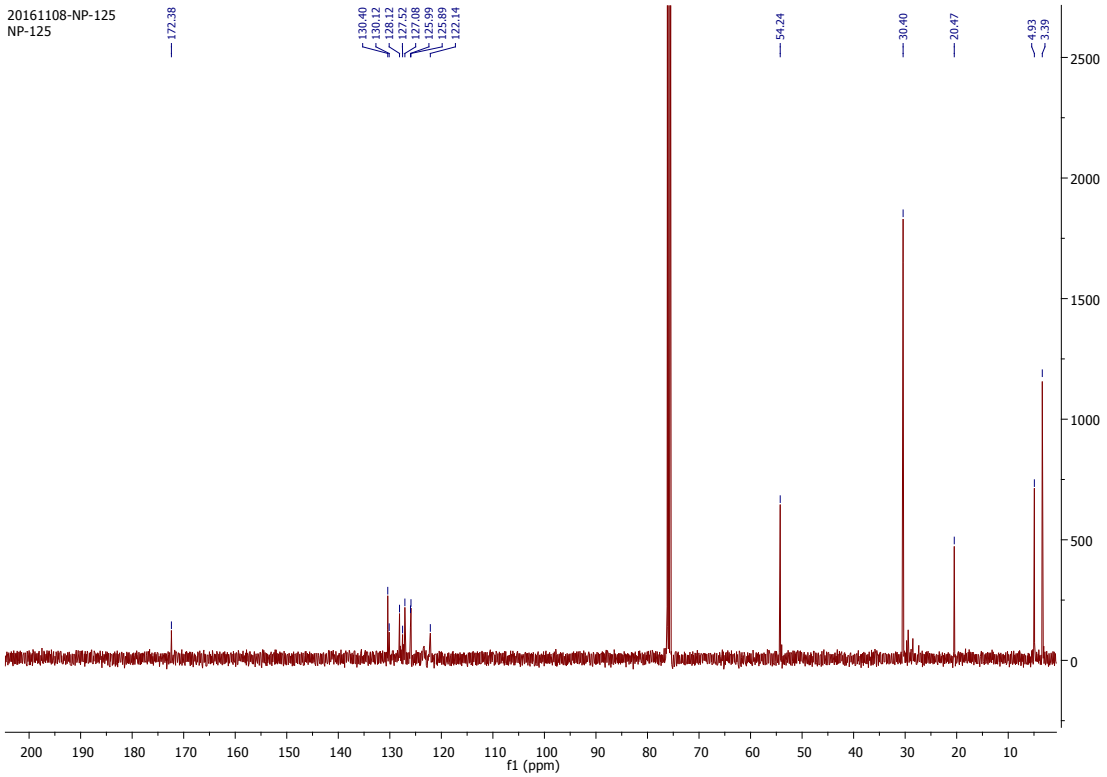

^{29}Si NMR Spectrum (79.495 MHz, $CDCl_3$) of **3**

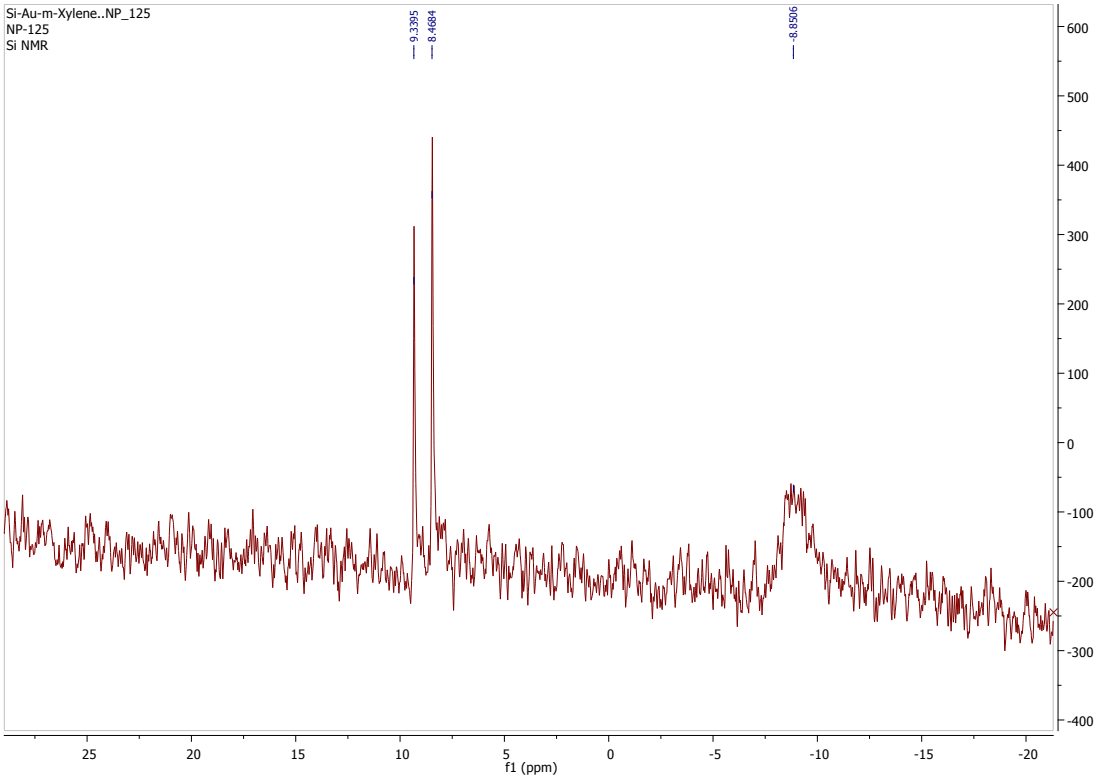

^{1}H NMR spectrum (400.31 MHz, $CDCl_3$) of compound **4**

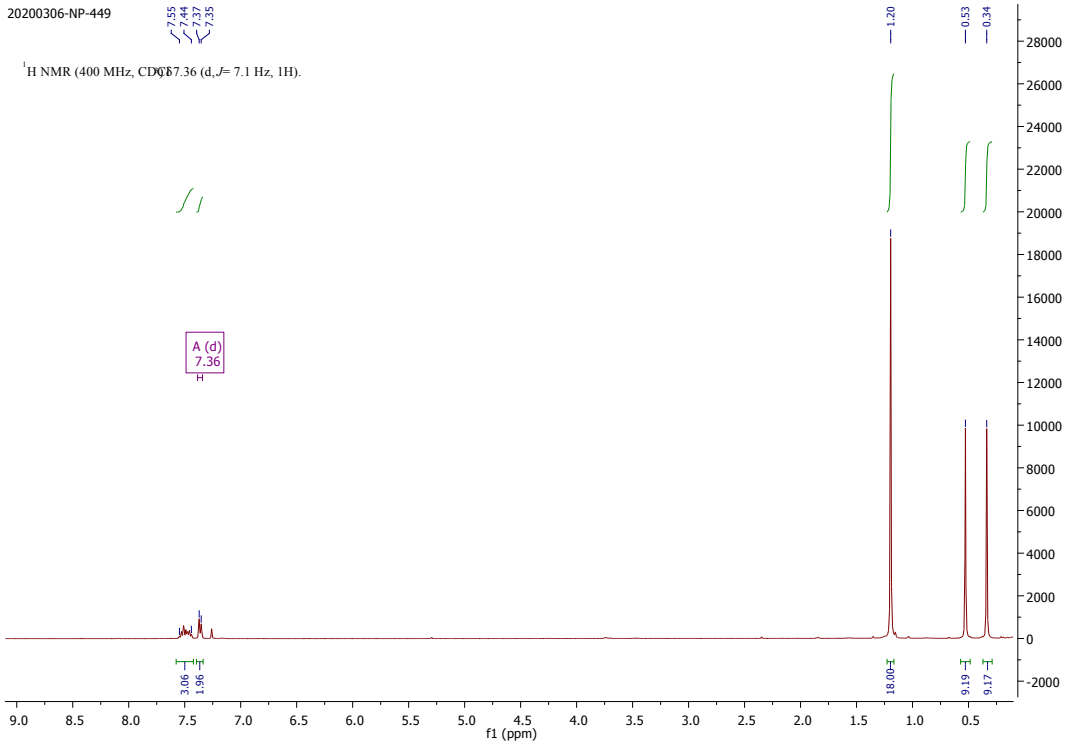

^{13}C NMR Spectrum (100.67 MHz, $CDCl_3$) of compound **4**

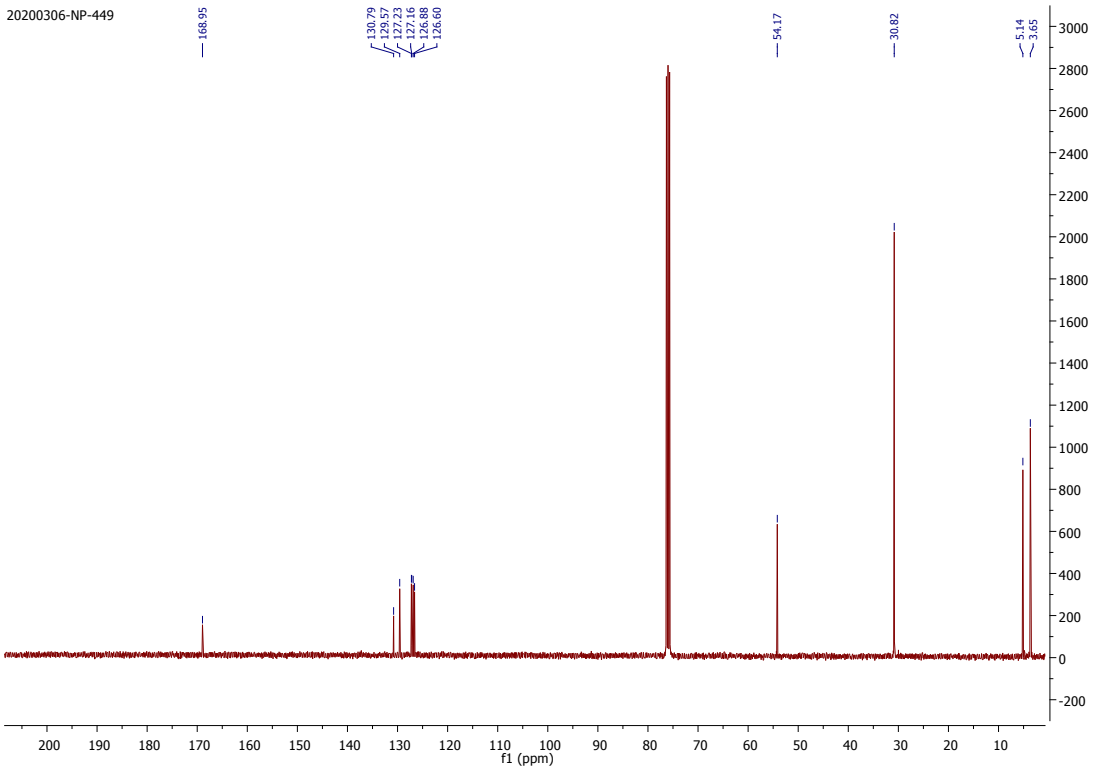

^{1}H NMR spectrum (400.31 MHz, $CDCl_3$) of compound **5**

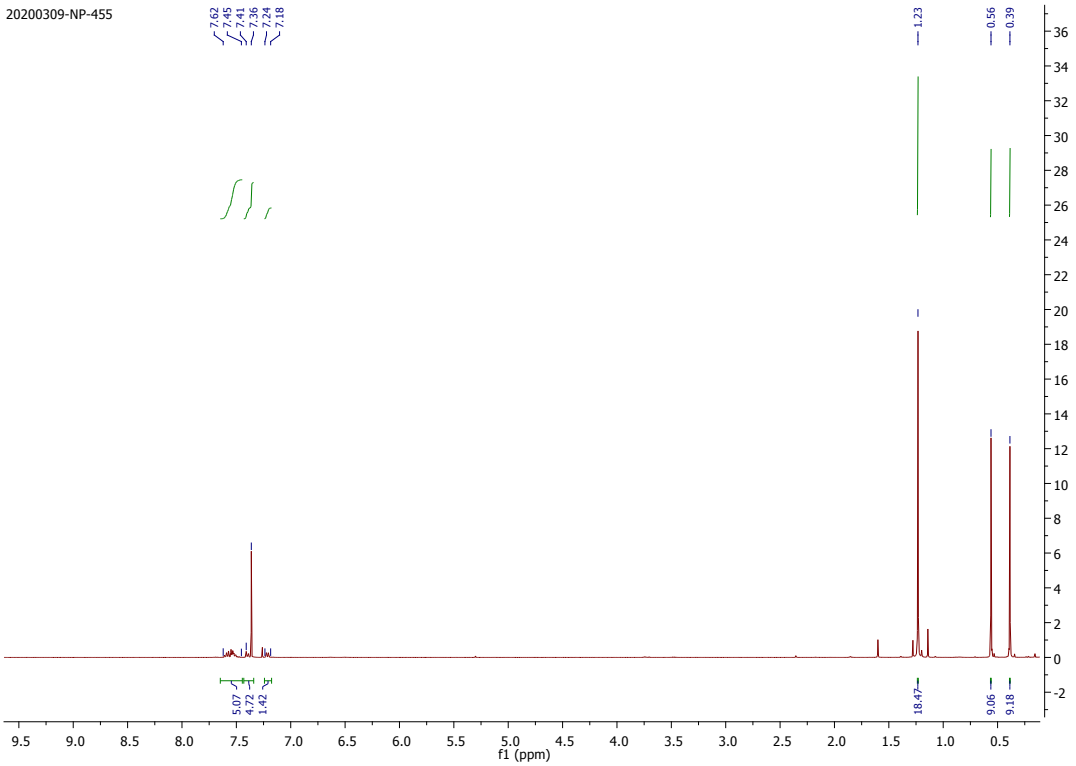

^{13}C NMR Spectrum (100.67 MHz, $CDCl_3$) of compound **5**

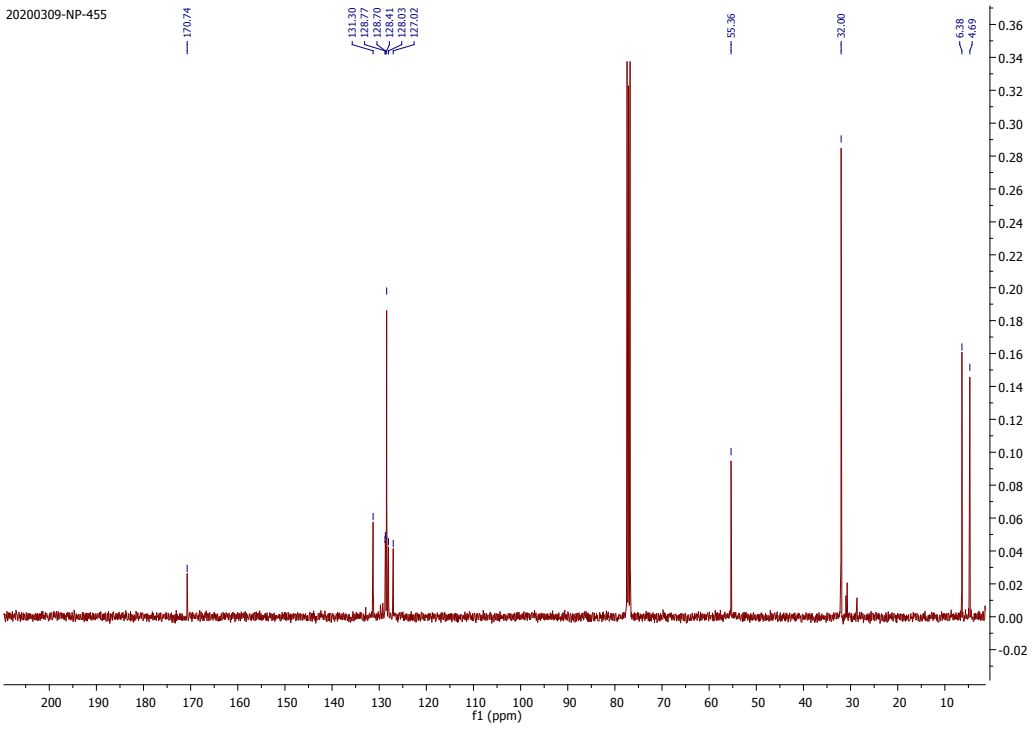

^{1}H NMR spectrum (400.31 MHz, $CDCl_3$) of compound **6**

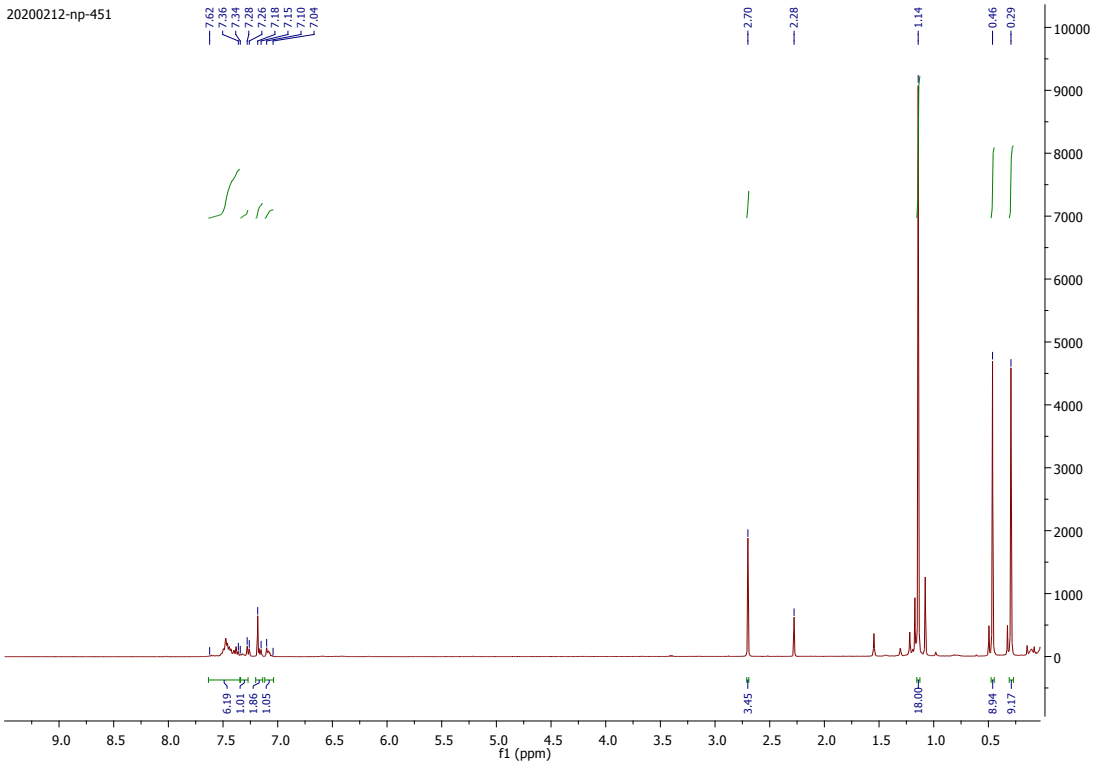

^{13}C NMR Spectrum (100.67 MHz, $CDCl_3$) of compound **6**

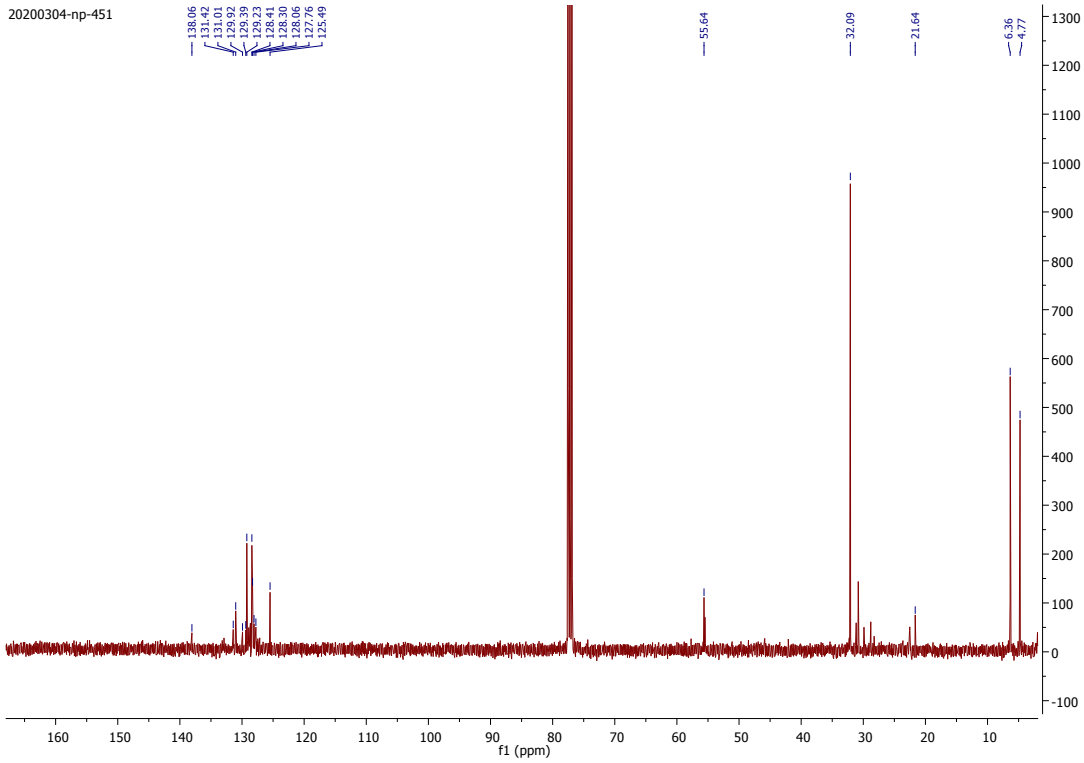

^{1}H NMR spectrum (400.31 MHz, $CDCl_3$) of compound **8**

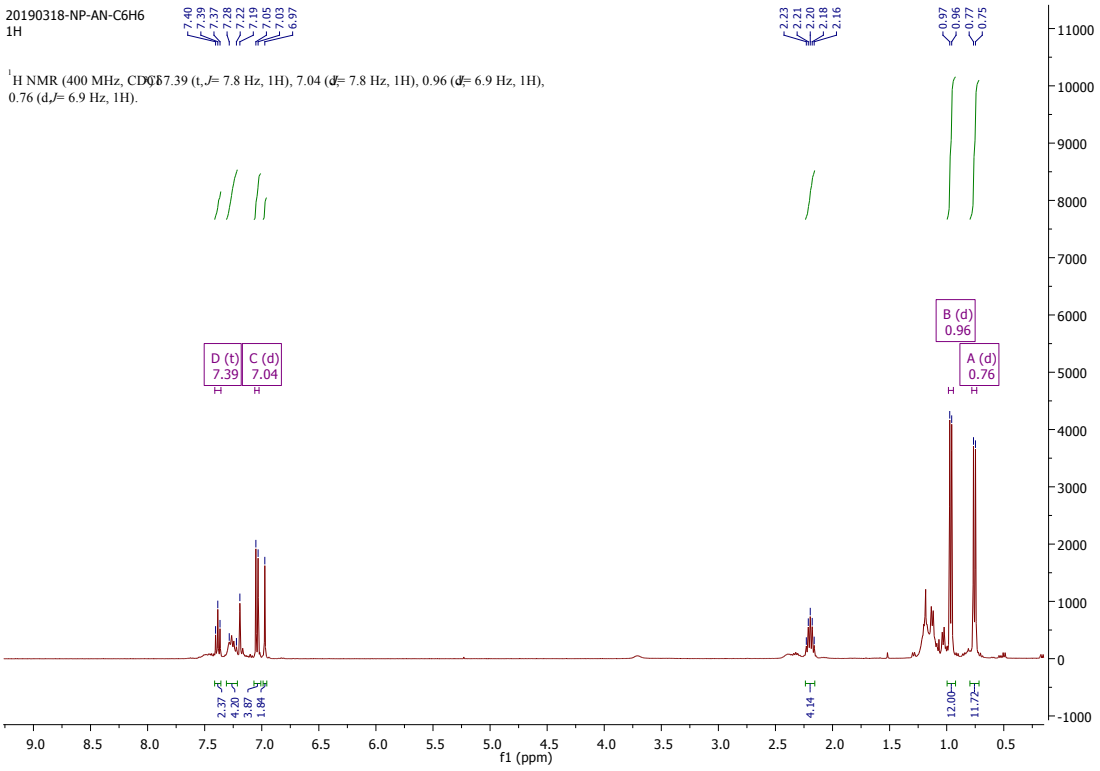

^{13}C NMR Spectrum (100.67 MHz, $CDCl_3$) of compound **8**

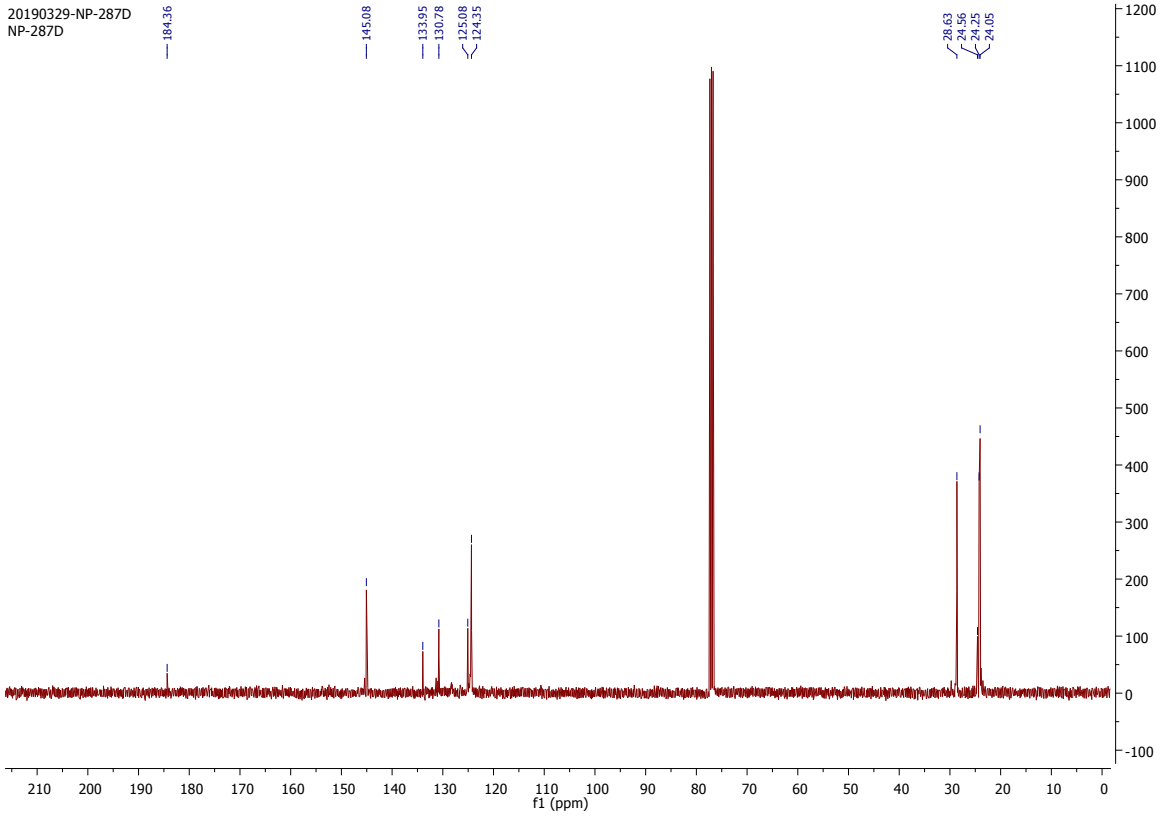

^{1}H NMR spectrum (400.31 MHz, $CDCl_3$) of compound **9**

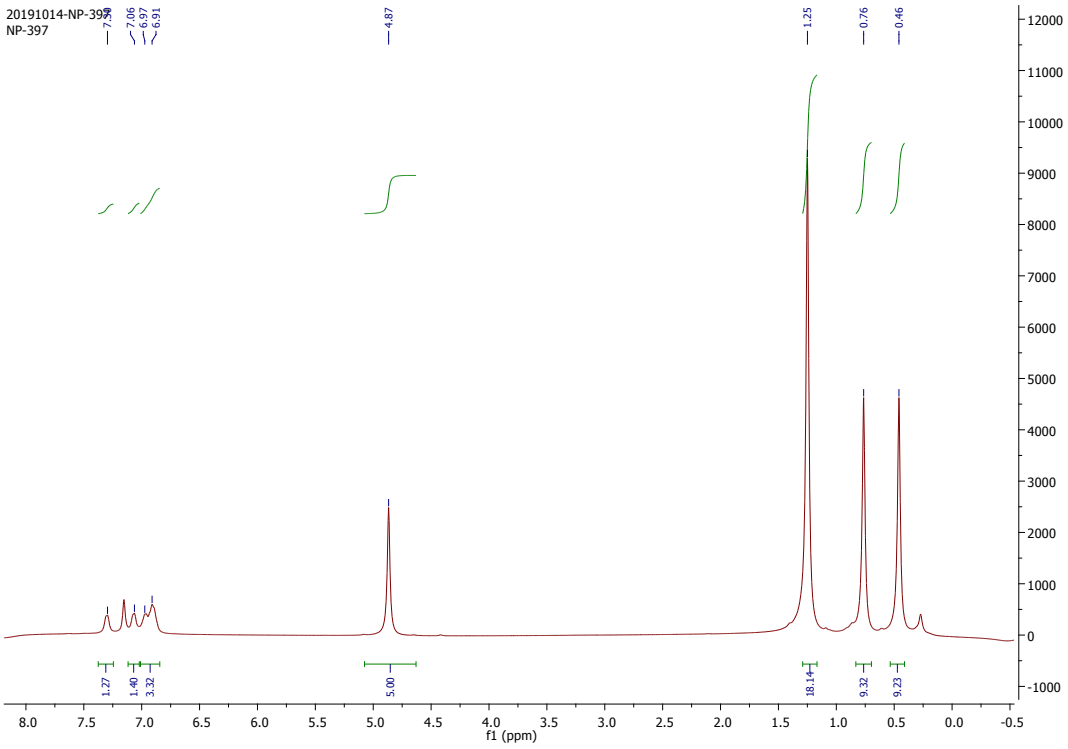

^{29}Si NMR Spectrum (79.495 MHz, $CDCl_3$) of **9**

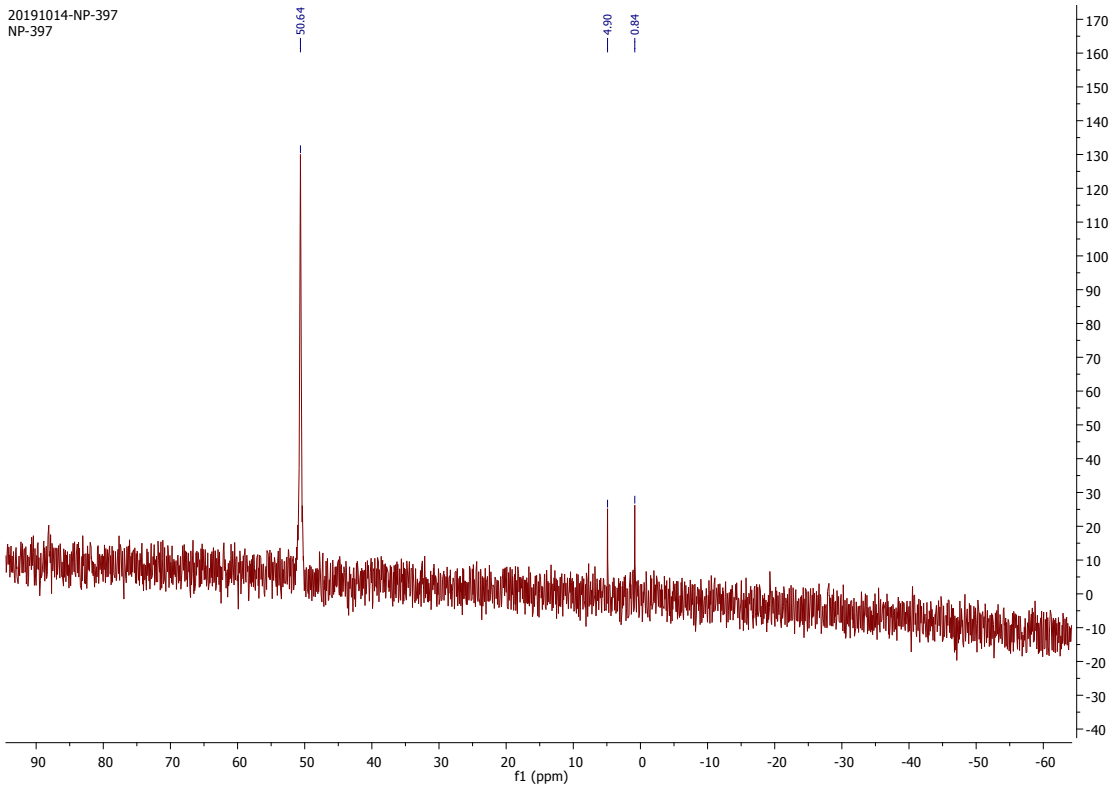

^{1}H NMR spectrum (400.31 MHz, $CDCl_3$) of compound **10**

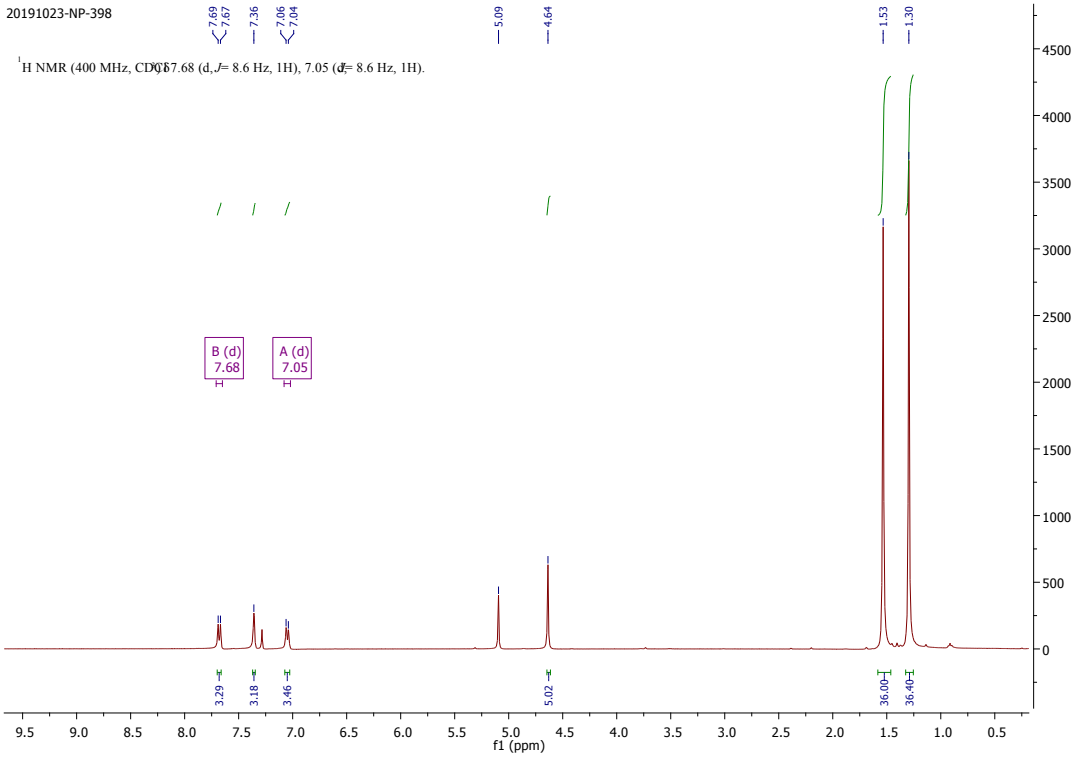

^{31}P NMR spectrum (161.976 MHz, $CDCl_3$) of **10**

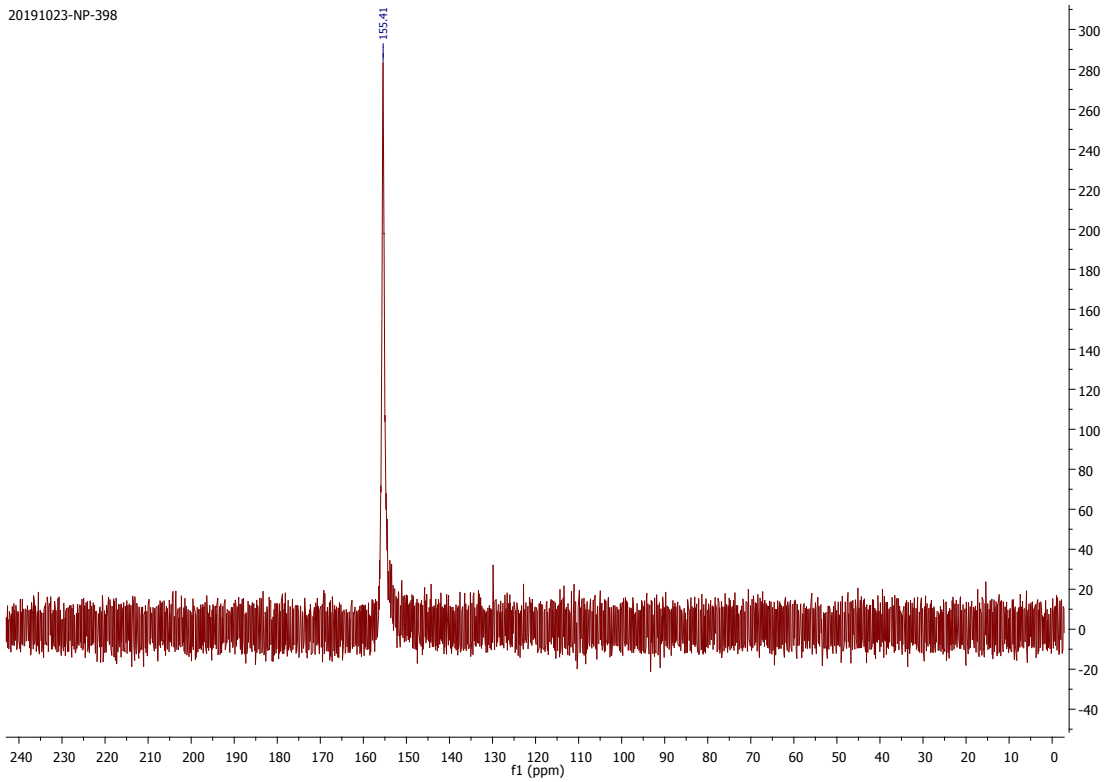
20191023-NP-398
155.41
300
280
260
240
220
200
180
160
140
120
100
80
60
40
20
0
-20
-40
240 230 220 210 200 190 180 170 160 150 140 130 120 110 100 90 80 70 60 50 40 30 20 10 0
f1 (ppm)

^{1}H NMR Spectrum (400.31 MHz, $CDCl_3$) of compound **12b**

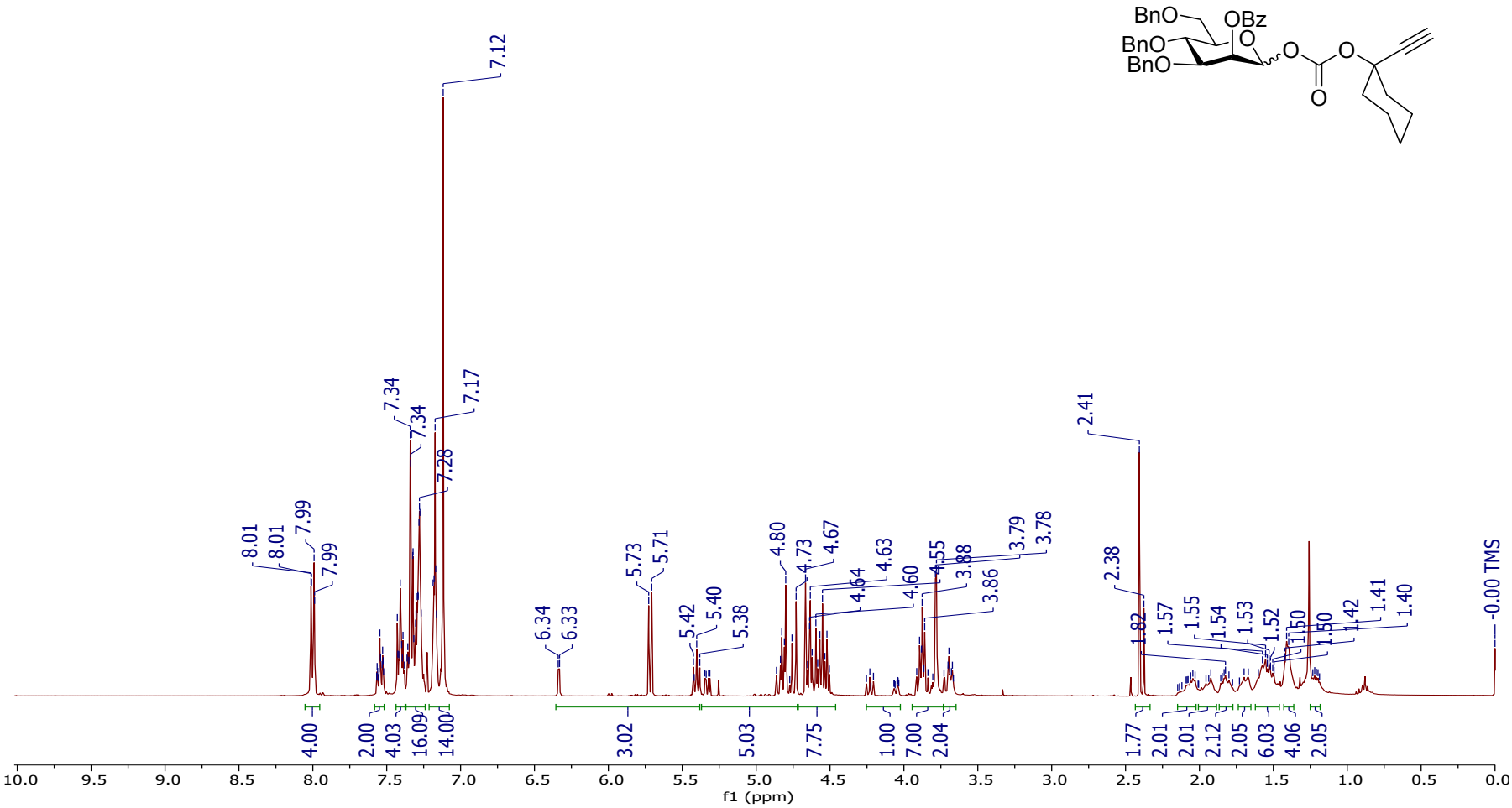

^{13}C NMR Spectrum (100.67 MHz, $CDCl_3$) of compound **12b**

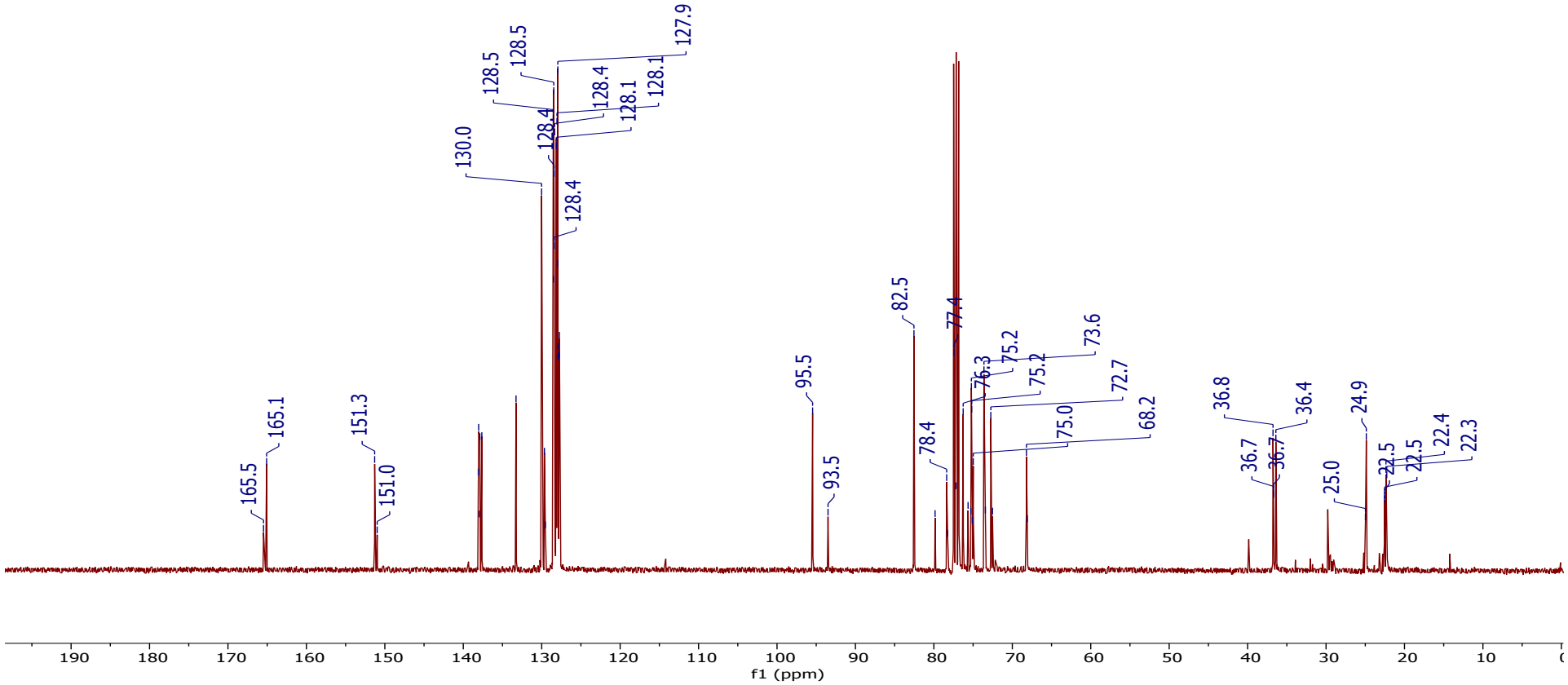

DEPT NMR Spectrum (100.67 MHz, $CDCl_3$) of compound **12b**

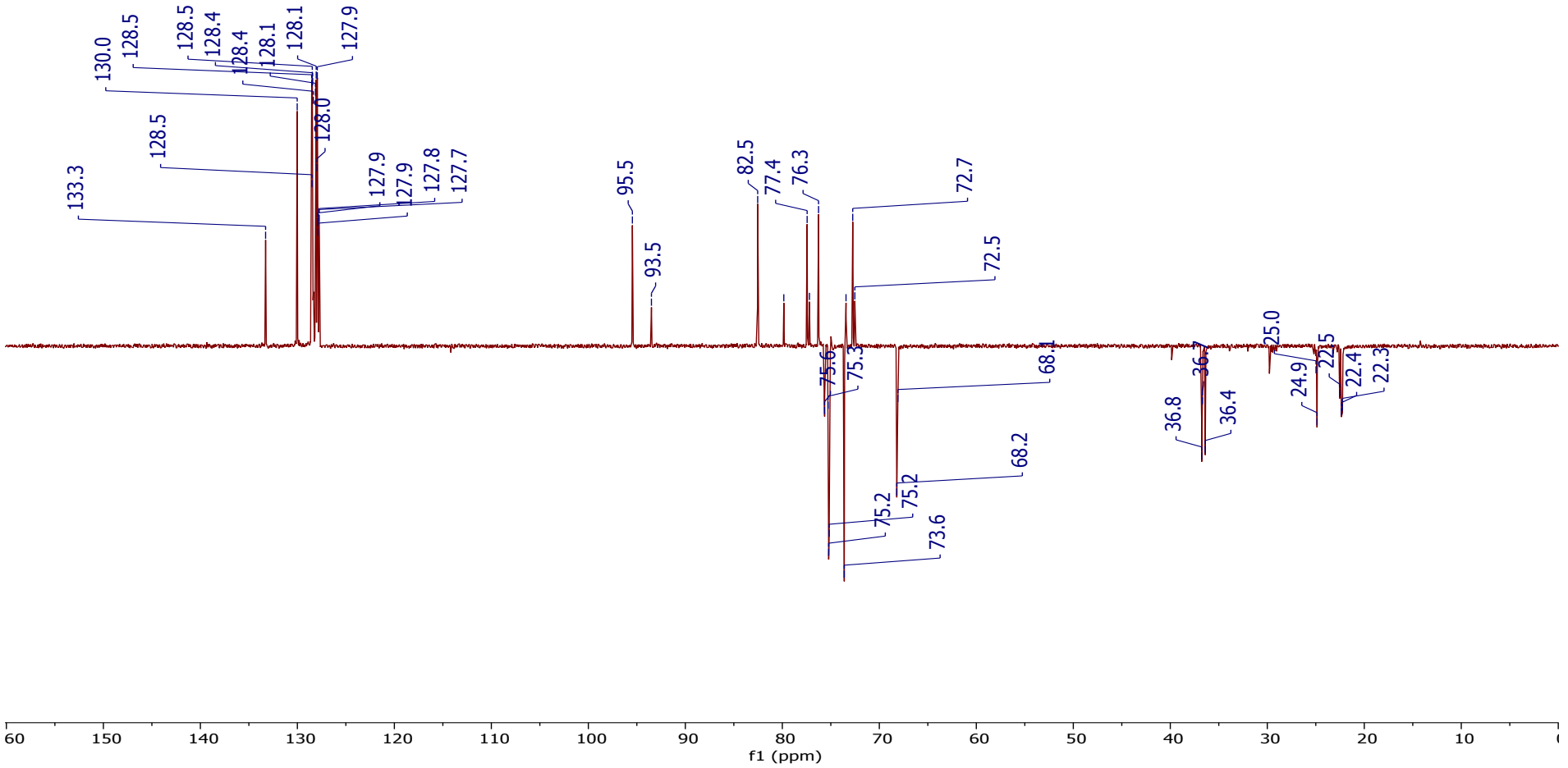

^{1}H NMR Spectrum (400.31 MHz, $CDCl_3$) of Compound **12d**

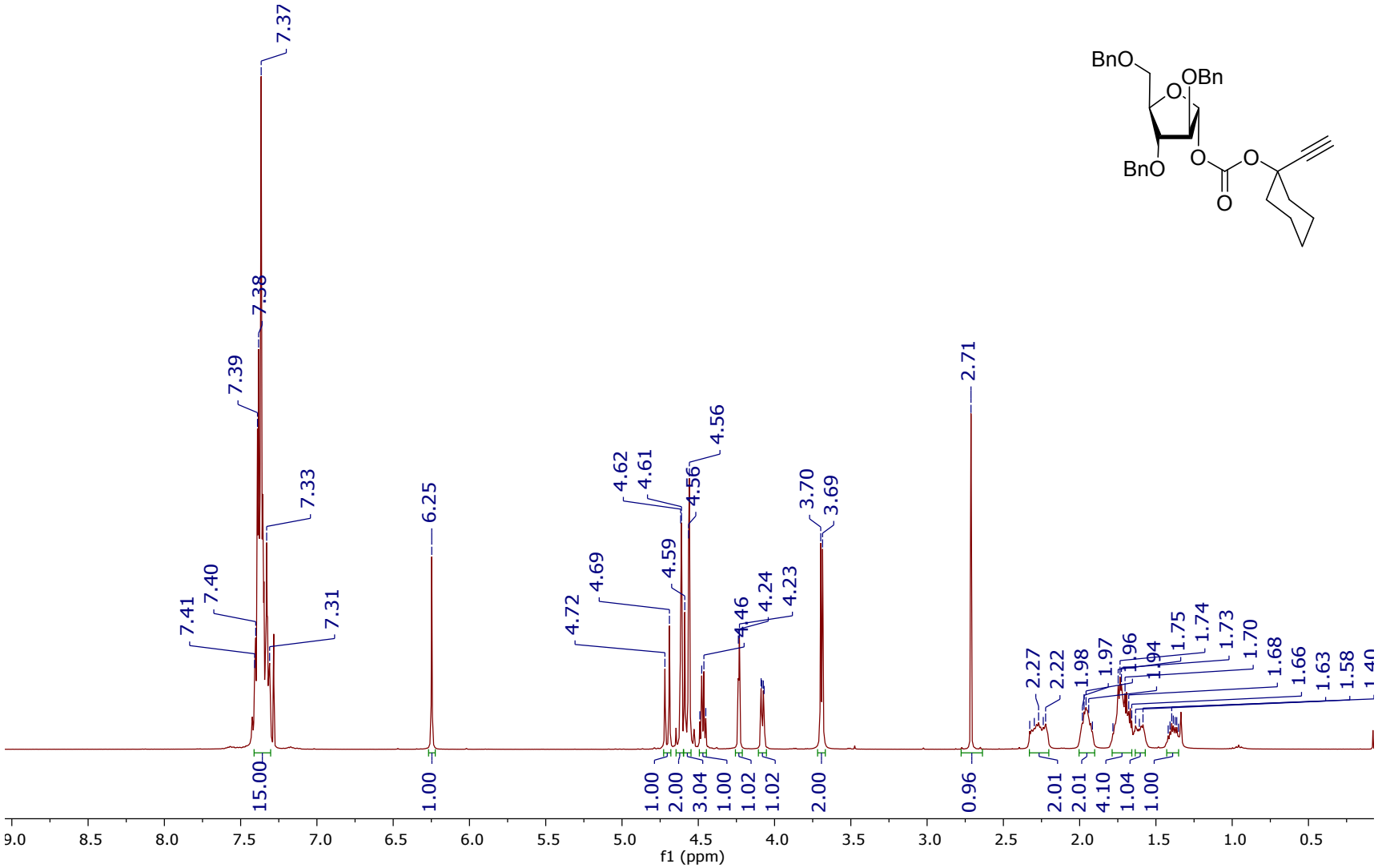

^{13}C NMR Spectrum (100.67 MHz, $CDCl_3$) of Compound **12d**

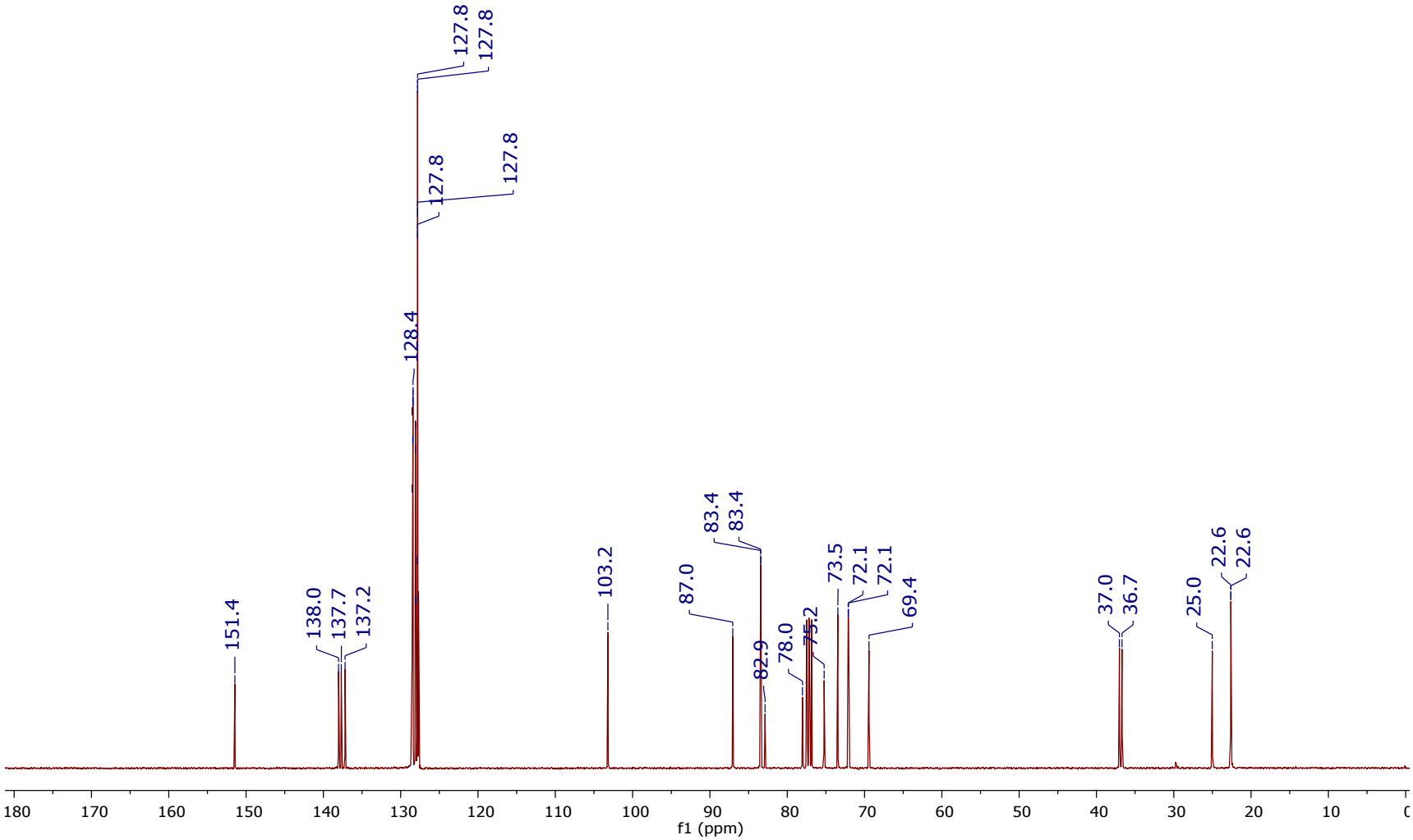

DEPT NMR Spectrum (100.67 MHz, $CDCl_3$) of Compound **12d**

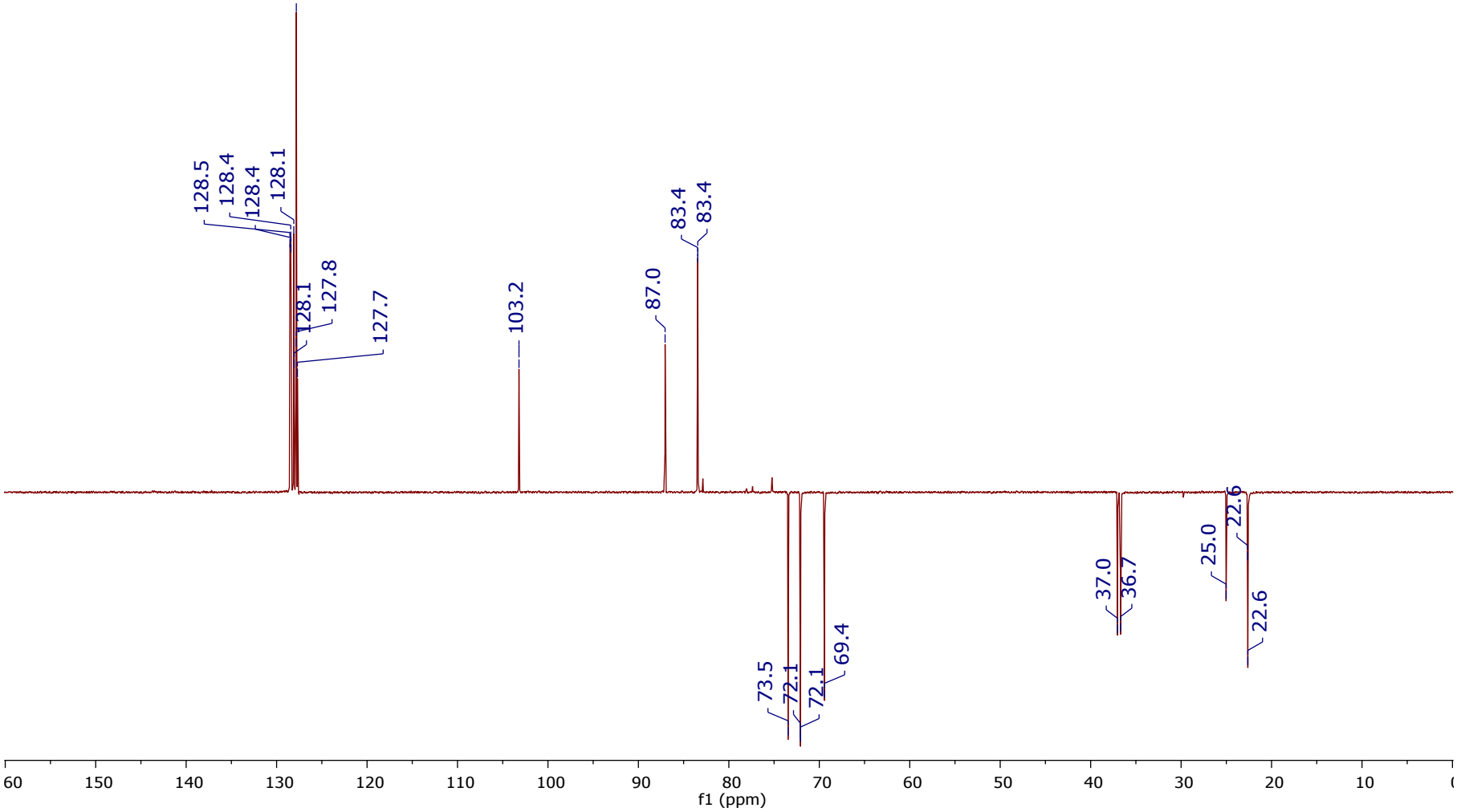

^{1}H NMR Spectrum (400.31 MHz, $CDCl_3$) of Compound **14a**

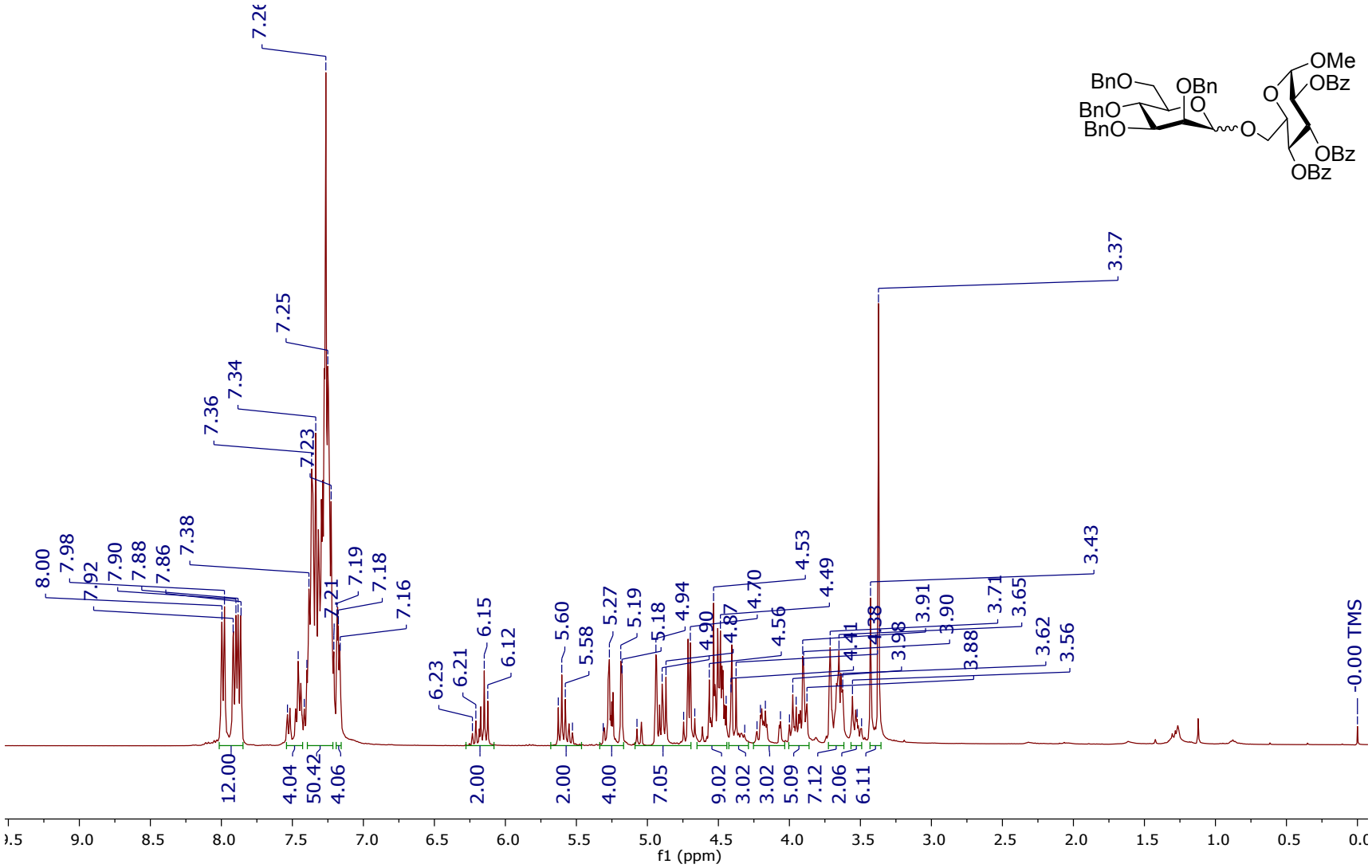

^{13}C NMR Spectrum (100.67 MHz, $CDCl_3$) of Compound **14a**

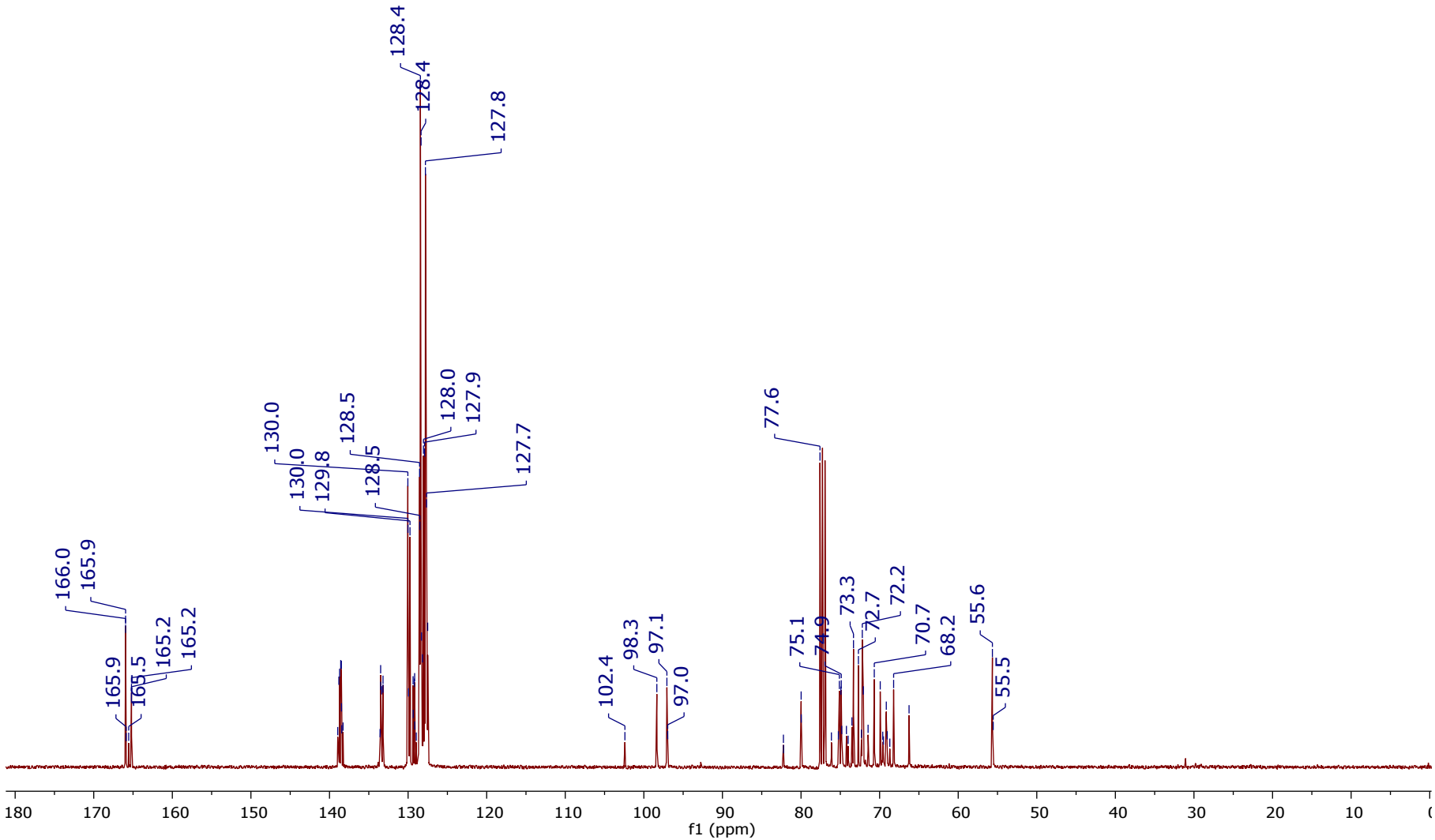

DEPT NMR Spectrum (100.67 MHz, $CDCl_3$) of Compound **14a**

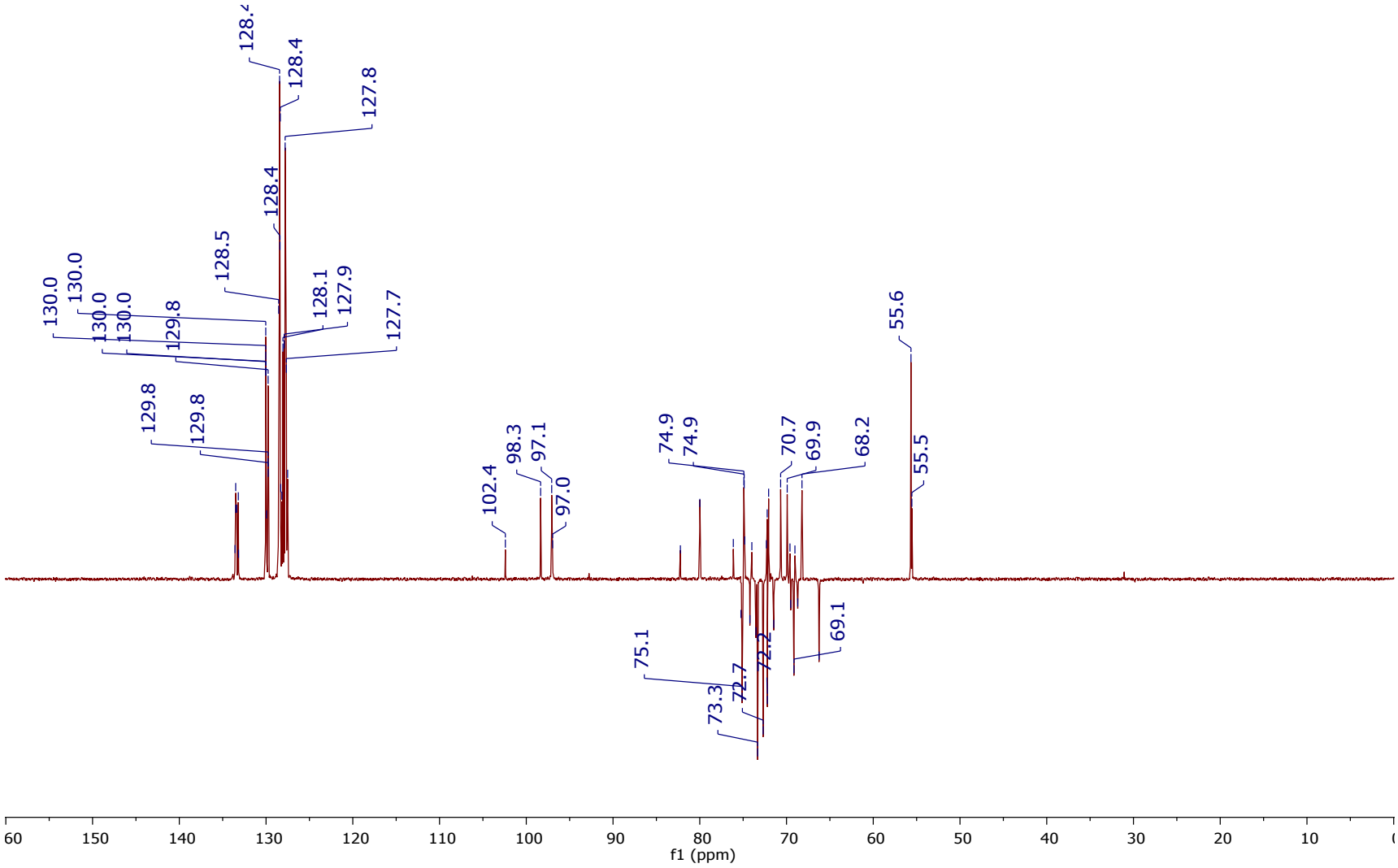

^{1}H NMR Spectrum (400.31 MHz, $CDCl_3$) of Compound **14b**

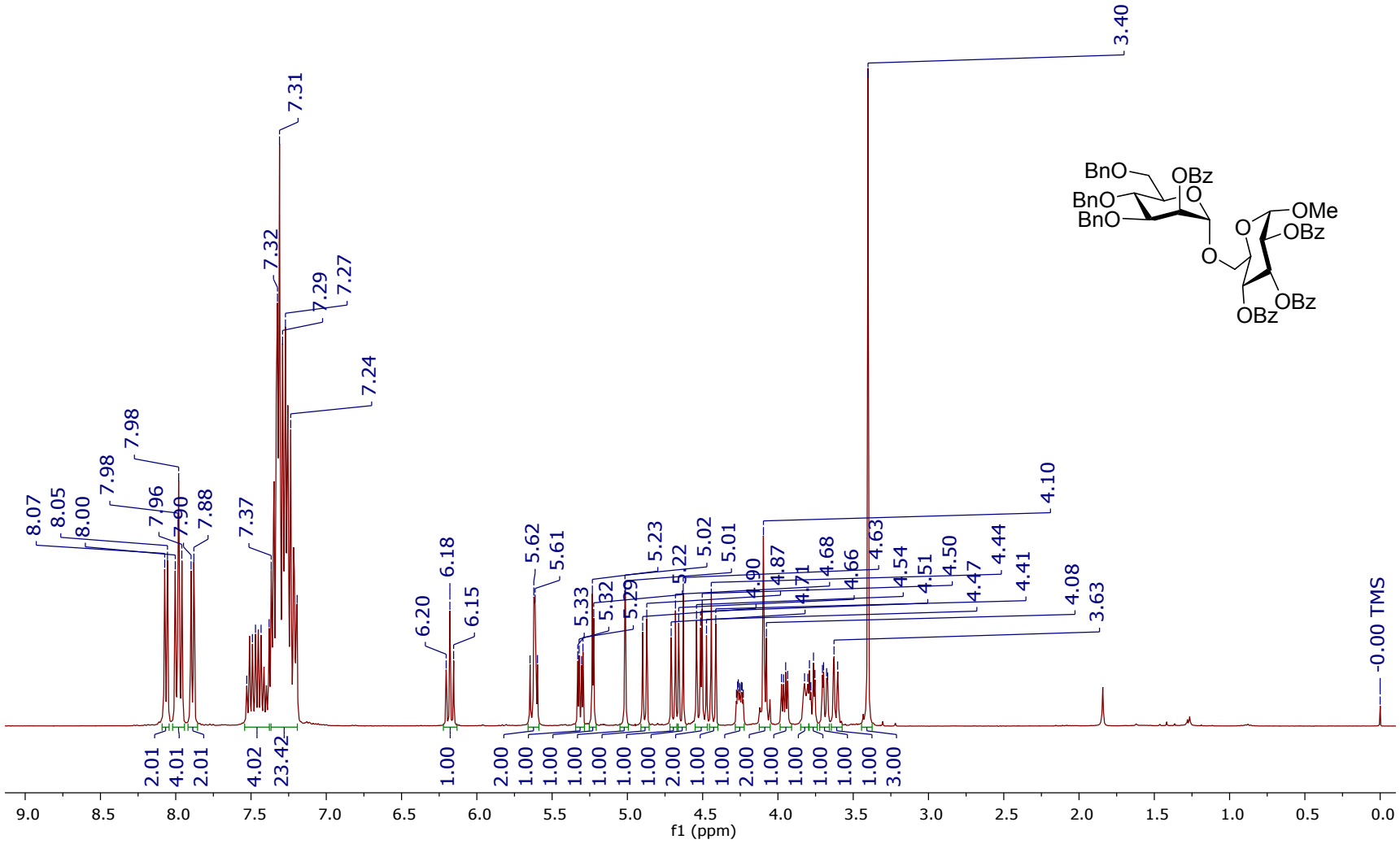

^{13}C NMR Spectrum (100.67 MHz, $CDCl_3$) of Compound **14b**

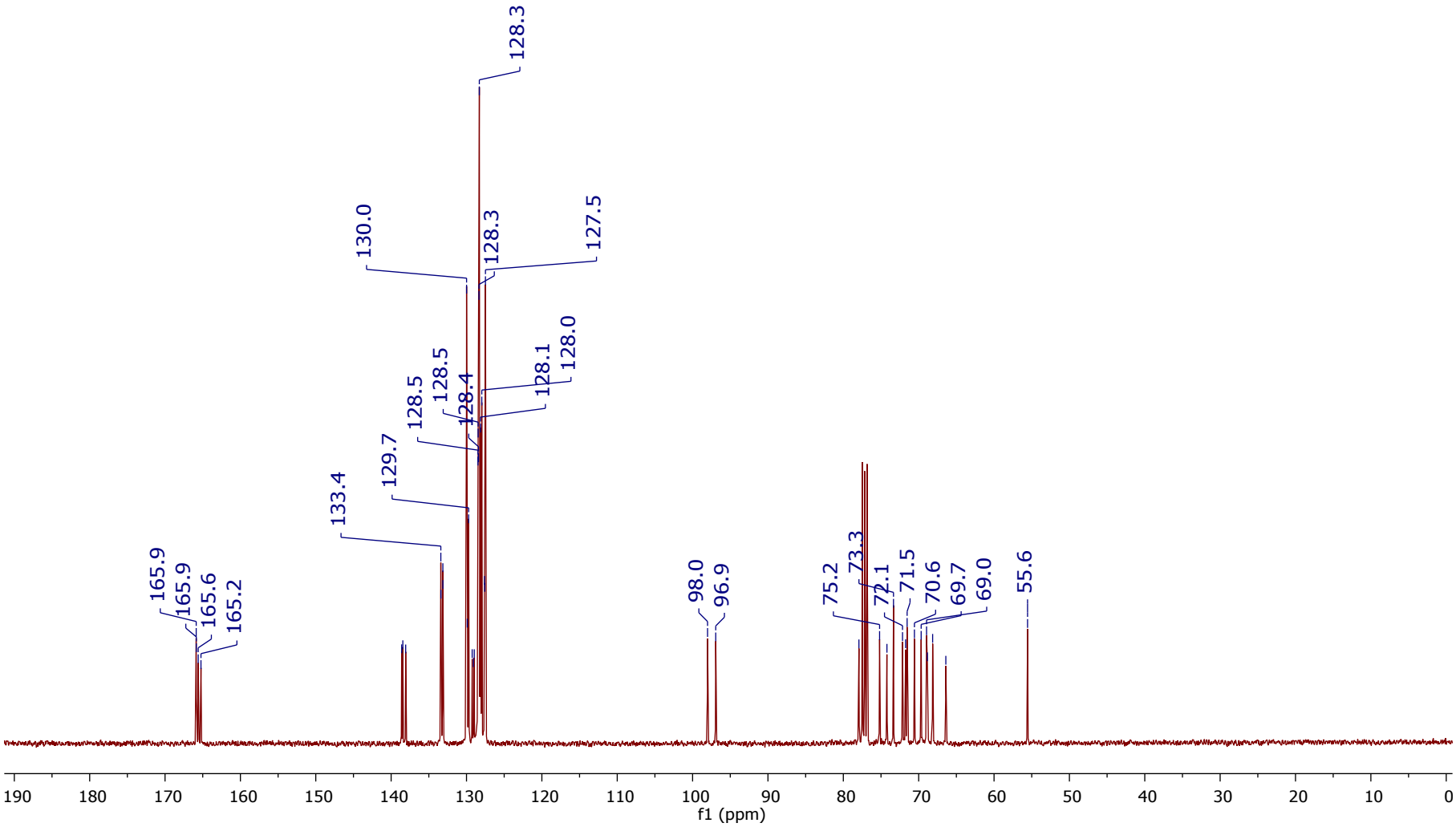

DEPT NMR Spectrum (100.67 MHz, $CDCl_3$) of Compound **14b**

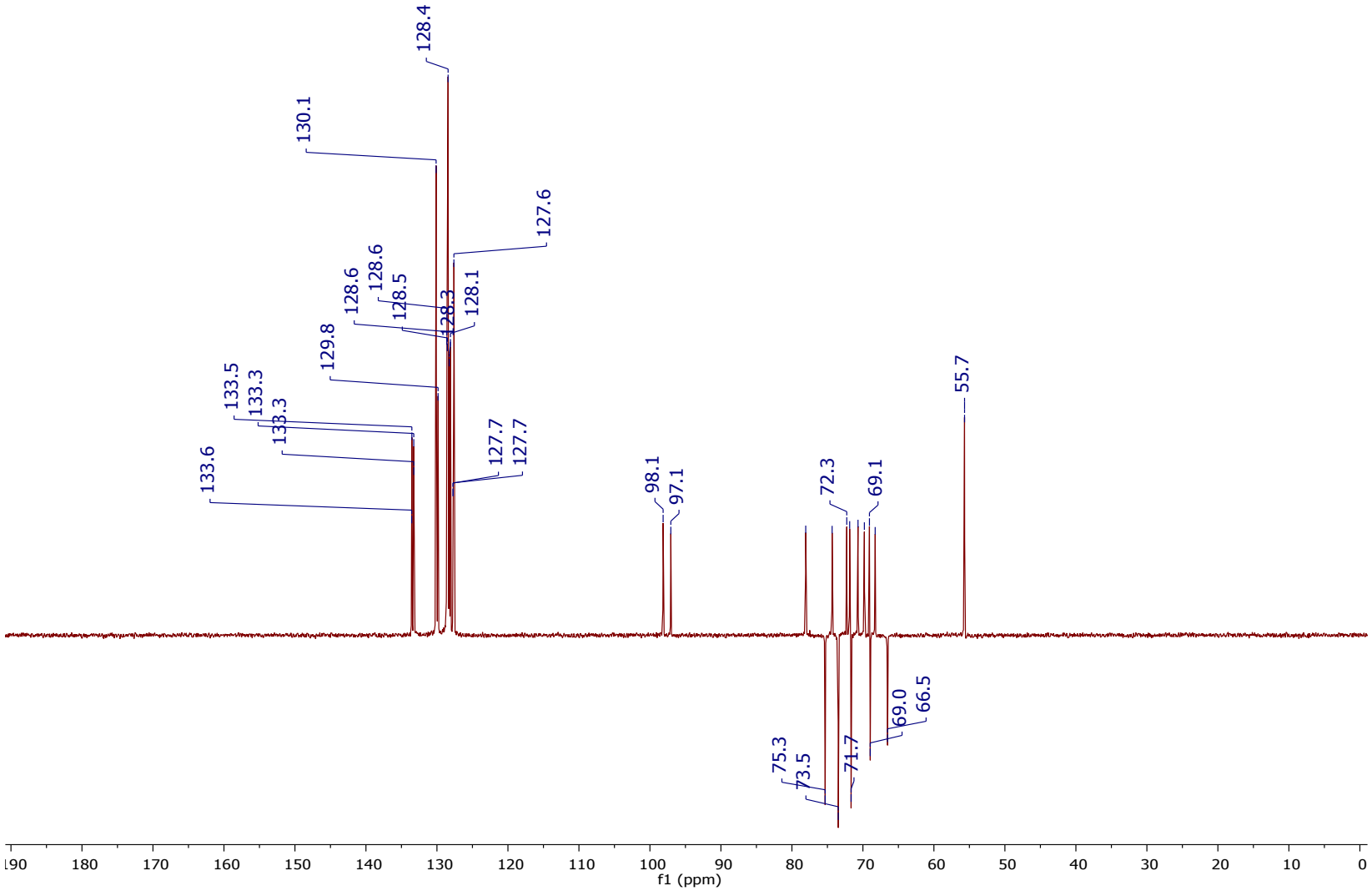

^{1}H NMR Spectrum (400.31 MHz, $CDCl_3$) of Compound **14c**

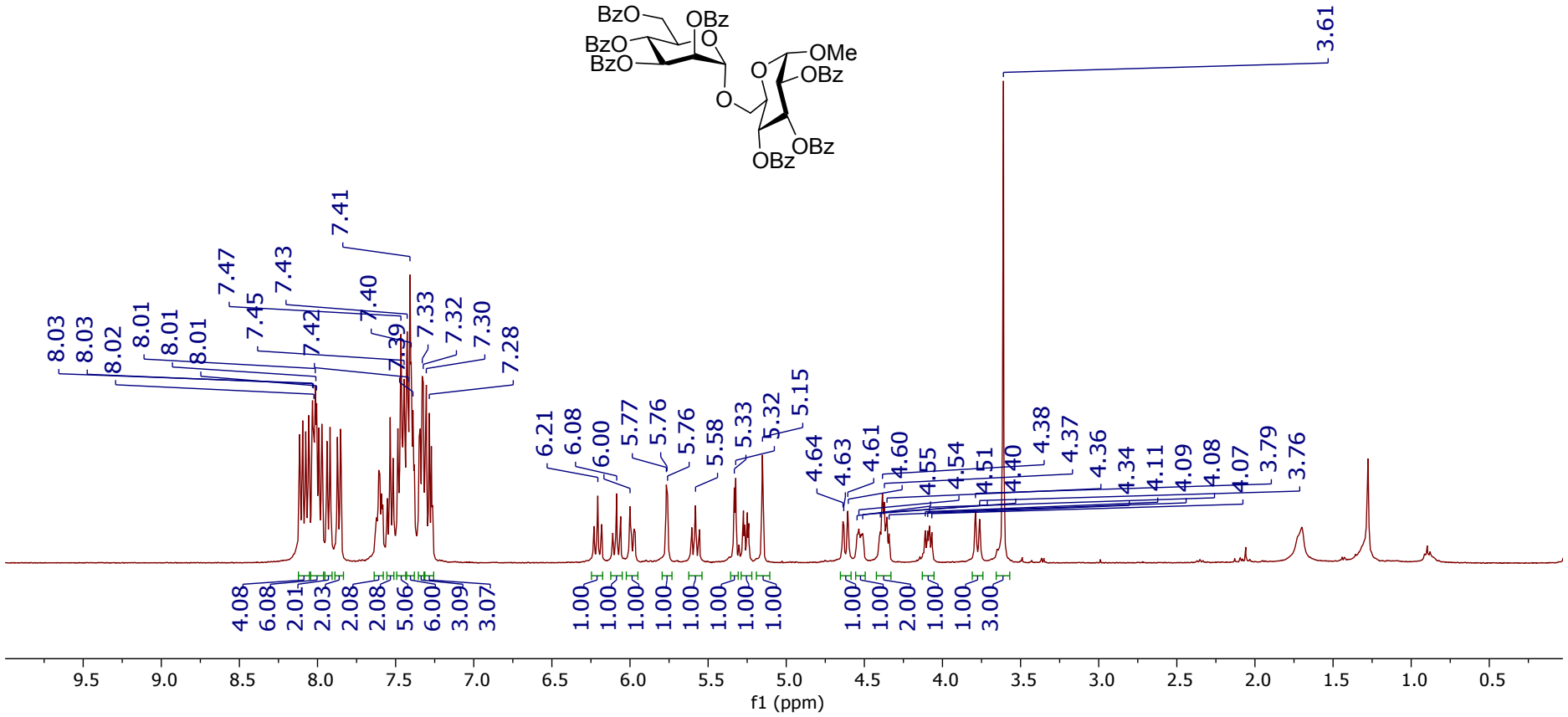

^{13}C NMR Spectrum (100.67 MHz, $CDCl_3$) of Compound **14c**

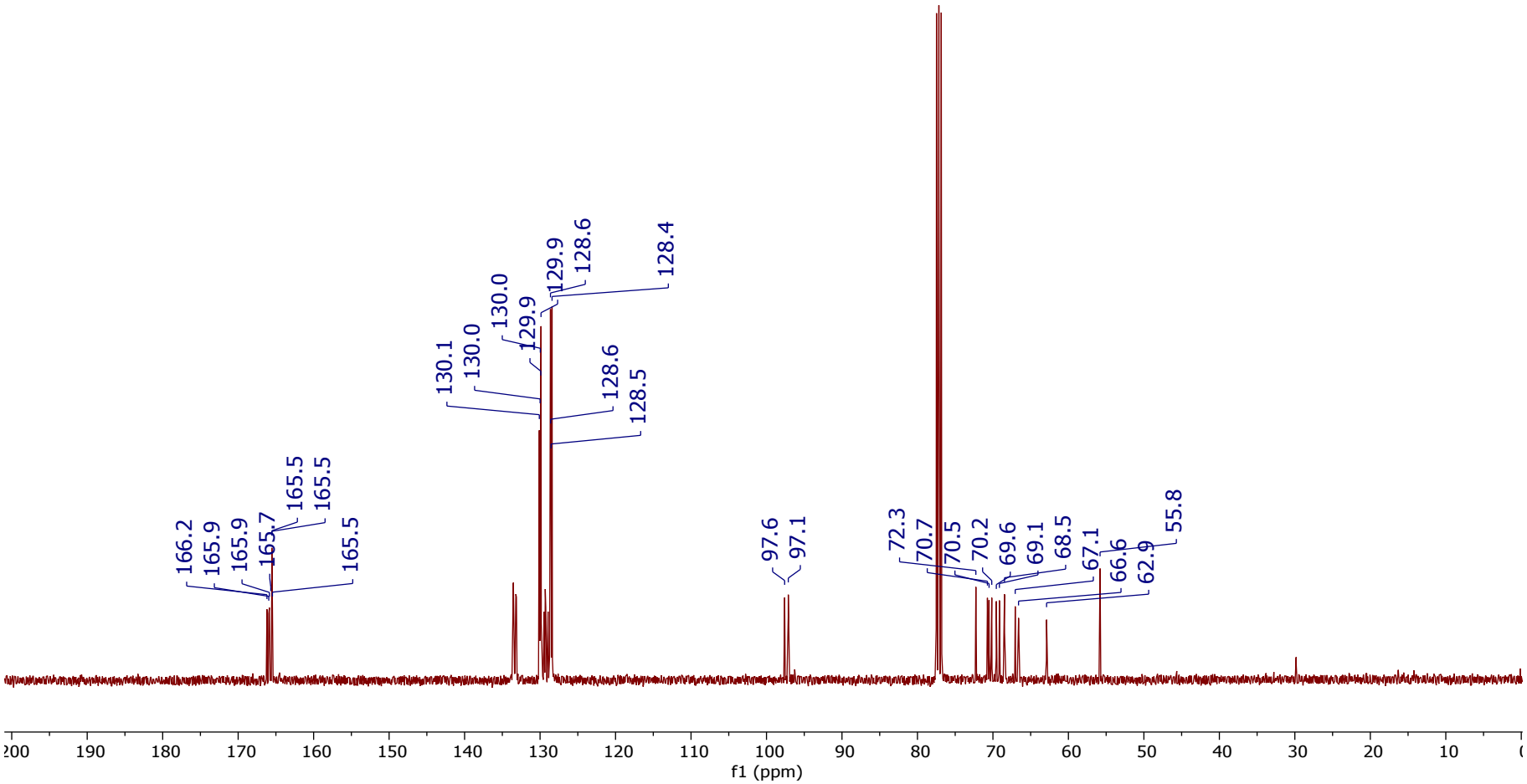

DEPT NMR Spectrum (100.67 MHz, $CDCl_3$) of Compound **14c**

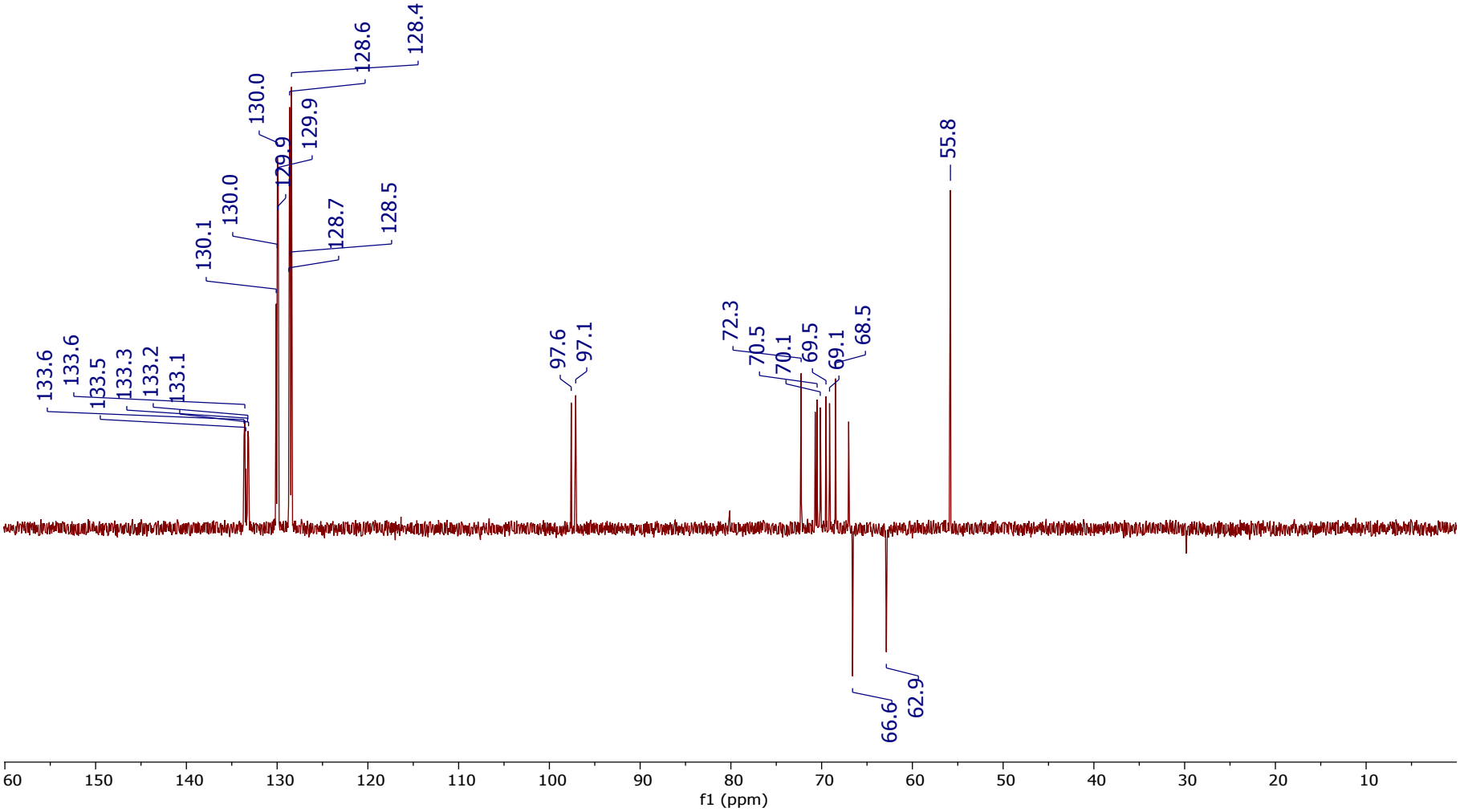

^{1}H NMR Spectrum (400.31 MHz, $CDCl_3$) of Compound **14d**

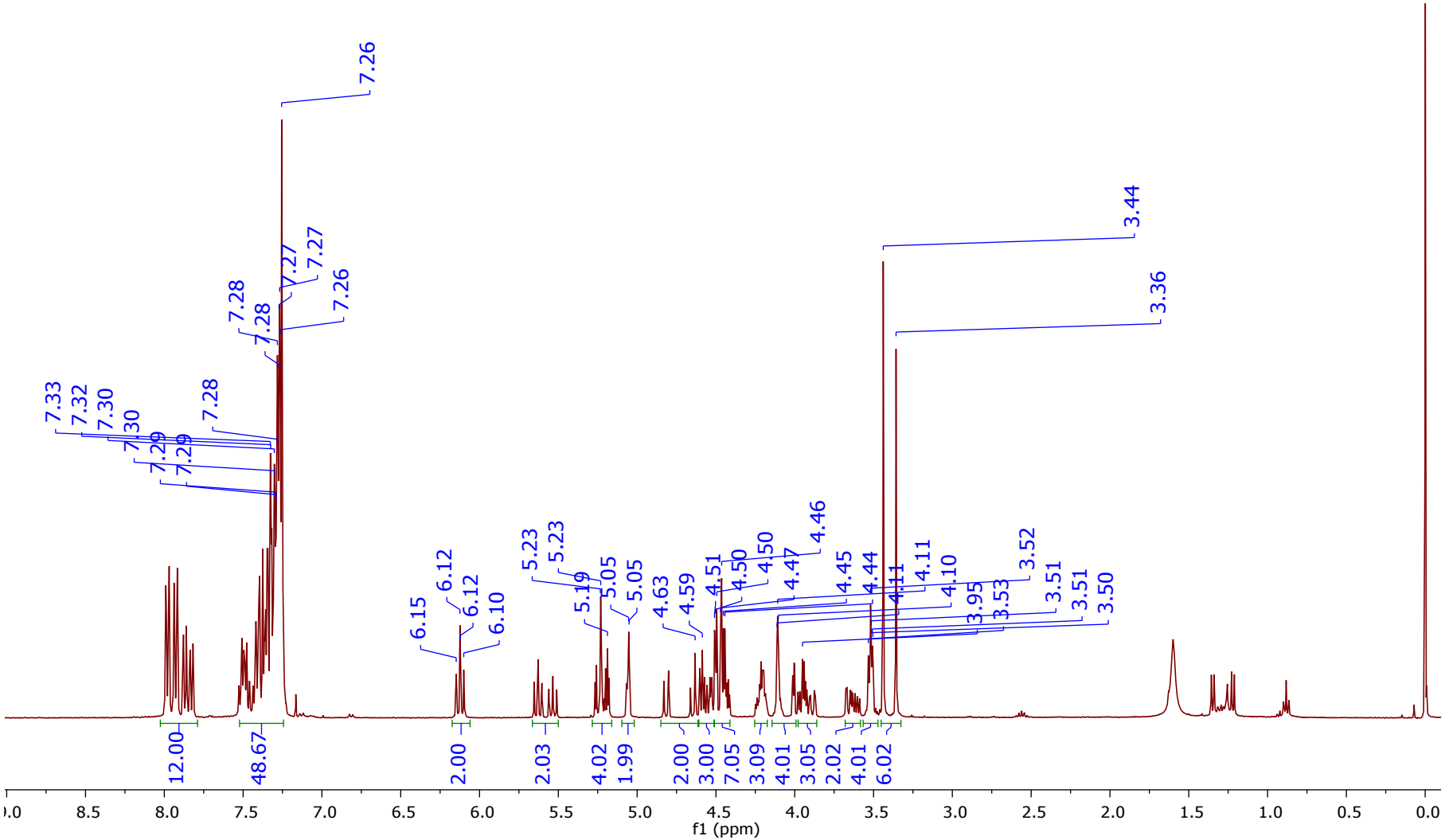

^{13}C NMR Spectrum (100.67 MHz, $CDCl_3$) of Compound **14d**

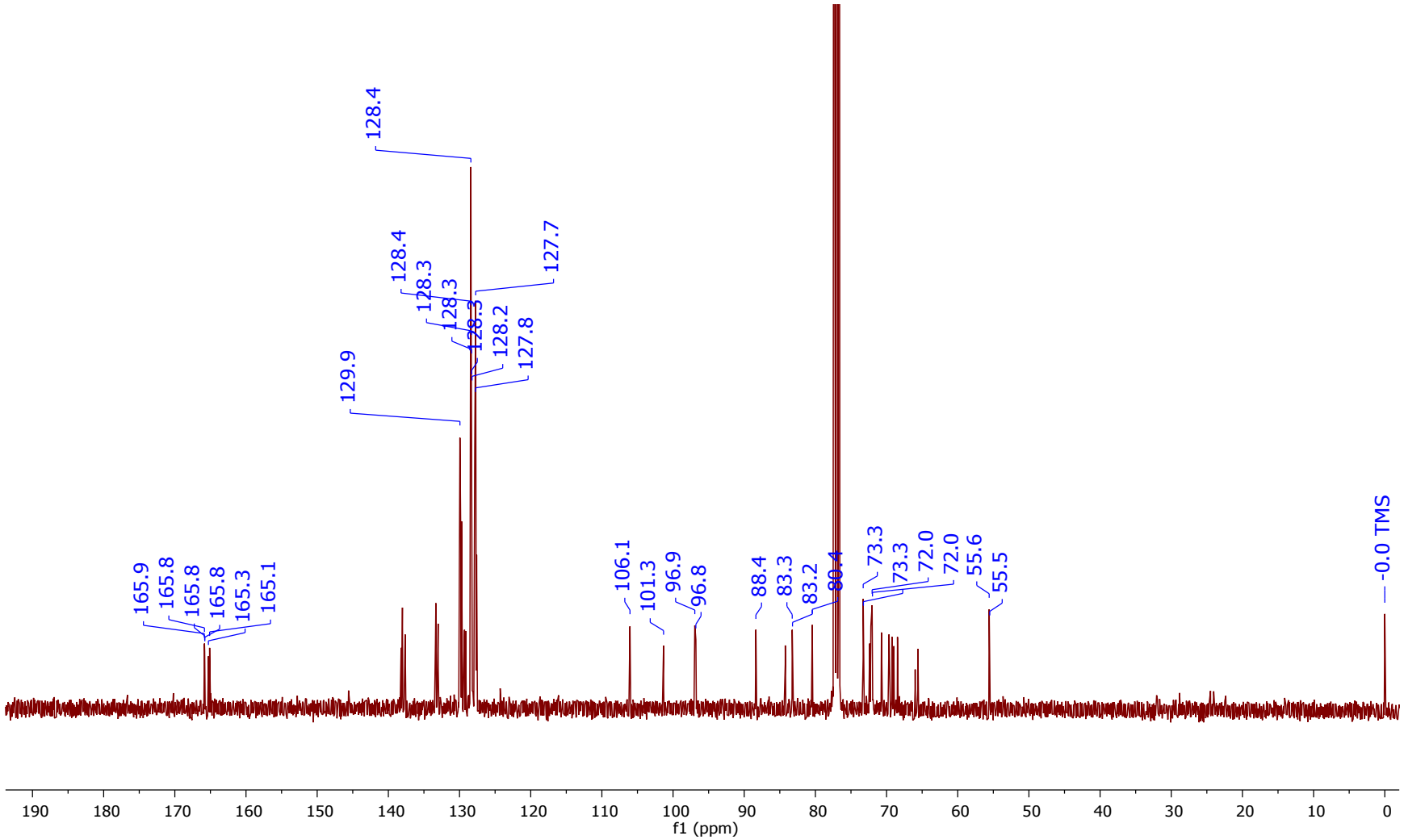

DEPT NMR Spectrum (100.67 MHz, $CDCl_3$) of Compound **14d**

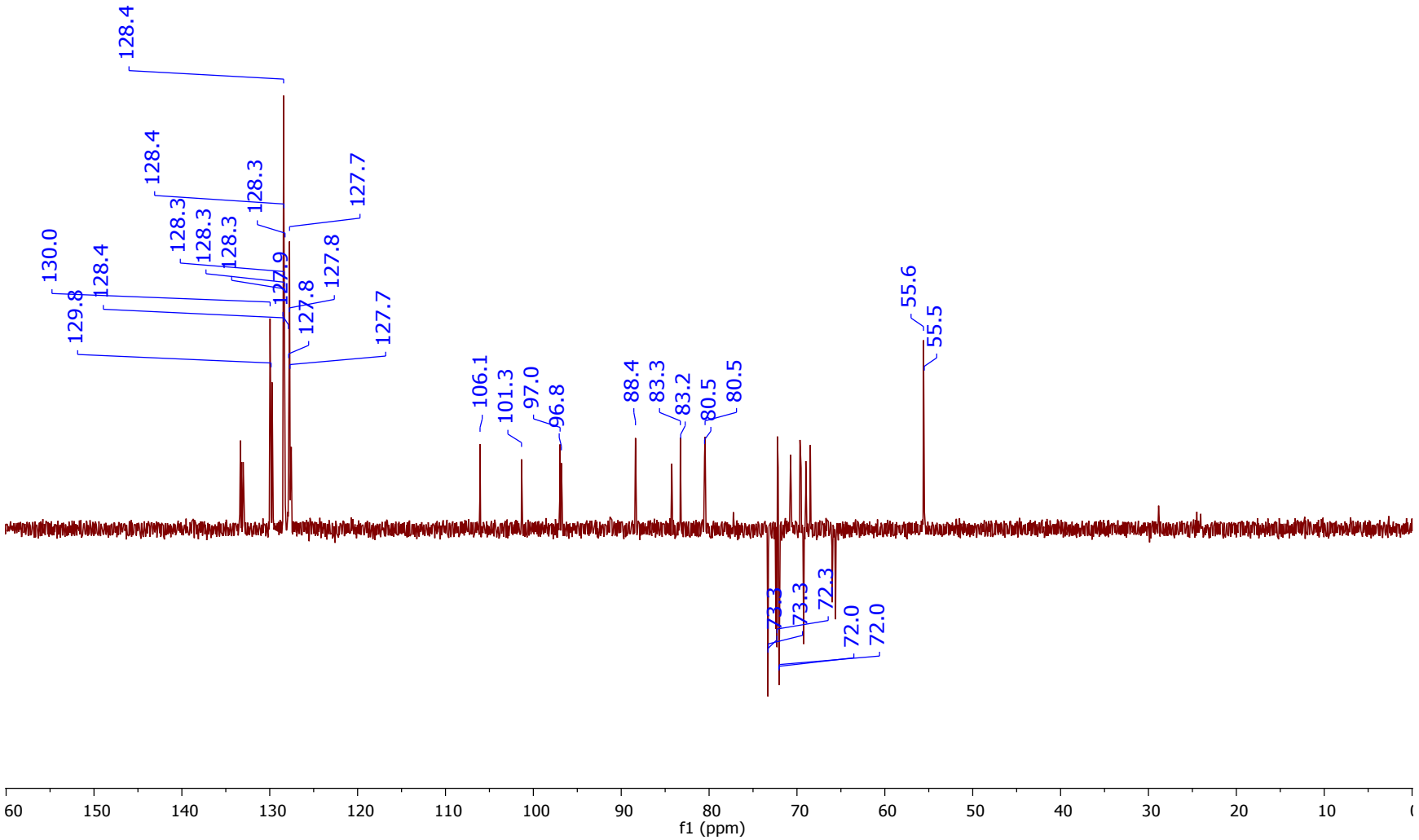

^{1}H NMR Spectrum (400.31 MHz, $CDCl_3$) of Compound **14f**

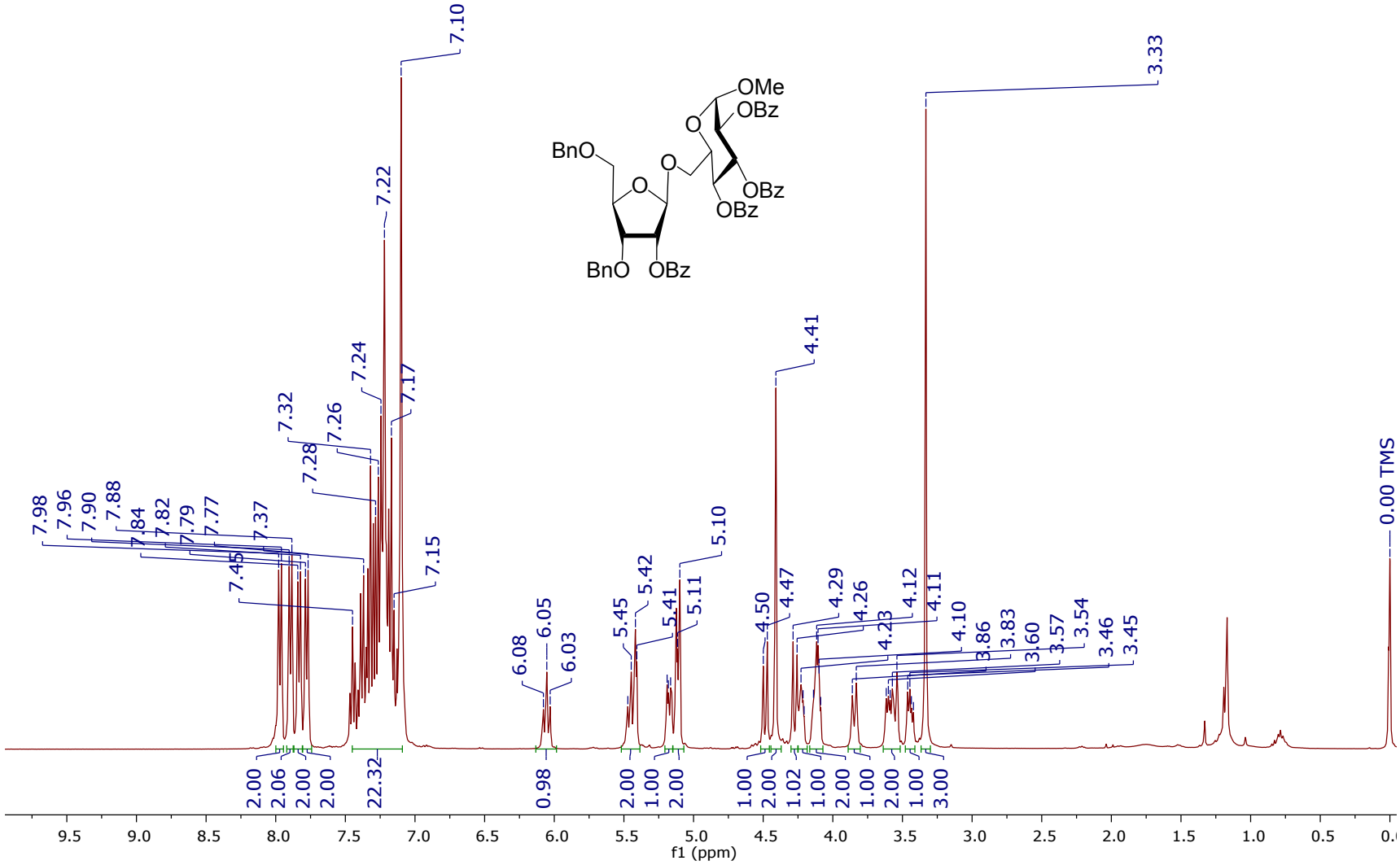

^{13}C NMR Spectrum (100.67 MHz, $CDCl_3$) of Compound **14f**

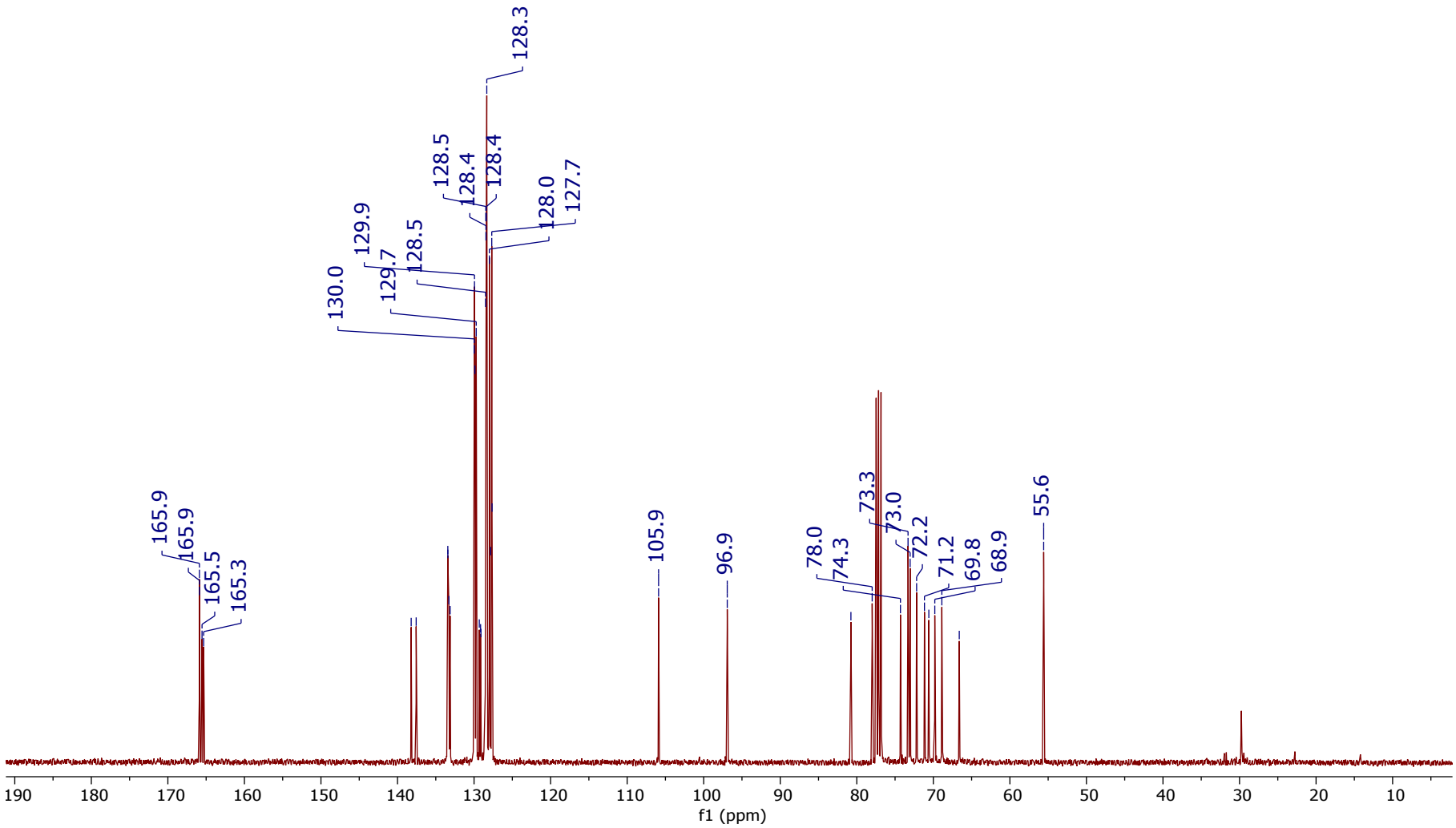

DEPT NMR Spectrum (100.67 MHz, $CDCl_3$) of Compound **14f**

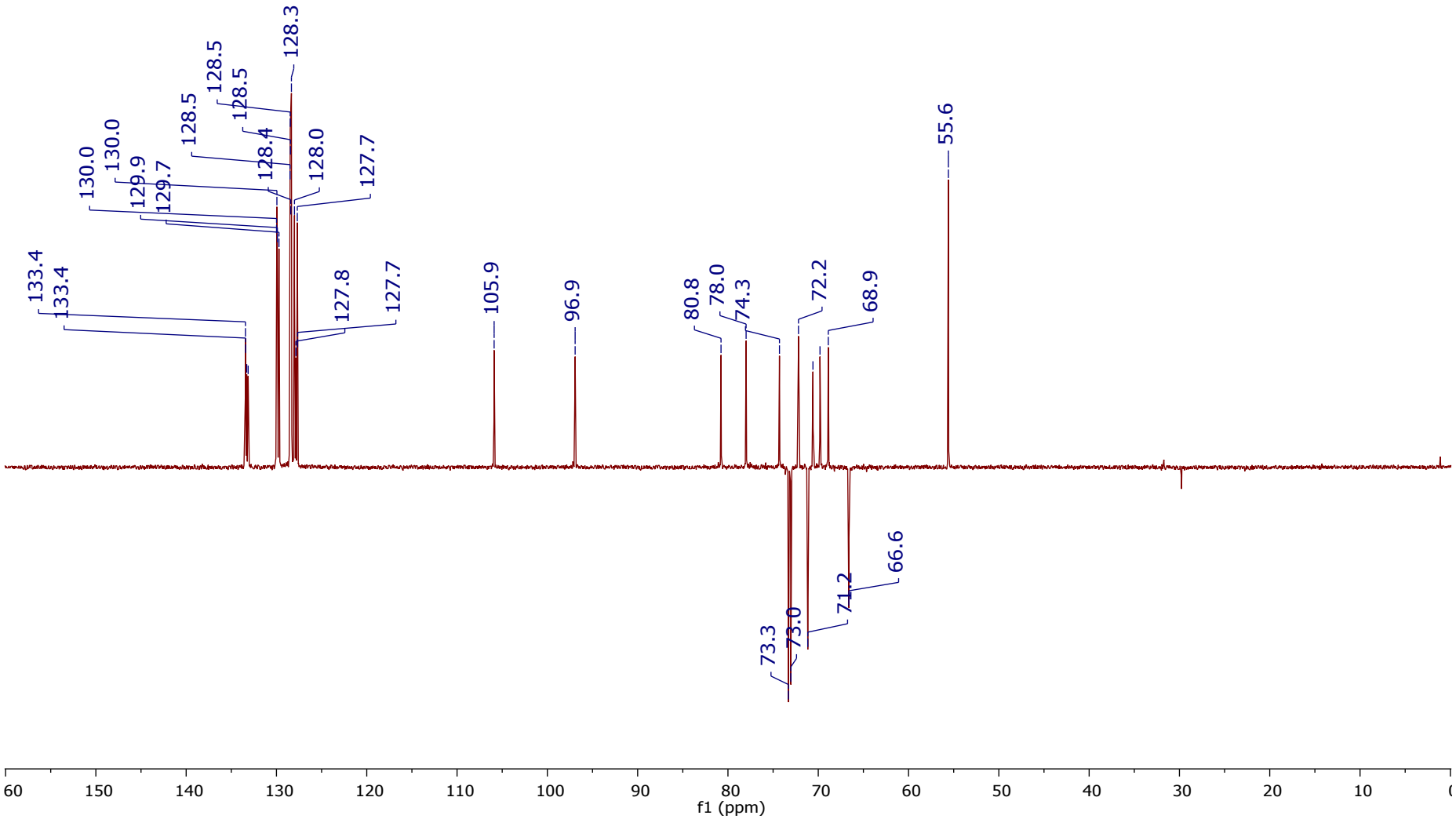
133.4
133.4
130.0
130.0
129.9
129.7
128.5
128.5
128.5
128.4
128.3
128.0
127.8
127.7
127.7
105.9
96.9
80.8
78.0
74.3
72.2
68.9
55.6
66.6
71.2
73.0
73.3
60
150
140
130
120
110
100
90
80
70
60
50
40
30
20
10
f1 (ppm)

^{1}H NMR Spectrum (400.31 MHz, $CDCl_3$) of Compound **17**

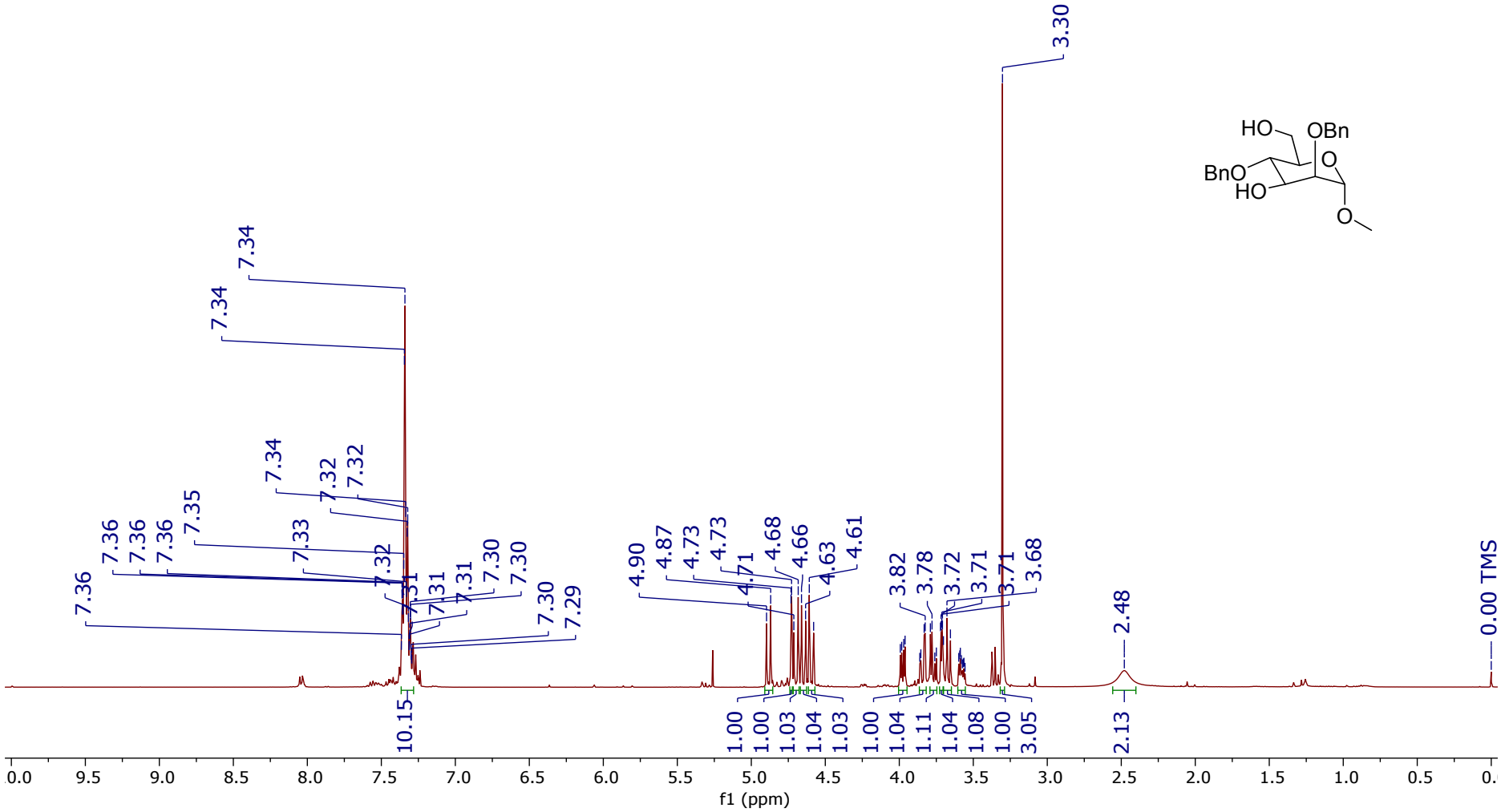

^{13}C NMR Spectrum (100.67 MHz, $CDCl_3$) of Compound **17**

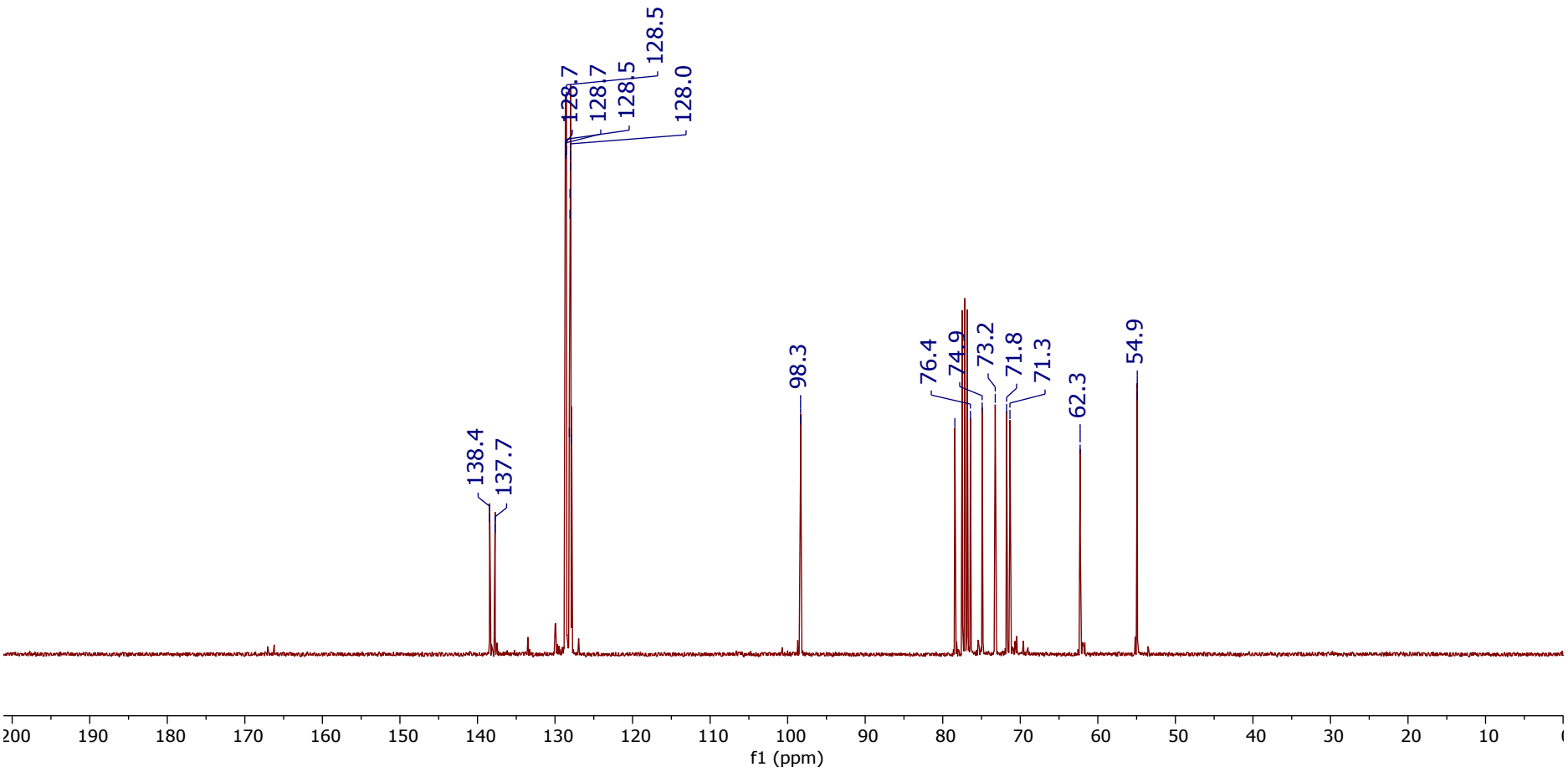

DEPT NMR Spectrum (100.67 MHz, $CDCl_3$) of Compound **17**

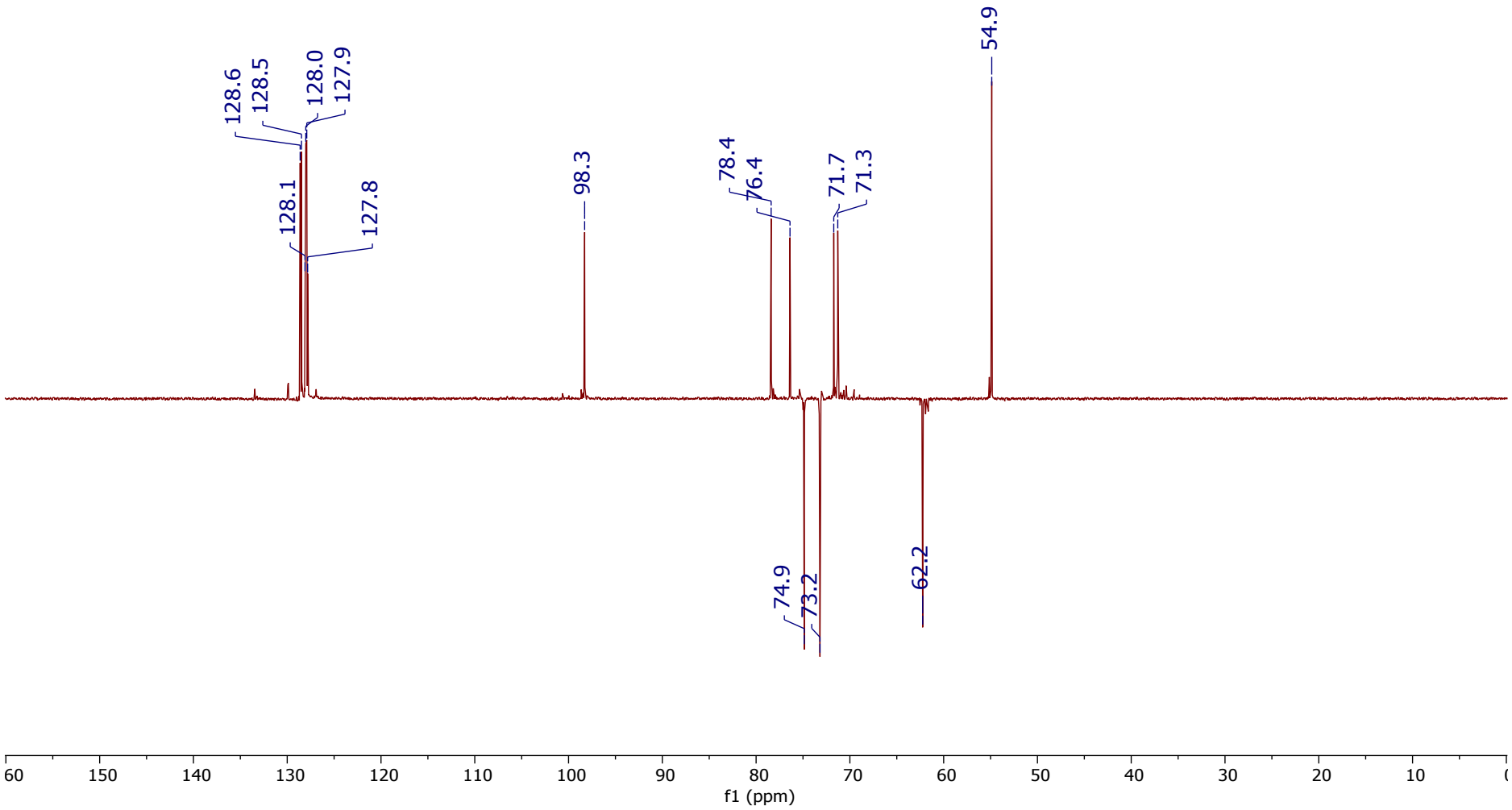

^{1}H NMR Spectrum (400.31 MHz, $CDCl_3$) of compound **18**

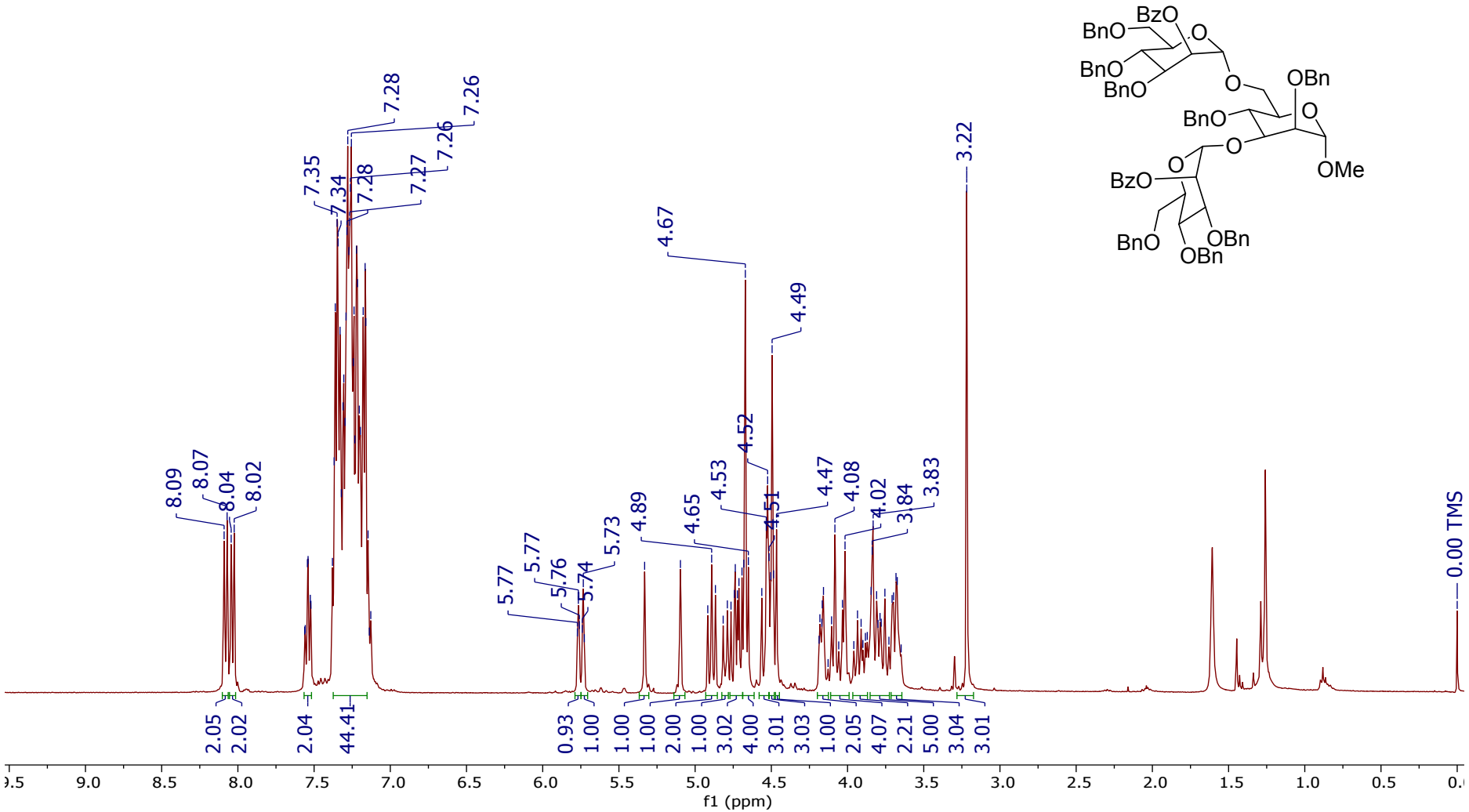

^{13}C NMR Spectrum (100.67 MHz, $CDCl_3$) of compound **18**

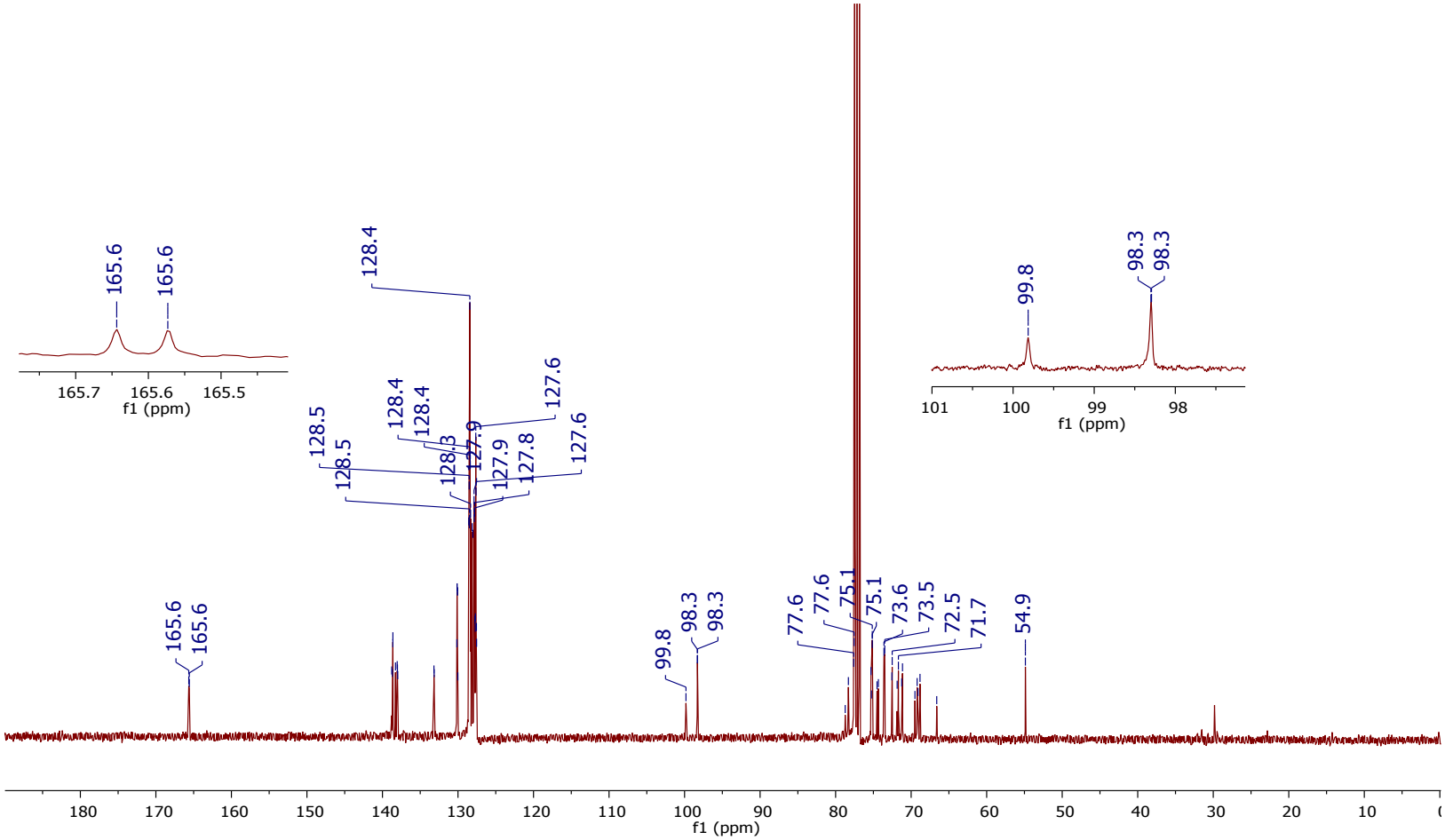

DEPT NMR Spectrum (100.67 MHz, $CDCl_3$) of compound **18**

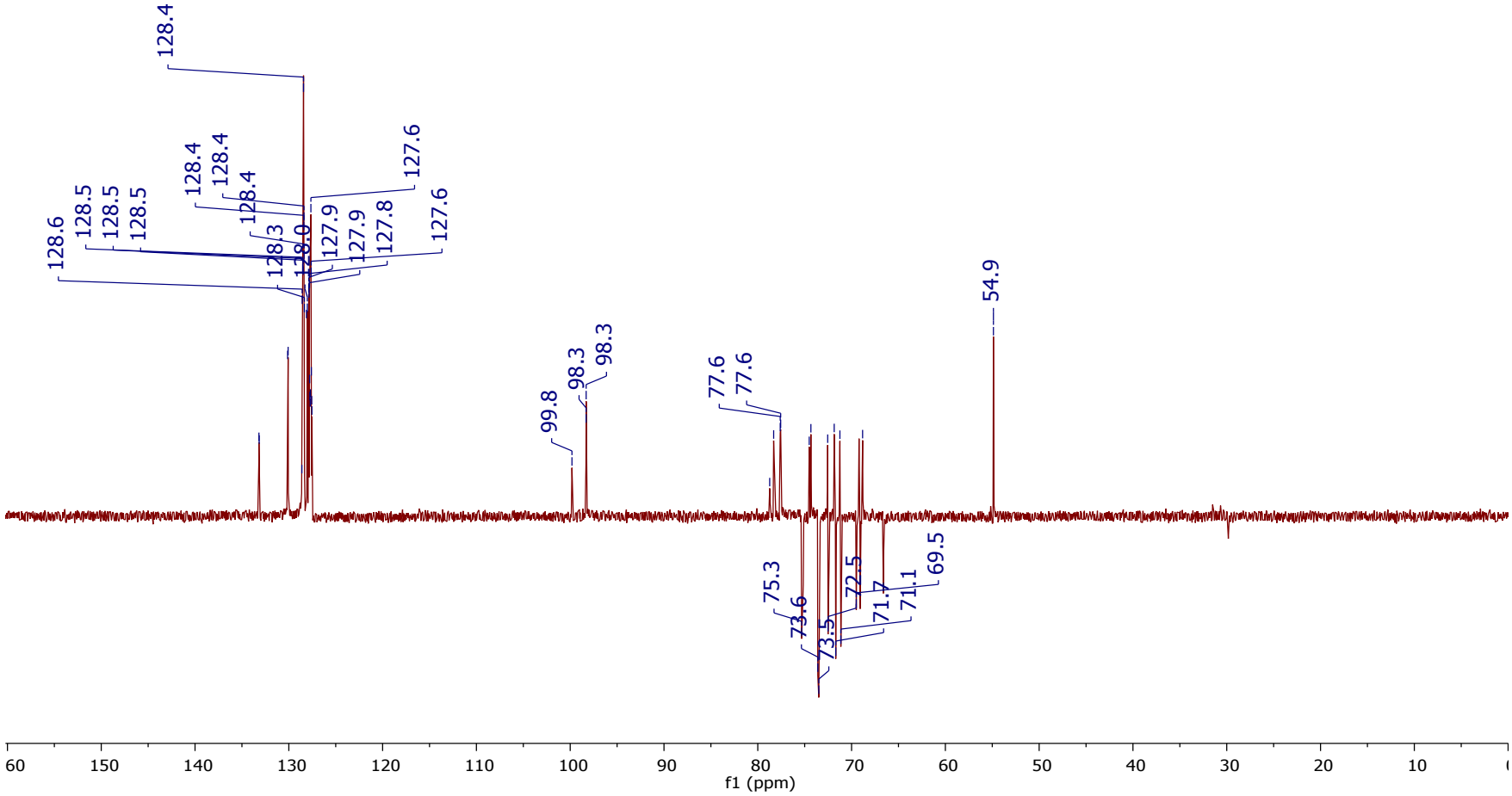

^{1}H NMR Spectrum (400.31 MHz, $CDCl_3$) of compound **19**

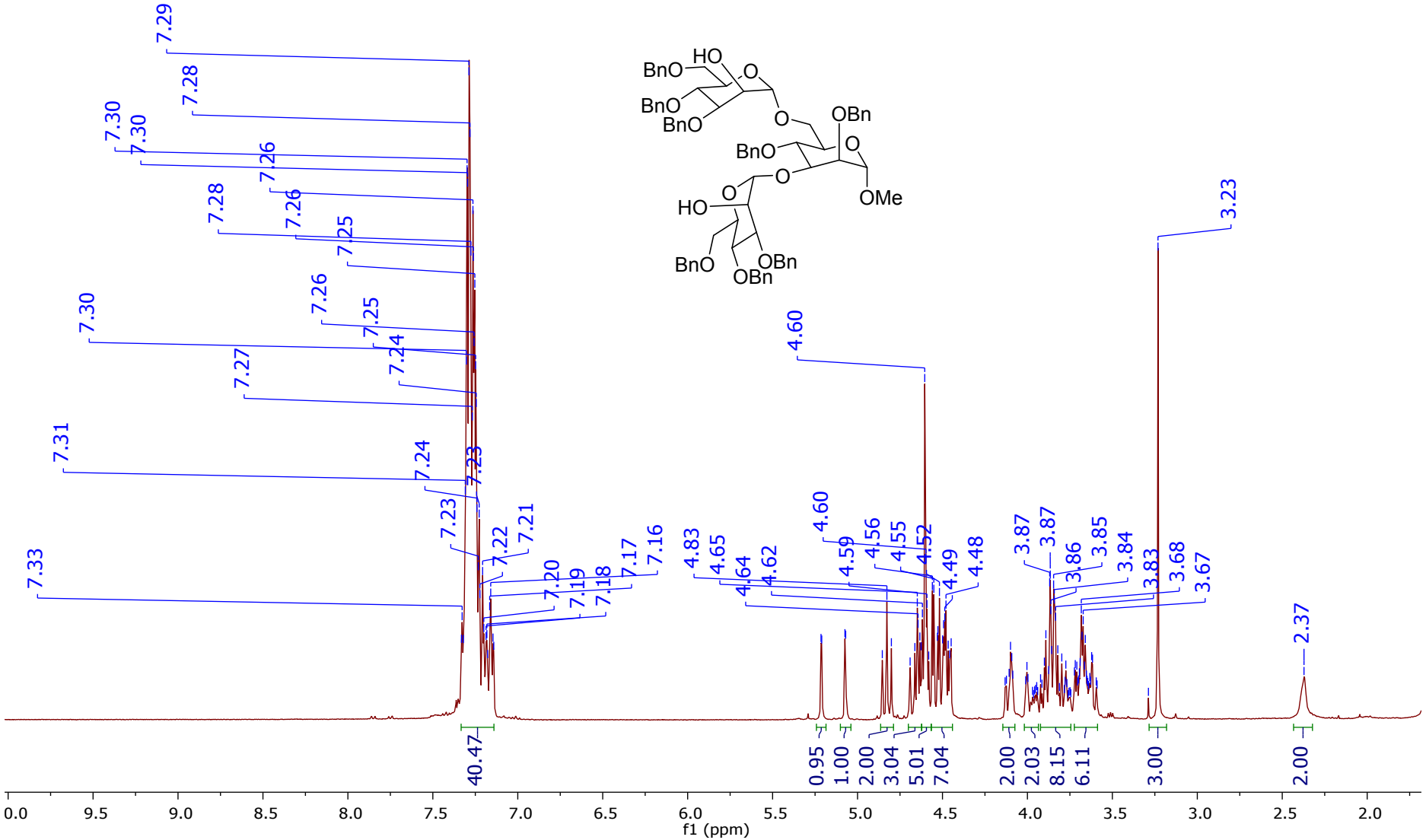

^{13}C NMR Spectrum (100.67 MHz, $CDCl_3$) of compound **19**

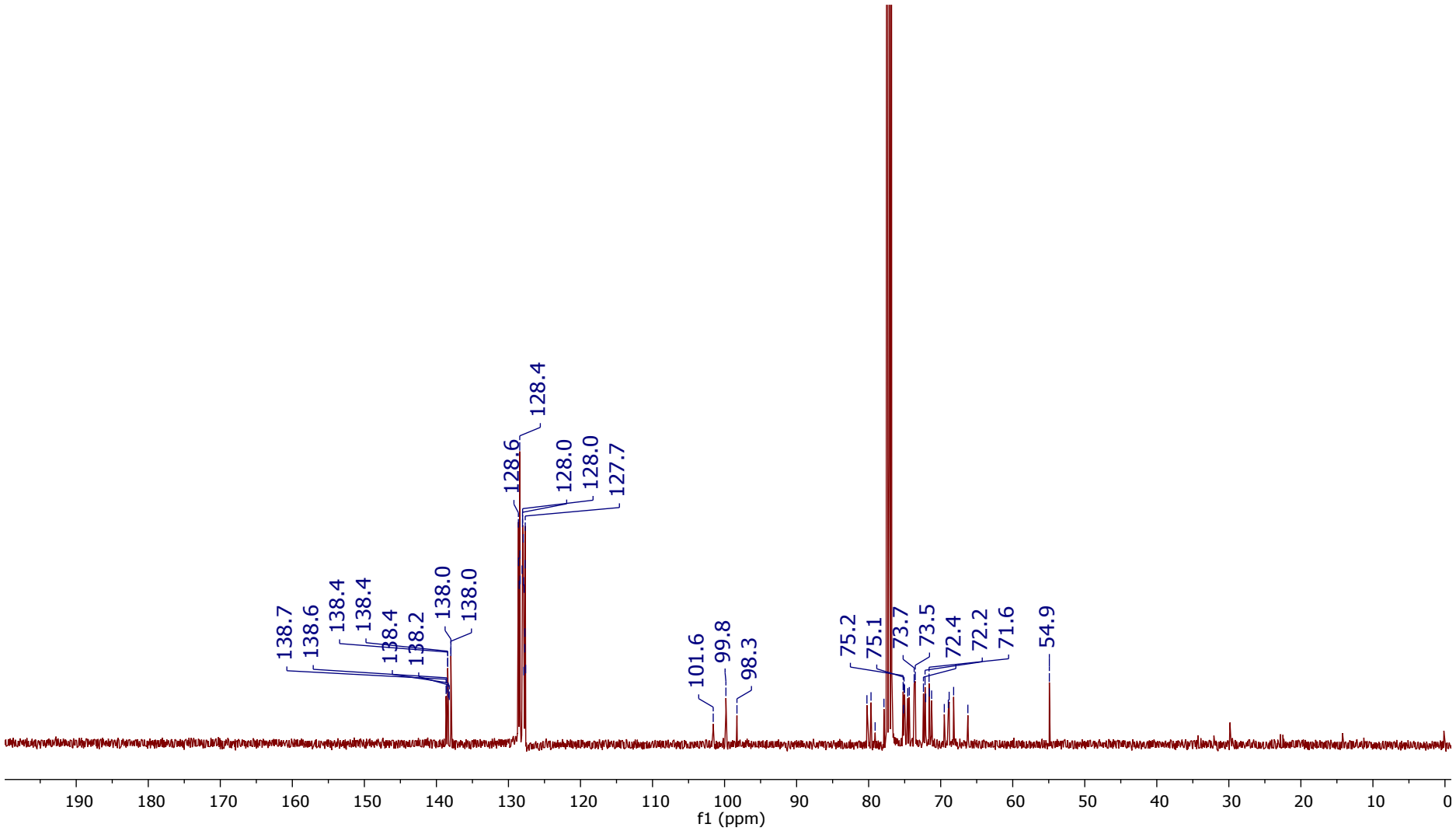

DEPT NMR Spectrum (100.67 MHz, $CDCl_3$) of compound **19**

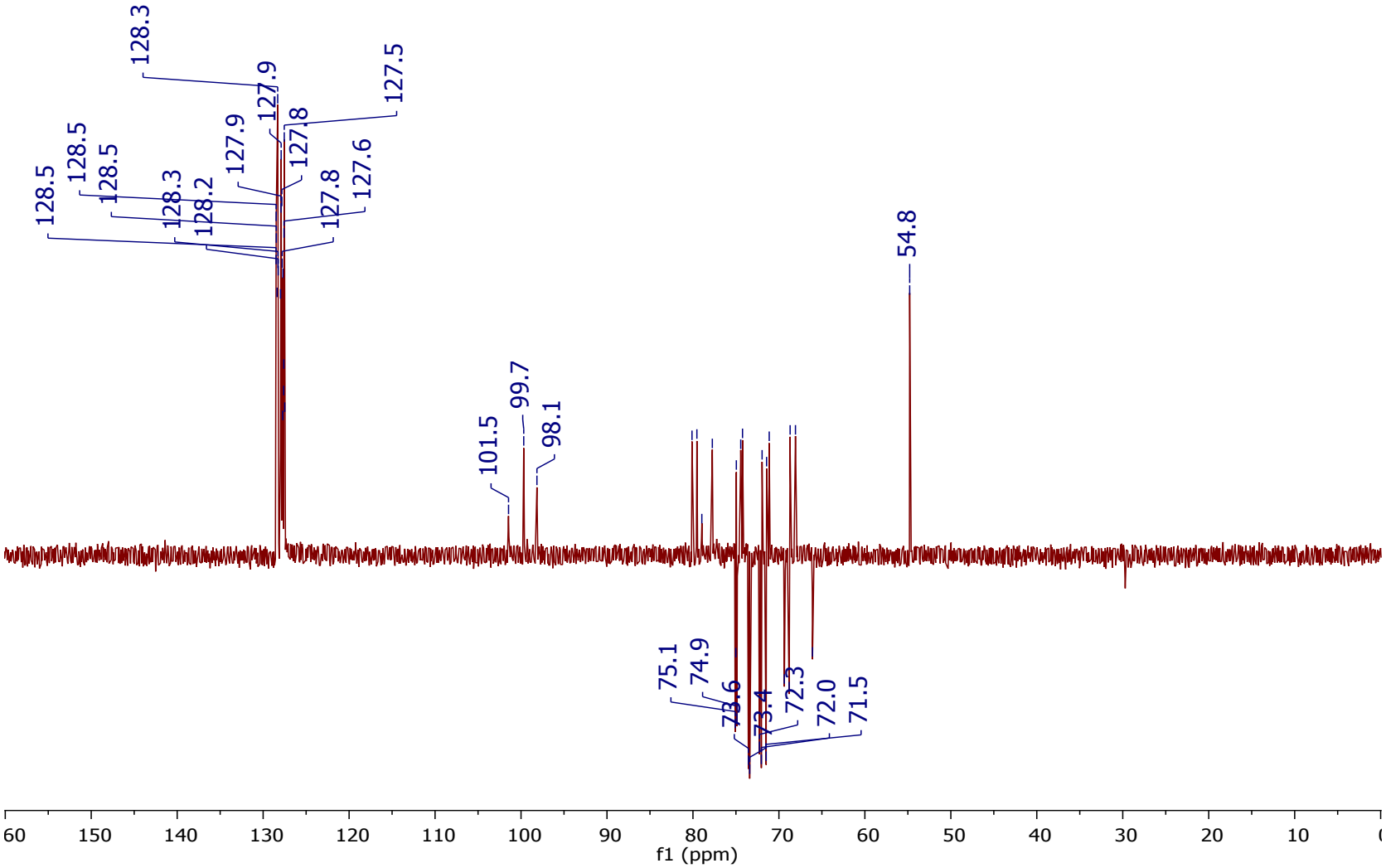

^{1}H NMR Spectrum (400.31 MHz, $CDCl_3$) of compound **20**

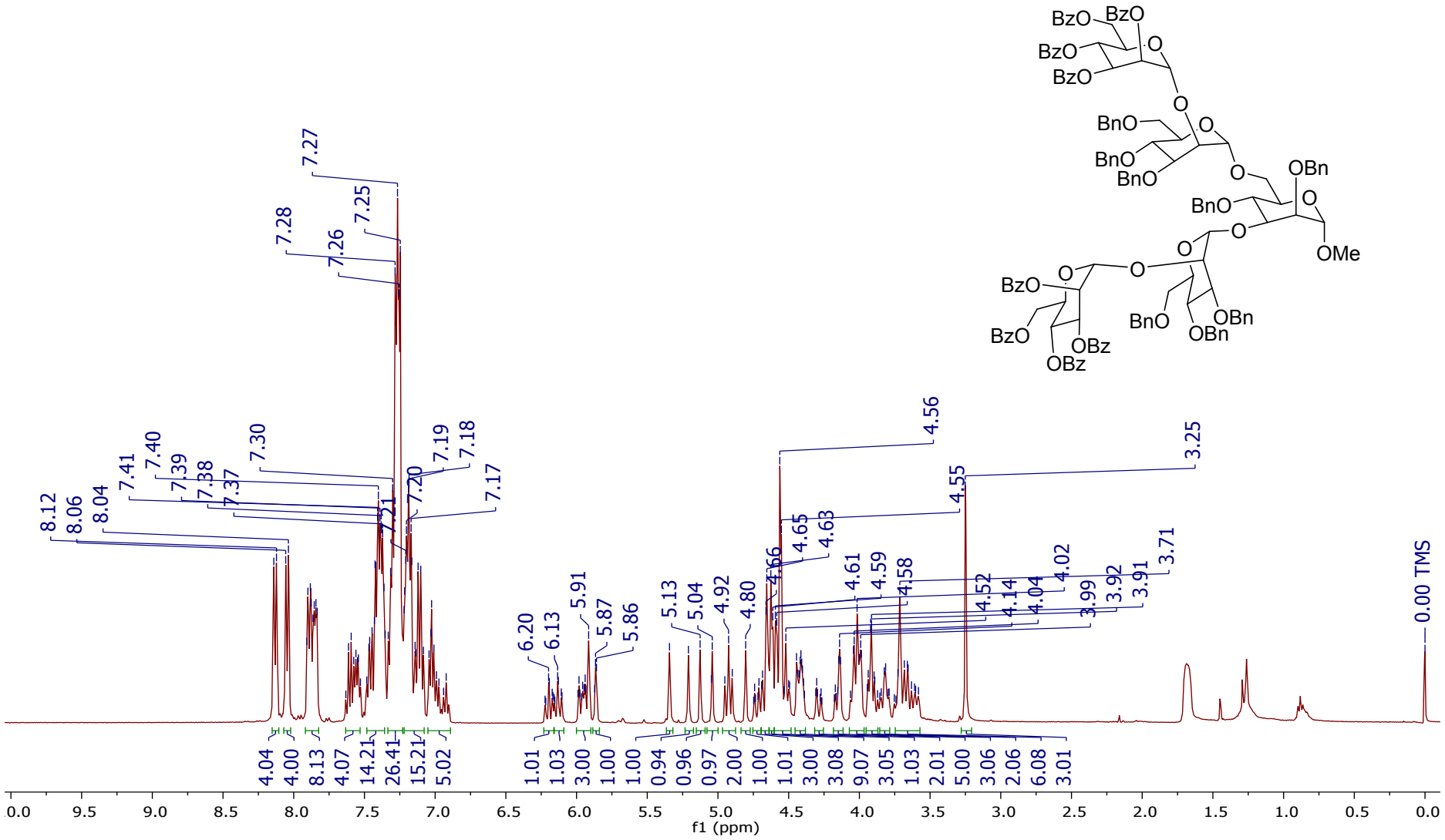

^{13}C NMR Spectrum (100.67 MHz, $CDCl_3$) of compound **20**

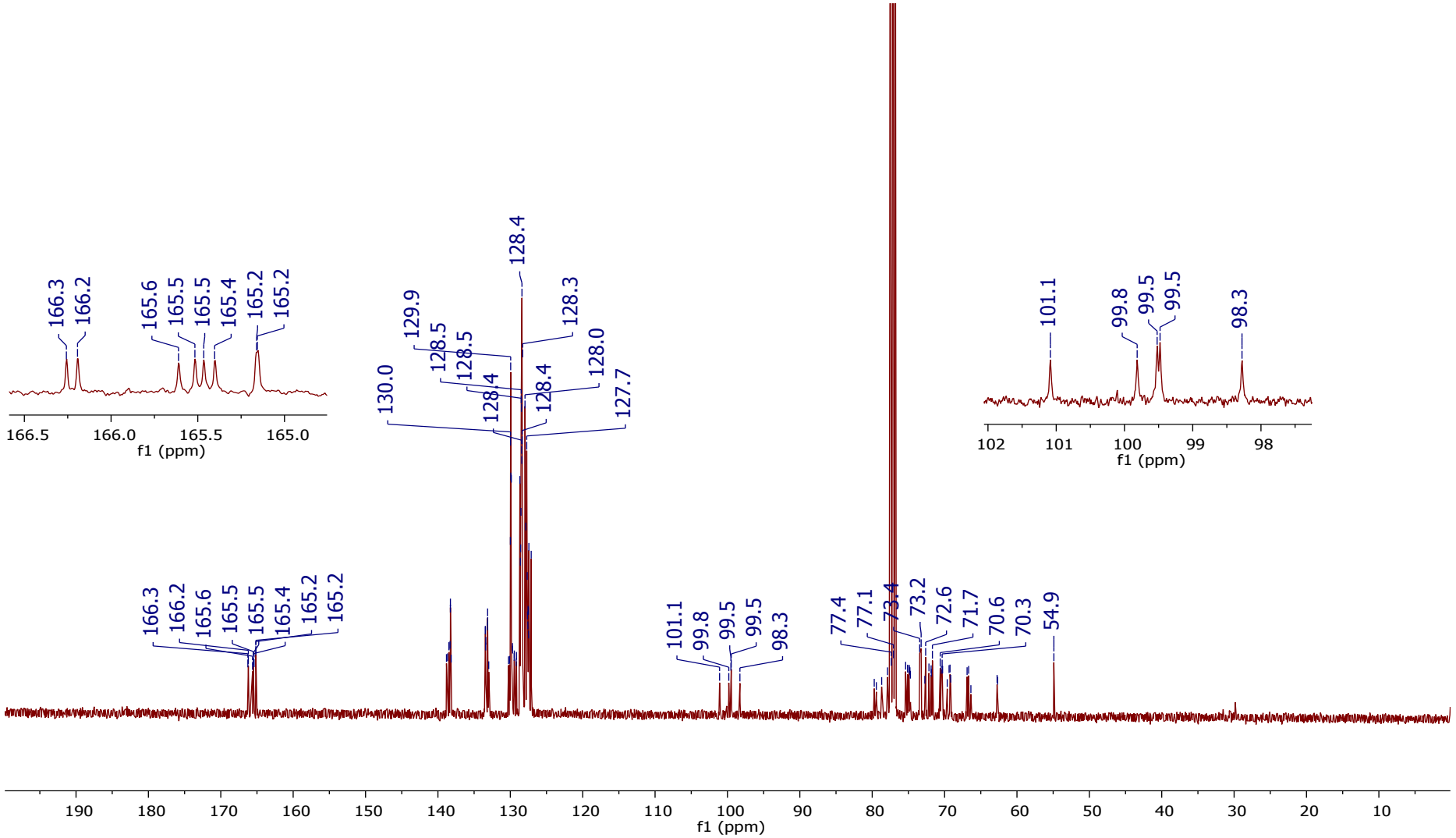

DEPT NMR Spectrum (100.67 MHz, $CDCl_3$) of compound **20**

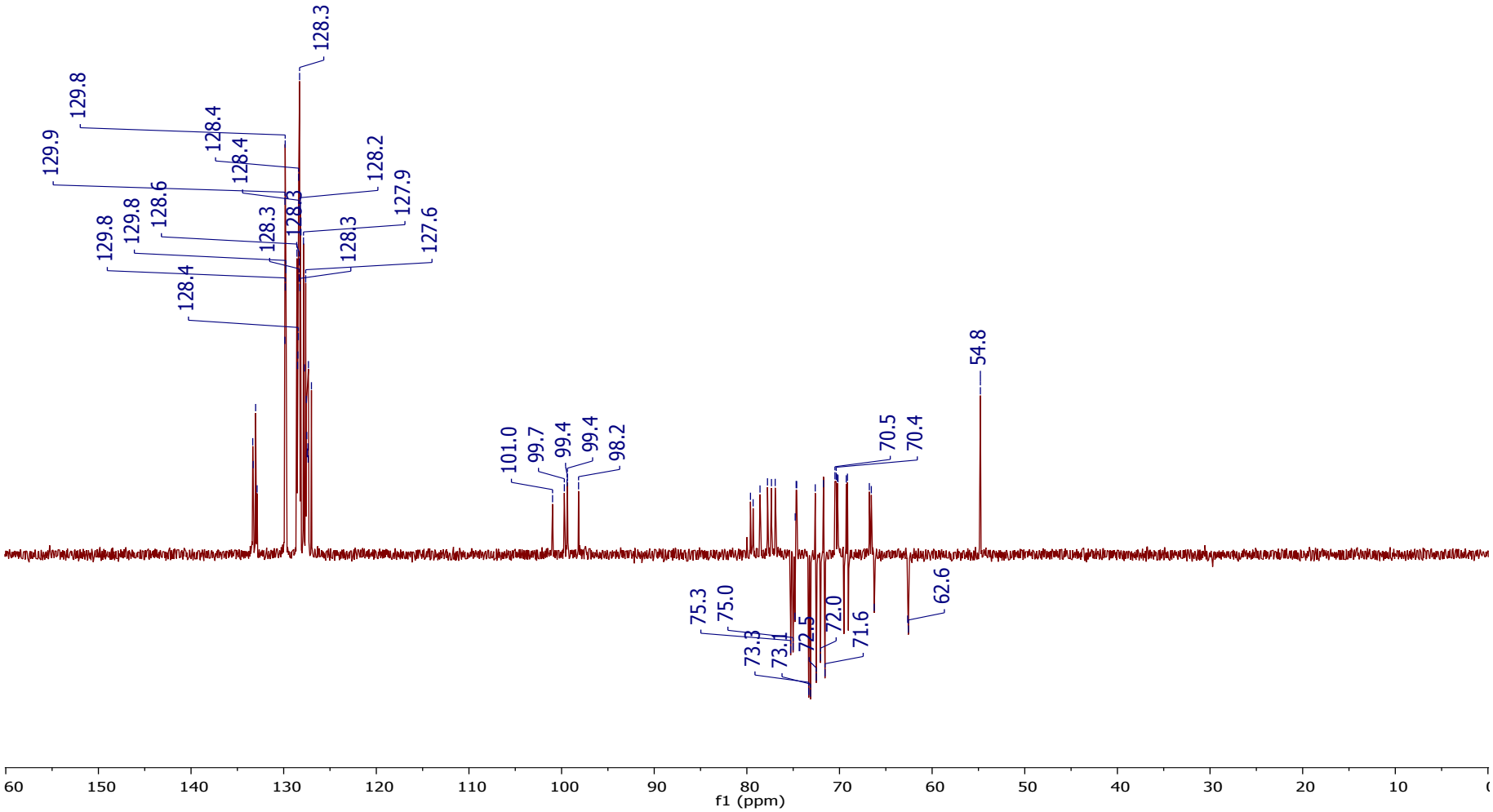
128.3
129.8
129.9
128.4
128.4
128.2
127.9
128.6
129.8
129.8
128.3
128.3
128.3
127.6
128.4
54.8
101.0
99.7
99.4
99.4
98.2
70.5
70.4
75.3
75.0
73.3
73.1
72.5
72.0
71.6
62.6
60
150
140
130
120
110
100
90
80
70
60
50
40
30
20
10
f1 (ppm)